

**CaMKII-dependent regulation of ion channels and its  
role in cardiac arrhythmias**

Dissertation  
zur Erlangung des Doktorgrades  
der Mathematisch-Naturwissenschaftlichen Fakultäten  
der Georg-August-Universität zu Göttingen

vorgelegt von  
Nataliya Dybkova  
aus Kiew/Ukraine

Göttingen 2008

D7

Referent: Prof. Dr. R. Hardeland

Korreferent Prof. Dr. D. Doenecke

Tag der mündlichen Prüfung: 3 Juli 2008

## Contents

<b>List of figures</b> .....	I
<b>Abbreviations</b> .....	III
<b>Summary</b> .....	1
<b>1 Introduction</b> .....	2
1.1 Ca <sup>2+</sup> as a critical second messenger in cardiac myocytes .....	2
1.2 Cardiac excitation-contraction coupling .....	2
1.3 Modulation of E-C coupling via Ca <sup>2+</sup> /calmodulin-dependent protein kinase II .....	4
1.3.1 Structure of Ca <sup>2+</sup> /calmodulin-dependent protein kinase II .....	5
1.3.2 Phosphorylation of L-type Ca <sup>2+</sup> channels by CaMKII results in Ca <sup>2+</sup> - dependent I <sub>Ca</sub> facilitation .....	7
1.3.3 Enhancement of SERCA2a activity and SR Ca <sup>2+</sup> uptake upon PLB phosphorylation by CaMKII .....	8
1.3.4 Regulation of RyR2 channel by CaMKII .....	8
1.4 Role of CaMKII in the development of heart failure .....	10
1.5 Involvement of CaMKII in cardiac arrhythmias .....	11
1.6 Cardiac voltage-gated Na <sup>+</sup> channels .....	14
1.6.1 The structure and function of Na <sup>+</sup> channels .....	14
1.6.2 Regulation of Na <sup>+</sup> channel by protein kinases .....	16
1.6.3 Na <sup>+</sup> channel involvement in arrhythmias .....	17
1.7 Mutations in cardiac RyR2 gene as a cause for cardiac arrhythmias .....	18
1.7.1 RyR2 regulates cardiac contraction and rhythm .....	18
1.7.2 Catecholaminergic polymorphic ventricular tachycardia .....	18
1.8 Aim of study .....	20
<b>2 Materials</b> .....	<b>21</b>
2.1 Animals .....	21
2.2 Adenovirus constructs .....	21
2.3 Oligonucleotides for polymerase chain reaction .....	21
2.4 Antibodies .....	22
2.5 Enzymes and nucleotides .....	24
2.6 Detection, purification and synthesis systems (kits) .....	24
2.7 Inhibitors .....	24
2.8 Stock solutions .....	25
2.9 Chemicals .....	27

## Contents

2.10 Detergents.....	28
2.11 Proteins and protein standards.....	28
2.12 Fluorescent dyes.....	29
2.13 Other materials.....	29
2.14 Instruments.....	29
<b>3 Methods.....</b>	<b>32</b>
3.1 Polymerase chain reaction (PCR).....	32
3.1.1 Electrophoresis conditions.....	33
3.1.2 Visualization of DNA in the gel.....	33
3.2 Adenoviral transfection and culture of adult rabbit ventricular cardiomyocytes.....	34
3.2.1 Preparation of laminin culture dishes.....	35
3.2.2 Calculation of virus quantity taken for transfection.....	35
3.3 Total protein homogenate preparation.....	36
3.3.1 Protein lysate preparation from rabbit ventricular cardiomyocytes.....	36
3.3.2 Protein homogenate preparation from mouse heart tissue.....	37
3.4 Co-immunoprecipitation.....	38
3.4.1 Formation of the antigen-antibody complex.....	38
3.4.2 Precipitation of immune complexes.....	38
3.4.3 Analysis.....	39
3.5 Immunoblotting.....	40
3.5.1 Casting of SDS-polyacrylamide gel.....	40
3.5.2 SDS-polyacrylamide gel electrophoresis (SDS-PAGE) and electrophoretic transfer.....	40
3.5.3 Staining the membrane with Ponceau S.....	41
3.5.4 Immunovisualization.....	41
3.6 Co-immunocytochemical analysis.....	45
3.6.1 Preparation and fixation of cells.....	45
3.6.2 Incubation with antibodies.....	46
3.7 Back-phosphorylation.....	47
3.7.1 Immunoprecipitation of Na <sup>+</sup> channel from mouse cardiac homogenates.....	47
3.7.2 Preactivation of endogenous CaMKII and immunoprecipitation of Na <sup>+</sup> channels from rabbit myocytes.....	48
3.7.3 Preactivation of exogenous CaMKII and back-phosphorylation.....	48
3.8 Isolation of mouse ventricular myocytes.....	50

## Contents

3.9	Measurement of cell shortening and Ca <sup>2+</sup> transients using an epifluorescence microscope.....	52
3.10	Measurement of the Ca <sup>2+</sup> sparks using confocal microscope.....	55
3.11	Echocardiographic measurements.....	56
3.12	Statistical analysis.....	56
<b>4</b>	<b>Results.....</b>	<b>57</b>
4.1	Association with and phosphorylation of Na <sup>+</sup> channels by CaMKII.....	57
4.1.1	CaMKII associates with Na <sup>+</sup> channels.....	57
4.1.2	Immunocolocalization of CaMKII and Na <sup>+</sup> channels in single cardiomyocytes....	59
4.1.3	CaMKII-dependent phosphorylation of Na <sup>+</sup> channels.....	61
4.1.4	Protein expression level of Na <sup>+</sup> channels.....	63
4.2	Generation and identification of mutant mice.....	65
4.2.1	PCR-mediated verification of genotypes of mutant mice.....	65
4.2.2	Cardiac overexpression of CaMKII $\delta_C$ in CaMKII $\delta_C$ TG and RyR2 <sup>R4496C+/-</sup> mice induces cardiac hypertrophy and mortality.....	66
4.3	Echocardiographic analysis of RyR2 <sup>R4496C+/-</sup> , CaMKII $\delta_C$ /RyR2 <sup>R4496C</sup> , CaMKII $\delta_C$ and WT mice.....	68
4.4	Analysis of cardiomyocyte shortening and Ca <sup>2+</sup> transients using an epifluorescence microscope.....	72
4.4.1	Fractional shortening and intracellular Ca <sup>2+</sup> transients.....	72
4.4.2	Frequency-dependence of shortening, intracellular Ca <sup>2+</sup> transients and relaxation.....	75
4.4.3	SR Ca <sup>2+</sup> content and NCX function.....	78
4.5	Expression levels of important Ca <sup>2+</sup> transport proteins in mouse hearts.....	82
4.6	Measurement of Ca <sup>2+</sup> release from the SR using confocal microscopy.....	85
4.7	Increased arrhythmogenic events in RyR2 <sup>R4496C+/-</sup> , CaMKII $\delta_C$ /RyR2 <sup>R4496C</sup> and CaMKII $\delta_C$ mice.....	88
<b>5</b>	<b>Discussion.....</b>	<b>91</b>
5.1	CaMKII $\delta_C$ associates with and phosphorylates cardiac Na <sup>+</sup> channels.....	91
5.2	Functional characterization of RyR2 <sup>R4496C+/-</sup> mice harboring a human CPVT mutation.....	94
5.3	Overexpression of CaMKII $\delta_C$ in mouse hearts bearing the R4496C mutation leads to arrhythmias and increased mortality.....	97
<b>6</b>	<b>References.....</b>	<b>102</b>

Contents

<b>Acknowledgements</b> .....	<b>116</b>
<b>Appendix</b> .....	<b>117</b>

## List of figures

	Page	
Fig. 1	General scheme of Ca <sup>2+</sup> cycle in a cardiac ventricular myocyte	3
Fig. 2	Effects of CaMKII $\delta_C$ on excitation-contraction coupling	5
Fig. 3	Domain layout and oligomeric organization of CaMKII	6
Fig. 4	Cardiac pathology in CaMKII $\delta_C$ TG mice	11
Fig. 5	Representative Ca <sup>2+</sup> sparks in CaMKII $\delta_C$ TG versus WT mice	12
Fig. 6	Structure of cardiac Na <sup>+</sup> channel Nav1.5 (SCN5A)	14
Fig. 7	Association of CaMKII with all Na <sup>+</sup> channel isoforms (Pan Na <sub>v</sub> ) in Triton X-100-solubilized cardiac mouse homogenate and rabbit lysates.	57
Fig. 8	Association of CaMKII with the cardiac Na <sup>+</sup> channel (Na <sub>v</sub> 1.5) isoform in Triton X-100-solubilized cardiac mouse homogenate and rabbit lysates	58
Fig. 9	Co-localization of CaMKII and Na <sup>+</sup> channels in mouse and rabbit cardiomyocytes	60
Fig. 10	Phosphorylation of Na <sup>+</sup> channel in cardiac mouse homogenate and rabbit lysates by either exogenous or endogenous CaMKII	62
Fig. 11	Protein expression levels of Na <sup>+</sup> channel in mice (CaMKII $\delta_C$ TG versus WT) and in transfected rabbit myocytes (CaMKII $\delta_C$ versus $\beta$ -gal, MOI of 100, 24 hours)	64
Fig. 12	PCR confirmation of CaMKII $\delta_C$ TG, RyR2 <sup>R4496C<math>\pm</math></sup> knock-in and WT mouse genotypes	65
Fig. 13	CaMKII $\delta_C$ overexpression in mouse hearts induced cardiac hypotrophy	67
Fig. 14	Overexpression of CaMKII $\delta_C$ led to sudden premature death	68
Fig. 15	Dilated cardiomyopathy and cardiac dysfunction at the whole heart level in vivo in CaMKII $\delta_C$ /RyR2 <sup>R4496C</sup> and CaMKII $\delta_C$ mice.	69
Fig. 16	Averaged structural echocardiographic parameters for WT, RyR2 <sup>R4496C<math>\pm</math></sup> , CaMKII $\delta_C$ /RyR2 <sup>R4496C</sup> and CaMKII $\delta_C$ mice	70
Fig. 17	Averaged functional echocardiographic parameter for WT, RyR2 <sup>R4496C<math>\pm</math></sup> , CaMKII $\delta_C$ /RyR2 <sup>R4496C</sup> and CaMKII $\delta_C$ mice	71
Fig. 18	Frequency-dependent changes in Ca <sup>2+</sup> transient amplitude in isolated	73

	cardiomyocytes measured using Fluo-3	
Fig. 19	Frequency-dependent changes in fractional shortening in isolated cardiomyocytes measured using a sarcomere length detection system	74
Fig. 20	Frequency-dependent changes in $\text{Ca}^{2+}$ transients and fractional shortening	76
Fig. 21	Frequency-dependent acceleration of relaxation	77
Fig. 22	Caffeine-induced $\text{Ca}^{2+}$ transients	79
Fig. 23	SR $\text{Ca}^{2+}$ content in cardiomyocytes	80
Fig. 24	NCX function	80
Fig. 25	Fractional SR $\text{Ca}^{2+}$ release	81
Fig. 26	(A) Representative Western blots of important $\text{Ca}^{2+}$ cycling proteins from cardiac homogenates prepared from hearts of $\text{RyR2}^{\text{R4496C}/-}$ and WT mice. (B) Quantification of the protein expression level in $\text{RyR2}^{\text{R4496C}/-}$ versus WT mice.	83
Fig. 27	(A) Representative Western blots of important $\text{Ca}^{2+}$ cycling proteins from cardiac homogenates prepared from hearts of $\text{CaMKII}\delta_{\text{C}}/\text{RyR2}^{\text{R4496C}}$ and WT mice. (B) Quantification of the protein expression level in $\text{CaMKII}\delta_{\text{C}}/\text{RyR2}^{\text{R4496C}}$ versus WT mice	84
Fig. 28	$\text{Ca}^{2+}$ sparks in mouse ventricular myocytes measured using Fluo-4	86
Fig. 29	$\text{Ca}^{2+}$ spark characteristics	87
Fig. 30	Cellular arrhythmias recorded in electrically paced isolated ventricular myocytes from $\text{RyR2}^{\text{R4496C}/-}$ , $\text{CaMKII}\delta_{\text{C}}/\text{RyR2}^{\text{R4496C}}$ and $\text{CaMKII}\delta_{\text{C}}$ mouse hearts	90



## Abbreviations

Ab	Antibody
AC3-I	Autocamtide-2 inhibitory peptide
Ad	Adenovirus
AIP	Autocamtide-2 related inhibitory peptide
AM	acetoxymethyl ester
AMP	Adenosine monophosphate
AP	Action potential
APS	Ammonium persulfate
ATP	Adenosine triphosphate
BCA	Bicinchoninic acid
BDM	2,3-butanedione monoxime
bp	Base pair
CaM	Calmodulin
CaMK	Ca <sup>2+</sup> /calmodulin-dependent protein kinase
CaMKII	Ca <sup>2+</sup> /calmodulin-dependent protein kinase II
CaMKII $\delta_C$	Cytosolic isoform of Ca <sup>2+</sup> /calmodulin-dependent protein kinase II
CaMKII $\delta_C$ /RyR2 <sup>R4496C</sup>	Crossbred RyR2 <sup>R4496C/+</sup> knock-in with CaMKII $\delta_C$ TG mice
cAMP	Cyclic adenosine-3',5'-monophosphate
CaSpF	Ca <sup>2+</sup> spark frequency
Ci	Curie
CHAPS	3-[(3-cholamidopropyl)dimethylammonio]-1-propane sulphonate
CPVT	Catecholaminergic polymorphic ventricular tachycardia
CSQ	Calsequestrin
DAD	Delayed afterdepolarization
dd H <sub>2</sub> O	Double distilled water
DEPC	Diethylpyrocarbonate
DM	Double mutant
DMSO	Dimethylsulfoxide
DNA	Desoxyribonucleic acid

dNTP	Deoxyribonucleoside triphosphate
DTT	Dithiothreitol
EAD	Early afterdepolarization
E-C coupling	Excitation-contraction coupling
EDTA	Ethylenedinitrilo-N, N, N', N'-tetraacetic acid
EGTA	ethylene glycol tetraacetic acid
$E_m$	Membrane potential
FDAR	Frequency-dependent acceleration of relaxation
FS	Fractional shortening
g	Gravity
GAPDH	Glyceraldehyde-3-phosphate dehydrogenase
HA	Hemagglutinin
HEK	Human embryonic kidney
HEPES	2-(4-(2-hydroxyethyl)-piperazinyl)-1-ethansulfonate
HF	Heart failure
HPLC	High performance liquid chromatography
HRP	Horseradish peroxidase
$I_{Ca}$	Calcium current
ICC	Immunocytochemical staining
IFM	Isoleucine-phenylalanine-methionine
IgG	Immunoglobulin G
IP	Immunoprecipitation
kDa	Kilodalton
KN-93	2-[N-(2-hydroxyethyl)-N-(4-methoxybenzenesulfonyl)] amino-N-(4-chlorocinnamyl)-N-methylbenzylamine
LQT3	Long-QT syndrome 3
LQTS	Long QT syndrome
MOI	Multiplicity of infection
NCX	$Na^+/Ca^{2+}$ -exchanger
PAAG	Polyacrylamide Gel
PBS	Phosphate buffered saline
PCR	Polymerase chain reaction
pfu	Plaque-forming unit
PKA	cAMP-dependent protein kinase

PKC	Ca <sup>2+</sup> -dependent protein kinase
PLB	Phospholamban
PLB-KO	PLB deficient mice
RyR	Ryanodine receptor
RyR2	Cardiac ryanodine receptor
RyR2 <sup>R4496C+/-</sup>	Knock-in mice harboring the R4496C mutation in RyR2
SCN5A	Human cardiac sodium channel
SDS	Sodium dodecylsulfate
SDS-PAGE	SDS-polyacrylamide gel electrophoresis
SEM	Standard error of the mean
SERCA2a	Cardiac sarcoplasmic reticulum Ca <sup>2+</sup> -ATPase
SR	Sarcoplasmic reticulum
TAC	Transverse aortic constriction
TBE	Tris-borate-EDTA buffer
TEMED	N, N, N', N'-tetramethylethylenediamine
TG	Transgenic
Tris	Tris-(hydroxymethyl)-aminomethane
UV	Ultraviolet
VT	Ventricular tachyarrhythmias
WB	Western blot
WT	Wild type
β-gal	β-Galactosidase

## Summary

Intracellular calcium ( $\text{Ca}^{2+}$ ) is a central second messenger, which translates the electrical signal into cardiac contraction. This process is termed excitation-contraction coupling (E-C coupling). Recently, it has become clear that several  $\text{Ca}^{2+}$ -dependent proteins contribute to the fine tuning of E-C coupling. One of these is the  $\text{Ca}^{2+}$ /calmodulin-dependent protein kinase II (CaMKII). Its major cardiac isoform is CaMKII $\delta$  with the  $\delta_C$  splice variant being localized to the cytosol. CaMKII can phosphorylate and alter the function of several  $\text{Ca}^{2+}$  handling proteins including sarcoplasmic reticulum  $\text{Ca}^{2+}$  release channels also known as ryanodine receptors (RyR). Increased CaMKII activity has been linked to heart failure (HF) and ventricular arrhythmias. Expression levels and activity of CaMKII in human HF and in animal HF models are increased 2- to 3- fold. HF is associated with an increased risk of sudden death mainly caused by ventricular arrhythmias. Altered sodium ( $\text{Na}^+$ ) channel function has been shown to underlie ventricular arrhythmias. Another mechanism for ventricular arrhythmias is catecholaminergic polymorphic ventricular tachycardia (CPVT). CPVT is a disease caused by mutations (e.g. R4497C) in the cardiac RyR2 gene in individuals with structurally normal hearts.

In the present work it has been investigated 1) whether CaMKII $\delta_C$  associates with and phosphorylates cardiac  $\text{Na}^+$  channels in rabbit myocytes and mouse heart tissue thereby regulating its function possibly leading to ventricular arrhythmias; 2) intracellular  $\text{Ca}^{2+}$  handling in mouse myocytes harboring the R4496C mutation in RyR2; 3) possible alterations of E-C coupling and arrhythmogenic effects due to overexpression of CaMKII $\delta_C$  in mouse hearts, carrying additionally the R4496C mutation in cardiac RyR2.

The present study shows that CaMKII $\delta_C$  associates with cardiac  $\text{Na}^+$  channels within the transverse tubular system, and that CaMKII $\delta_C$  can phosphorylate  $\text{Na}^+$  channels in both mouse and rabbit myocardium.

Studies with a mouse model harboring the R4496C mutation in RyR2 revealed abnormal  $\text{Ca}^{2+}$  release through RyR2. Overexpression of CaMKII $\delta_C$  in these mice leads to severe heart failure, contractile dysfunction and altered intracellular  $\text{Ca}^{2+}$  handling in vitro causing arrhythmogenic events in isolated myocytes under basal conditions and increased mortality in vivo as compared to mice overexpressing CaMKII $\delta_C$  only.

# 1 Introduction

## 1.1 $\text{Ca}^{2+}$ as a critical second messenger in cardiac myocytes

Calcium ( $\text{Ca}^{2+}$ ) is a critical second messenger in cardiac muscle. Elevated intracellular  $\text{Ca}^{2+}$  levels can activate numerous  $\text{Ca}^{2+}$ -regulated enzymes, which have different subcellular localizations and may respond to distinct modes of  $\text{Ca}^{2+}$  mobilization. Intracellular cytosolic  $\text{Ca}^{2+}$  concentrations are regulated carefully to remain at  $\sim 100$  nM under resting conditions. This occurs even when extracellular levels of  $\text{Ca}^{2+}$  are increased. Acute increases in intracellular  $\text{Ca}^{2+}$  are needed to elicit physiological responses in cells. In cardiac muscle,  $\text{Ca}^{2+}$  plays a central role in the regulation of contractility, hypertrophy, gene expression and apoptosis. Changes in intracellular  $\text{Ca}^{2+}$  generate both acute and chronic effects on cardiac function. The  $\text{Ca}^{2+}$  transients, which accompany each cardiac cycle, trigger cardiac muscle contraction, a process termed excitation-contraction (E-C) coupling that occurs on the millisecond time scale. The key amplification step in E-C coupling is under tight control of the strictly local  $\text{Ca}^{2+}$  concentration. In contrast, sustained or chronic (minutes to hours/days) alterations in  $\text{Ca}^{2+}$  signaling could result in activation of gene expression, the process known as excitation-transcription coupling. These pathways are involved in hypertrophy and heart failure, and they can alter the expression of some  $\text{Ca}^{2+}$  regulatory proteins involved in E-C coupling (Maier and Bers, 2002; Bers, 2001; Bers and Guo, 2005).

## 1.2 Cardiac excitation-contraction coupling

Upon myocyte membrane depolarization  $\text{Ca}^{2+}$  enters the cell mainly through voltage dependent L-type  $\text{Ca}^{2+}$  channels and triggers  $\text{Ca}^{2+}$  release from the sarcoplasmic reticulum (SR) via ryanodine receptors (RyR) to amplify  $\text{Ca}^{2+}$  current ( $I_{\text{Ca}}$ ), a process termed  $\text{Ca}^{2+}$ -induced  $\text{Ca}^{2+}$  release (Bers, 2002). The resultant rise in global intracellular  $\text{Ca}^{2+}$  causes  $\text{Ca}^{2+}$  binding to troponin C, which in turn activates the myofilaments to produce cardiac contraction. To allow cardiac muscle to relax, cytosolic  $\text{Ca}^{2+}$  must be quickly removed. The main mechanisms for  $\text{Ca}^{2+}$  removal is mediated by SR  $\text{Ca}^{2+}$ -ATPase (SERCA2a), which pumps  $\text{Ca}^{2+}$  back into SR, and by  $\text{Na}^+/\text{Ca}^{2+}$ -exchanger (NCX), which extrudes  $\text{Ca}^{2+}$  out of myocytes but may also contribute to systolic  $\text{Ca}^{2+}$  influx in its reverse mode (Bers, 2002). Quantitatively, during steady-state conditions, the same amount of  $\text{Ca}^{2+}$  that entered

the cell upon activation via voltage dependent L-type  $\text{Ca}^{2+}$  channels and reverse mode NCX is transported out of the cell, mainly via NCX, with a very minor contribution by the sarcolemmal  $\text{Ca}^{2+}$ -ATPase. Likewise, the amount of  $\text{Ca}^{2+}$  previously released from the SR must be taken back up by SERCA2a. Of note, only a small  $\text{Ca}^{2+}$  flux (1-2 %) contributes to E-C coupling by the mitochondrial uniporter (Fig. 1)

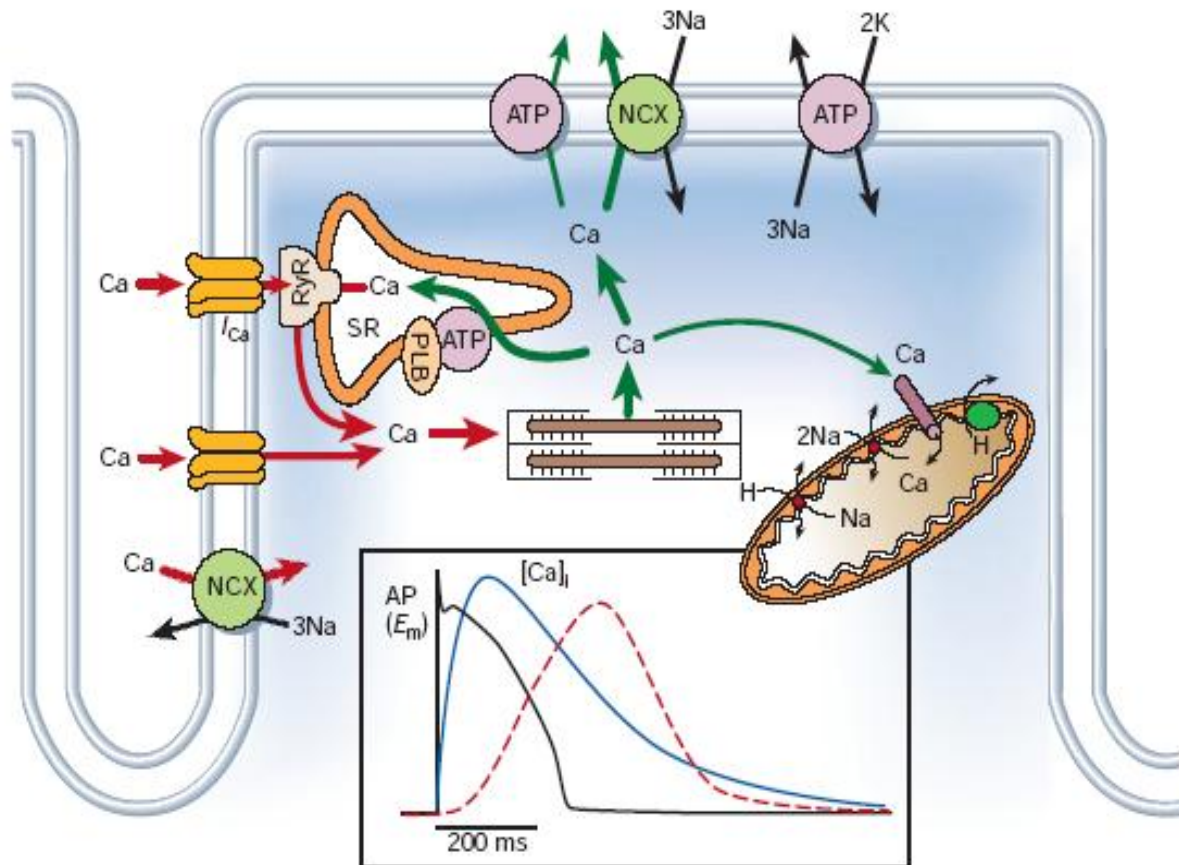


**Figure 1. General scheme of  $\text{Ca}^{2+}$  cycle in a cardiac ventricular myocyte.**  $\text{Ca}^{2+}$  can enter the cell via  $\text{Ca}^{2+}$  channels ( $I_{\text{Ca}}$ ) and  $\text{Na}^+/\text{Ca}^{2+}$  exchange (NCX).  $\text{Ca}^{2+}$  influx controls SR  $\text{Ca}^{2+}$  release by the ryanodine receptor (RyR).  $\text{Ca}^{2+}$  is removed from cytosol by the SR  $\text{Ca}^{2+}$ -ATPase pump (ATP), modulated by phospholamban (PLB), NCX and only to a minor extent by sarcolemmal  $\text{Ca}^{2+}$ -ATPase pump and mitochondrial uniporter (from Bers, 2002).

This well coordinated process of E-C coupling occurring at approximately 60 times per minute in man and up to 500 times per minute in mouse during rest, consists of thousands of synchronized local events. About 25 L-type  $\text{Ca}^{2+}$  channel proteins and 100 RyR2 proteins are co-localized in the junctional microdomain between the SR and the

sarcolemmal membrane forming a local SR  $\text{Ca}^{2+}$  release unit called junction or couplon (Bers and Guo, 2005). Spontaneous  $\text{Ca}^{2+}$  releases from an individual couplon ( $\text{Ca}^{2+}$  sparks) during diastole in cardiac myocytes can be monitored by confocal microscopy.  $\text{Ca}^{2+}$  influx through  $I_{\text{Ca}}$  raises local intracellular  $\text{Ca}^{2+}$  from 0.1 to  $> 10 \mu\text{M}$ , and local  $\text{Ca}^{2+}$  release from a cluster of RyR2s further increases local cleft  $\text{Ca}^{2+}$  to  $> 100 \mu\text{M}$ , whereas global intracellular  $\text{Ca}^{2+}$  only reaches  $\sim 1 \mu\text{M}$  (at a later time). A critical aspect of this discrete local signaling is that as local intracellular  $\text{Ca}^{2+}$  declines between junctions, it is not sufficient to trigger SR  $\text{Ca}^{2+}$  release at neighboring junctions 1-2  $\mu\text{m}$  away (Bers, 2002). However, physiologically these local SR  $\text{Ca}^{2+}$  release events are synchronized by action potentials and simultaneous activation of  $I_{\text{Ca}}$  at all junctions to produce a relatively homogenous increase in intracellular  $\text{Ca}^{2+}$  throughout the cytosol. Therefore,  $\text{Ca}^{2+}$  sparks are the elementary units of SR release both at rest and during the normal  $\text{Ca}^{2+}$  transient during E-C coupling (Bers, 2002; Cheng et al., 1993; Fill and Copello, 2002).

### **1.3 Modulation of E-C coupling via $\text{Ca}^{2+}$ /calmodulin-dependent protein kinase II**

There is considerable evidence that changes in intracellular  $\text{Ca}^{2+}$  handling are not only involved in the direct myofilament activation leading to contraction, but also indirectly modify the activity of ion channels and transporters via calmodulin (CaM) and  $\text{Ca}^{2+}$ /calmodulin-dependent protein kinase II (CaMKII) (Maier and Bers, 2002). CaM is an important signaling messenger in nearly all cell types, where  $\text{Ca}^{2+}$ /CaM regulates proteins involved in  $\text{Ca}^{2+}$  transport, ion channels, cell contraction, protein kinases, cell metabolism, gene expression and cell proliferation (Cheung, 1980; Vogel, 1994).  $\text{Ca}^{2+}$ /calmodulin-dependent protein kinases (CaMKs) are one of the targets for CaM binding. This multifunctional serine/threonine family consists of CaMKI, -II, and -IV and has a wide tissue distribution. CaMKI and CaMKIV are monomeric enzymes that are activated by phosphorylation through an upstream kinase (Lee and Edelman, 1994; Tokumitsu et al., 1995). These isoforms are expressed at very low levels in the heart (Edman and Schulman, 1994; Colomer et al., 2003). In contrast, CaMKII is a multimer of 6-12 subunits encoded by four separate genes:  $\alpha$ ,  $\beta$ ,  $\gamma$ , and  $\delta$  (Braun and Schulman, 1995). Binding of  $\text{Ca}^{2+}$ /CaM to CaMKII leads to its activation and subsequent autophosphorylation, rendering it capable of autoactivation in the absence of  $\text{Ca}^{2+}$ /CaM (Braun and Schulman, 1995). CaMKII can

modulate E-C coupling by phosphorylating several important  $\text{Ca}^{2+}$  transport proteins in the heart in response to  $\text{Ca}^{2+}$  signals, including RyR2 (Witcher et al., 1991; Hain et al., 1995), PLB (Davis et al., 1983; Simmerman et al., 1986) and L-type  $\text{Ca}^{2+}$  channels (Maier and Bers, 2002) with multiple functional consequences (Fig. 2)

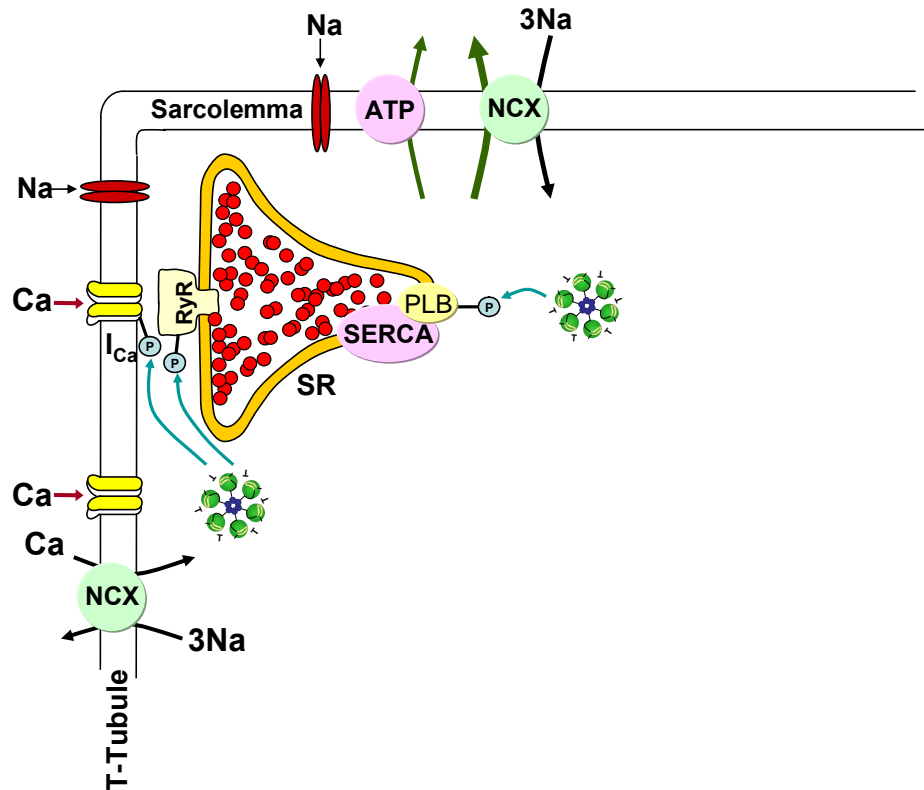


**Figure 2. Effects of CaMKII $\delta_C$  on excitation-contraction coupling.** CaMKII phosphorylates several  $\text{Ca}^{2+}$ -handling proteins including phospholamban (PLB), SR  $\text{Ca}^{2+}$  release channels (RyR), and L-type  $\text{Ca}^{2+}$  channels responsible for  $\text{Ca}^{2+}$  influx ( $I_{\text{Ca}}$ ) (modified from Maier and Bers, 2007).

### 1.3.1 Structure of $\text{Ca}^{2+}$ /calmodulin-dependent protein kinase II

The multimeric CaMKII holoenzyme consists of homo- or heteromultimers of 6-12 kinase subunits forming a wheel-like structure (Maier and Bers, 2002; Hook and Means, 2001) (Fig. 3). There are four closely related but different CaMKII genes ( $\alpha$ ,  $\beta$ ,  $\gamma$  and  $\delta$ ). The  $\alpha$  and  $\beta$  isoforms are expressed in the nervous tissue, whereas the  $\gamma$  and  $\delta$  isoforms are more ubiquitous. The  $\delta$  isoform is the predominant isoform of CaMKII in the heart. There are two splice variants of the  $\delta$  isoform:  $\delta_B$  is localized to the nucleus, whereas  $\delta_C$  is found in cytoplasm. Each CaMKII subunit has three structural domains: an amino-terminal catalytic



domain, a central regulatory domain (containing partially overlapping autoinhibitory and CaM binding regions) and a carboxy-terminal association domain responsible for oligomerization (Braun and Schulman, 1995; Maier and Bers, 2002). Resting CaMKII is blocked by the autoinhibitory region that acts as a pseudosubstrate, preventing a substrate from binding. When intracellular  $\text{Ca}^{2+}$  increases, such as during systole,  $\text{Ca}^{2+}/\text{CaM}$  complex binds to the regulatory domain of CaMKII and displaces the autoinhibitory domain by wrapping itself around it resulting in release of the active centre of the catalytic region, which then gains access to substrates. After this  $\text{Ca}^{2+}/\text{CaM}$ -dependent activation, CaMKII locks itself into the activated state by autophosphorylation of Thr-286 on the autoinhibitory segment of adjacent CaMKII subunits (Braun and Schulman, 1995; Zhang and Brown, 2004).

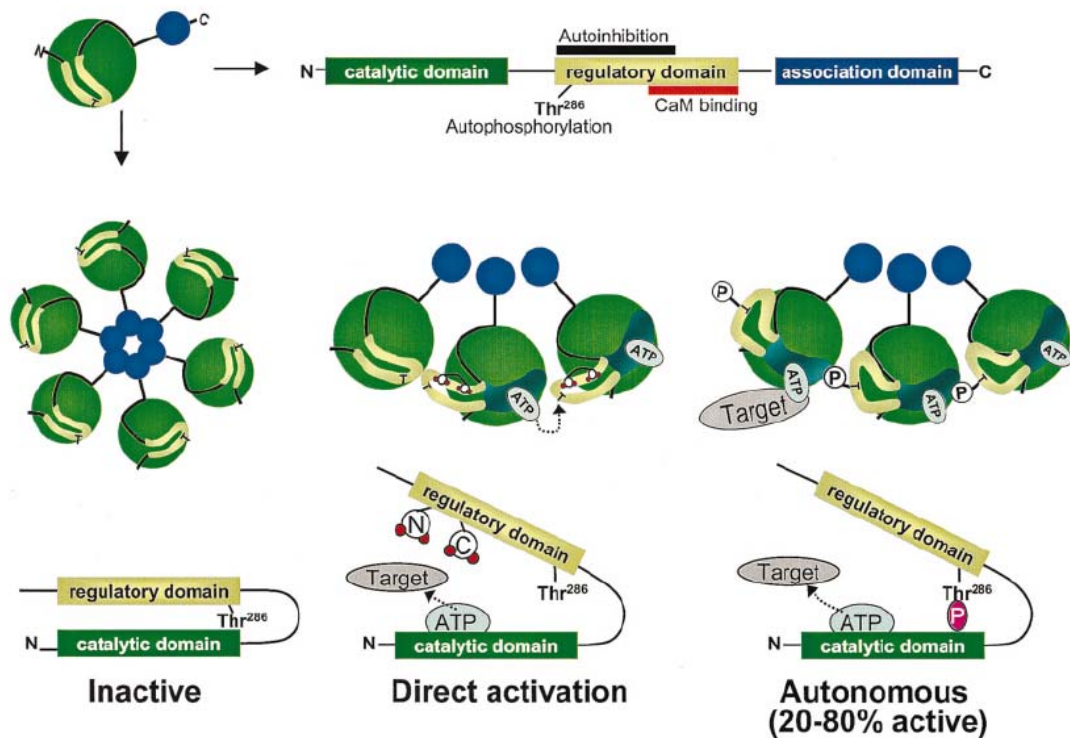


**Figure 3. Domain layout and oligomeric organization of CaMKII.** The three main domains of the CaMKII monomer are indicated in a linear layout (top). Middle left shows that CaMKII forms homo- or heteromultimers (6-12 monomers) in wheel-like structures (a second one may sit on top of the one shown, forming a double wheel). Lower middle and right panels show activation of CaMKII by  $\text{Ca}^{2+}/\text{CaM}$  binding and subsequent autophosphorylation at Thr-286 (P). CaM binding is sufficient to activate CaMKII allowing the active site (ATP) to interact and phosphorylate target proteins. Autophosphorylation maintains CaMKII active (20-80%) even after CaM dissociation (from Maier and Bers, 2002).

Autophosphorylation at Thr-286 in the autoinhibitory domain can maintain CaMKII active even after  $\text{Ca}^{2+}$  has declined, (e.g. during diastole) when  $\text{Ca}^{2+}/\text{CaM}$  has dissociated from its binding region, and will generate autonomous activity of CaMKII. Autophosphorylation is not essential for CaMKII activity, but it does have important consequences, i.e. by increasing the affinity of the  $\text{Ca}^{2+}/\text{CaM}$ -kinase complex (Meyer et al., 1992). This effect traps  $\text{Ca}^{2+}/\text{CaM}$  on the autophosphorylated subunit. Even after declining  $\text{Ca}^{2+}$  to resting levels during diastole (i. e.  $\sim 100$  nM), CaM is still trapped on the kinase for several seconds. As a result, the kinase remains fully active with CaM bound regardless of the  $\text{Ca}^{2+}$  level and partially active (20-80%) after CaM dissociation from this autonomous state (Meyer et al., 1992; Lai et al., 1986; Lou et al., 1986).

### ***1.3.2 Phosphorylation of L-type $\text{Ca}^{2+}$ channels by CaMKII results in $\text{Ca}^{2+}$ -dependent $I_{\text{Ca}}$ facilitation***

CaMKII modulates voltage-gated L-type  $\text{Ca}^{2+}$  channel and results in  $\text{Ca}^{2+}$ -dependent  $I_{\text{Ca}}$  facilitation, which is typically observed as increased  $I_{\text{Ca}}$  amplitude and slower inactivation over 2 to 5 pulses. Several groups demonstrated that  $\text{Ca}^{2+}$ -dependent  $I_{\text{Ca}}$  facilitation is regulated by CaMKII-dependent phosphorylation (Anderson et al., 1994; Xiao et al., 1994; Yuan and Bers, 1994). CaMKII can bind to the  $\alpha_{1\text{C}}$  subunit of the cardiac L-type  $\text{Ca}^{2+}$  channel and can phosphorylate the  $\alpha_{1\text{C}}$  subunit at carboxy tails (Hudmon et al., 2005). CaMKII also phosphorylates Thr-498 on the  $\beta_{2\text{a}}$ -subunit of the L-type  $\text{Ca}^{2+}$  channel, which may be involved in the functional effect of  $I_{\text{Ca}}$  facilitation (Grueter et al., 2006). At the single channel level this CaMKII-dependent  $I_{\text{Ca}}$  facilitation is manifested as longer single channel opening (Dzhura et al., 2000). This  $I_{\text{Ca}}$  facilitation is  $\text{Ca}^{2+}$ -dependent and CaMKII-dependent, because it could be abolished by a CaMKII inhibitory peptide and is not apparent with  $\text{Ba}^{2+}$  as the charge carrier.  $I_{\text{Ca}}$  facilitation is also a local event because it is still observed when the intracellular milieu of a cell is heavily  $\text{Ca}^{2+}$  buffered with 10 mM EGTA. The physiological role of  $I_{\text{Ca}}$  facilitation is not entirely clear, but it may partly offset reduced L-type  $\text{Ca}^{2+}$  channel availability at high heart rates (caused by direct  $\text{Ca}^{2+}$ -dependent inactivation). By overexpressing CaMKII $\delta_{\text{C}}$  in transgenic mouse myocytes as well as in adenovirus-mediated rabbit myocytes,  $I_{\text{Ca}}$  amplitude was increased and inactivation was slowed (Maier et al., 2003, Kohlhaas et al., 2006).  $I_{\text{Ca}}$  amplitude could be reduced back to control levels by blocking CaMKII with the organic inhibitor KN-93

(Maier et al., 2003) or with the autocamide-2 related inhibitory peptide (AIP) (Kohlhaas et al., 2006).

### ***1.3.3 Enhancement of SERCA2a activity and SR Ca<sup>2+</sup> uptake upon PLB phosphorylation by CaMKII***

Ca<sup>2+</sup> uptake into the SR is mediated by SERCA2a, which plays an important role in the declining phase of the Ca<sup>2+</sup> transient. The activity of SERCA2a, the isoform expressed in the heart, is regulated by intracellular Ca<sup>2+</sup> concentration and PLB. PLB is an endogenous inhibitor of SERCA2a in its unphosphorylated state (Brittsan and Kranias, 2000). PLB can be phosphorylated by cAMP-dependent protein kinase (PKA) at Ser-16 and by CaMKII at Thr-17 (Brittsan and Kranias, 2000, Simmerman et al., 1986). Bassani and colleagues (Bassani et al., 1995) demonstrated that CaMKII enhanced SR Ca<sup>2+</sup> uptake, and suggested that CaMKII phosphorylation of PLB might be responsible for the frequency-dependent acceleration of relaxation (FDAR) of twitches and SR Ca<sup>2+</sup> uptake. Some studies even showed that direct CaMKII-dependent SERCA2a phosphorylation stimulates its activity, although others failed to show the significant stimulatory function of CaMKII on SERCA2a (Maier and Bers, 2002). Hagemann and colleagues (Hagemann et al., 2000) showed a frequency-dependent increase in PLB Thr-17 phosphorylation in rat myocytes in the absence of Ser-16 phosphorylation, and that the level of CaMKII phosphorylation of PLB at Thr-17 correlated with the rate of relaxation.

Physiologically, FDAR could be an important intrinsic mechanism to allow faster relaxation when heart rate is increased. It has been hypothesized that FDAR might be due to enhanced SR Ca<sup>2+</sup> uptake via PLB phosphorylation by CaMKII, activated by the cyclic increase in Ca<sup>2+</sup> during E-C coupling. However, it was found that FDAR is still quite prominent in PLB deficient (PLB-KO) mice and still sensitive to CaMKII inhibition by KN-93 and AIP (DeSantiago et al., 2002). Thus, while PLB might contribute to FDAR, it cannot be the sole mechanism.

### ***1.3.4 Regulation of RyR2 channel by CaMKII***

CaMKII also affects RyR2 activity. Witcher and colleagues (Witcher et al., 1991) first reported that the unique phosphorylation site was Ser-2809 on RyR2 which regulated channel activity. Later Rodriguez and colleagues (Rodriguez et al., 2003) suggested that CaMKII may phosphorylate at least four sites in addition to Ser-2809. Wehrens and

colleagues (Wehrens et al., 2004) identified a CaMKII phosphorylation site on RyR2 at Ser-2815 using site-directed mutagenesis. Other studies also showed that RyR2 is a substrate of CaMKII (Hain et al., 1995; Lokuta et al., 1997), but the real functional effect of phosphorylation by CaMKII in vivo is still unclear and controversial. That is, CaMKII was suggested to either increase (Hain et al., 1995; Witcher et al., 1991) or decrease the RyR2 open probability (Lokuta et al., 1997). Most studies on CaMKII effects on RyR2 have been conducted using RyR2 in lipid bilayers or by measuring  $\text{Ca}^{2+}$  release from SR vesicles. It is important to study RyR2 behavior in its native cellular environment. In intact voltage clamped ventricular myocytes endogenous CaMKII increased the amount of SR  $\text{Ca}^{2+}$  release for a given SR  $\text{Ca}^{2+}$  content and  $I_{\text{Ca}}$  triggers (Li et al., 1997). This effect of CaMKII on RyR2 was evaluated when both L-type  $\text{Ca}^{2+}$  current and SR  $\text{Ca}^{2+}$  load were constant under control conditions and in the presence of the CaMKII inhibitor KN-93. However, Wu and colleagues (Wu et al., 2001) showed that constitutively active CaMKII inhibited  $\text{Ca}^{2+}$  transients, while a CaMKII inhibitor increased  $\text{Ca}^{2+}$  transients. Yang and colleagues (Yang et al., 2007) reported that phosphorylation of RyR2 by CaMKII negatively regulates  $\text{Ca}^{2+}$  spark and  $\text{Ca}^{2+}$  wave activities, thus serving as a stabilizing factor for SR  $\text{Ca}^{2+}$  release in intact cardiac myocytes.

Recent studies performed in isolated cardiac myocytes have provided new evidences indicating that CaMKII indeed is directly associated with RyR2 (Zhang et al., 2003; Wehrens et al., 2004; Currie et al., 2004) and overexpression of CaMKII increases fractional SR  $\text{Ca}^{2+}$  release as well as resting spontaneous SR  $\text{Ca}^{2+}$  spark frequency despite lower SR  $\text{Ca}^{2+}$  load and diastolic  $\text{Ca}^{2+}$  (Maier et al., 2003; Kohlhaas et al., 2006; Guo et al., 2006). In addition to this increased frequency (which is indicative of RyR2-mediated diastolic spontaneous SR  $\text{Ca}^{2+}$  sparks), width and duration of  $\text{Ca}^{2+}$  sparks were enhanced, demonstrating increased diastolic SR  $\text{Ca}^{2+}$  leak. In contrast,  $\text{Ca}^{2+}$  spark frequency decreases dramatically upon inhibition of CaMKII by KN-93 (Maier et al., 2003). These results in myocytes from CaMKII $\delta_{\text{C}}$  transgenic mouse hearts have been recently confirmed by acute CaMKII $\delta_{\text{C}}$  overexpression by adenovirus-mediated gene transfer in isolated rabbit myocytes (Kohlhaas et al., 2006) as well as direct application of preactivated CaMKII to permeabilized mouse myocytes (Guo et al., 2006). In rabbit hearts, AIP (CaMKII inhibitor peptide) decreased  $\text{Ca}^{2+}$  spark frequency, indicating that CaMKII activates RyR2 in myocytes (Currie et al., 2004). Wehrens and colleagues (Wehrens et al., 2004) also showed that CaMKII-dependent RyR2 phosphorylation increases the RyR2 open probability using

channel measurements in lipid bilayers. Taken together, CaMKII-dependent RyR2 phosphorylation seems to have strong stimulatory effects on RyR2 activity in vivo.

#### **1.4 Role of CaMKII in the development of heart failure**

As was discussed, CaMKII can phosphorylate and alter the function of several  $\text{Ca}^{2+}$  transport proteins and plays an important role in E-C coupling in cardiomyocytes. CaMKII is also associated with the development of hypertrophy and heart failure (HF). Heart failure is characterized by contractile dysfunction of the heart developing with hypertrophy and which is associated with changes in cardiomyocyte  $\text{Ca}^{2+}$  homeostasis. It has been reported that CaMKII expression and activity are increased 2- to 3-fold in patients with heart failure due to dilated cardiomyopathy. Initially, it was hypothesized that upregulation and activation of CaMKII might represent a compensatory mechanism to keep diseased hearts from contractile failure (Hoch et al., 1999; Kirchhefer et al., 1999). However, several transgenic (TG) mouse models have established a role for CaMK in the development of cardiac hypertrophy.

Overexpression of CaMKII $\delta_B$ , which is highly concentrated in cardiomyocyte nuclei, causes transcriptional activation of atrial natriuretic factor gene expression (a hypertrophic signaling marker) in neonatal rat ventricular myocytes (Ramirez et al., 1997). Similarly, transgenic mice that overexpress CaMKII $\delta_B$  induce cardiac hypertrophy and mild ventricular dilation (Zhang et al., 2002). CaMKIV, which is physiologically expressed at very low levels in the heart (Maier and Bers, 2002; Zhang and Brown, 2004), was also shown to contribute to the development of cardiac hypertrophy upon its overexpression in transgenic mice (Passier et al., 2000). Pressure overload hypertrophy induced by transverse aortic constriction (TAC) surgery in mouse hearts results in a rapid increase of CaMKII expression and activity (Zhang et al., 2003; Saito et al., 2003). It was hypothesized that the nuclear isoform CaMKII $\delta_B$  serves as a compensatory mechanism by initiating hypertrophic gene expression, while the cytoplasmic isoform CaMKII $\delta_C$  serves as a compensatory mechanism by improving  $\text{Ca}^{2+}$  handling. At an early stage of hypertrophy, these changes could be beneficial to the maintenance of normal cardiac function. However, at later stages, when CaMKII $\delta_C$  expression is upregulated and alteration in  $\text{Ca}^{2+}$  handling are sustained, CaMKII might contribute to the downward spiral leading to heart failure. Overexpression of the cytoplasmic isoform CaMKII $\delta_C$  in mouse hearts clearly results in

severe contractile dysfunction and heart failure (Zhang et al., 2003; Maier et al., 2003) (Fig. 4). In these animals alterations in intracellular  $\text{Ca}^{2+}$  handling were observed with a marked reduction in  $\text{Ca}^{2+}$  transients, SR  $\text{Ca}^{2+}$  content, and SERCA2a, PLB, and RyR2 protein expression and enhanced NCX function and expression, all of which are widely accepted as indicative for heart failure. In contrast RyR2 phosphorylation increases in  $\text{CaMKII}\delta_{\text{C}}$  versus wild type mouse hearts and appears to be responsible for the development of increased SR  $\text{Ca}^{2+}$  spark frequency despite reduced SR  $\text{Ca}^{2+}$  load and diastolic  $\text{Ca}^{2+}$ , which by themselves would normally reduce SR  $\text{Ca}^{2+}$  leak (Fig.5). This increased RyR2 phosphorylation most likely results directly from  $\text{CaMKII}\delta_{\text{C}}$  overexpression, because  $\text{Ca}^{2+}$  spark frequency could be reduced back to normal levels by blocking CaMKII (Maier et al., 2003, Zhang et al., 2003).



**Figure 4. Cardiac pathology in  $\text{CaMKII}\delta_{\text{C}}$  TG mice.** Images of the whole hearts from WT and TG mice aged 6 and 13 weeks (from Zhang et al, 2003).

### 1.5 Involvement of CaMKII in cardiac arrhythmias

Cardiac arrhythmias are a leading cause of death in patients with heart failure. Arrhythmia mechanisms in cardiomyopathy involve cellular remodeling. Cellular studies reveal an action potential (AP) duration prolongation and an increased propensity for afterdepolarizations that are important mechanisms for triggering arrhythmias (Zeng and Rudy, 1995; Priebe and Beuckelmann, 1998). These triggers are due to the increased net inward current and could occur as early afterdepolarizations (EAD) or delayed afterdepolarizations (DAD). EAD are named so because they occur early relative to the completion of action potential repolarization. EAD occur during the action potential

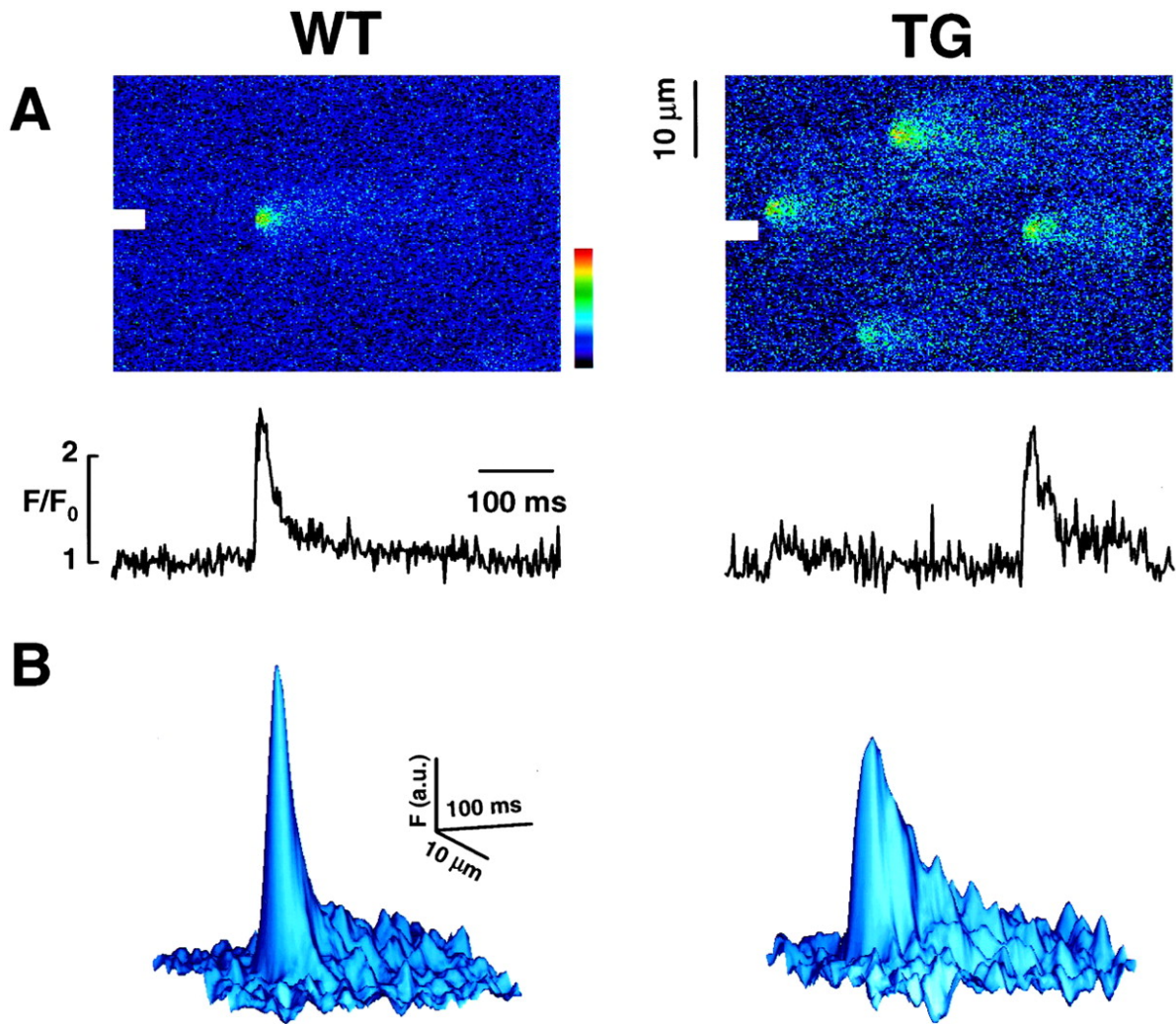


**Figure 5. Representative Ca<sup>2+</sup> sparks in CaMKII $\delta_C$  TG versus WT mice.** (A) Representative longitudinal line scan images, with line plots of Ca<sup>2+</sup> at sites indicated by white bars. (B) 3-D surface plot of signal averaged Ca<sup>2+</sup> sparks from the cells in A (from Maier et al., 2003).

plateau or phase II and III repolarization and are more likely during long action potential durations, long QT syndrome (LQTS), bradycardia, and are most often associated with repetitive L-type Ca<sup>2+</sup> channel openings (January and Riddle, 1989). EAD were suggested to initiate long QT- arrhythmias. Anderson and colleagues (Anderson et al., 1998) first reported that CaMKII is involved in the development of EAD and arrhythmias as a consequence of L-type Ca<sup>2+</sup> channel activation. They showed that EAD in isolated rabbit hearts were associated with an enhanced CaMK activity, and depended on the L-type Ca<sup>2+</sup> current. EAD can be suppressed by KN-93, the CaMKII inhibitor. Studies using rabbit ventricular myocytes demonstrated that L-type Ca<sup>2+</sup> current is augmented by a mechanism

involving the release of SR  $\text{Ca}^{2+}$  and the activation of CaMKII. The CaMKII inhibitory peptide AC3-I prevents afterdepolarizations and normalizes L-type  $\text{Ca}^{2+}$  channel opening (Wu et al, 1999). In another study, the same group developed a mouse model of cardiac hypertrophy using transgenic expression of CaMKIV. These mice show also a significantly increased CaMKII activity and expression as a side effect and suffer from increased arrhythmias, which could be increased by isoproterenol and decreased by KN-93 or a specific inhibiting peptide for CaMKII (AC3-I). CaMKIV TG mice showed also increased QT-intervals and prolonged action potential durations leading to EAD (Wu et al, 2002). In summary, these studies show that the increased CaMK activation is proarrhythmic during an action potential prolongation (Anderson et al., 1998; Wu et al, 1999, Wu et al, 2002).

Delayed afterdepolarizations owe their name to their occurrence after repolarization of the action potential to baseline. These afterdepolarization are widely accepted as being caused by spontaneous SR  $\text{Ca}^{2+}$  release events that occur during SR  $\text{Ca}^{2+}$  overload. This SR  $\text{Ca}^{2+}$  release causes a transient inward current that can alter the surface membrane potential and generate DAD. The latter in turn can lead to aftercontractions and triggered arrhythmias. CaMKII acts at key sites for  $\text{Ca}^{2+}$  homeostasis and increases L-type  $\text{Ca}^{2+}$  current as well as enhances the uptake and release of  $\text{Ca}^{2+}$  from the SR in ventricular myocytes. Thus, CaMKII activity could be important for the development of  $\text{Ca}^{2+}$  overload-dependent arrhythmias. Zhang and colleagues (Zhang et al., 2005) demonstrated a reduced sarcoplasmic reticulum  $\text{Ca}^{2+}$  content in a genetic mouse model of cardiac CaMKII inhibition (AC3-I) which results from diminished sarcoplasmic reticulum  $\text{Ca}^{2+}$  uptake, related to the reduced PLB phosphorylation by CaMKII. This reduction in sarcoplasmic reticulum  $\text{Ca}^{2+}$  content in AC3-I hearts was linked to a reduction in CaMKII activity rather than altered expression of sarcoplasmic reticulum proteins. Wu and colleagues (Wu et al., 1999) showed that elevated intracellular  $\text{Ca}^{2+}$  concentrations can activate transient inward current due to  $\text{Na}^+/\text{Ca}^{2+}$  exchanger activity in isolated ventricular rabbit myocytes and inhibition of CaMKII completely suppresses this transient inward current. These results show that CaMKII can enhance EAD as well as DAD and link these afterdepolarizations to arrhythmias.

However, not only heart failure can lead to arrhythmias. Rare genetic mutations in  $\text{Na}^+$  channels and RyR2 in patients with structurally normal hearts can increase the risk for arrhythmias and will be discussed below.



## 1.6 Cardiac voltage-gated Na<sup>+</sup> channels

### 1.6.1 The structure and function of Na<sup>+</sup> channels

Voltage-gated Na<sup>+</sup> channels are large membrane glycoproteins with a molecular mass of ~260 kDa. They are composed of a pore-forming  $\alpha$  subunit and auxiliary  $\beta$  subunits (Catterall 2000). The  $\alpha$  subunit is the major subunit of the channel essential for its function. Different isoforms of  $\alpha$  subunits of Na<sup>+</sup> channels have distinct distribution with the Nav1.5 (SCN5A) isoform being the predominant isoform in the heart (Fig 6). The auxiliary  $\beta$  subunits modulate channel gating, interact with extracellular matrix, and function as cell adhesion molecules (Isom et al., 1994; Isom, 2001). The cardiac  $\alpha$  subunit consists of four homologous domains (I-IV). Each domain has six transmembrane segments of 19-27 amino acids (S1-S6). The fourth transmembrane segment (S4) of each domain is highly

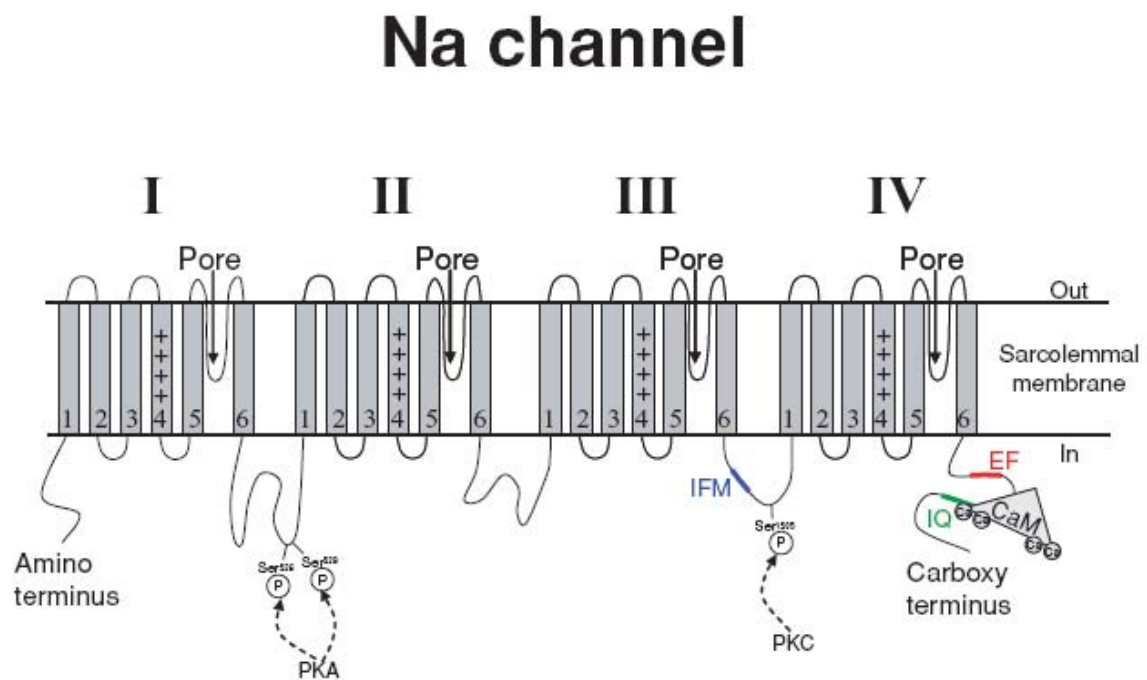


**Figure 6. Structure of cardiac Na<sup>+</sup> channel Nav1.5 (SCN5A).** The Na<sup>+</sup> channel has four domains (I-IV), each of which has six homologous repeating transmembrane regions (S1-S6) and a pore loop. Repetitive positively charged gating region in each S4 is indicated by ++++. Other noted sites are (1) PKA and PKC phosphorylation sites, (2) site possibly implicated in fast inactivation (inactivation gate; IFM), (3) IQ motif at the carboxy terminus, the putative site of Ca<sup>2+</sup>/CaM binding (from Wagner and Maier, 2006).

positively charged, with a number of conserved arginines or lysines located at each third position. These S4 regions span to move within the electric field in response to changes in membrane potential ( $E_m$ ): when the membrane becomes depolarized (outside negative), the voltage-sensing helices move toward the outer plasma membrane surface, causing an immediate conformational change in the gate segment that opens the channel for influx of  $\text{Na}^+$  ions. In each domain there is also a pore loop between S5 and S6 which dips back into the membrane and lines the pore. The pore segments determine the  $\text{Na}^+$  selectivity of the pore discriminating  $\text{Na}^+$  from  $\text{Ca}^{2+}$  ions (Bers, 2001). The central pore (through which the ions move) is formed by the four domains with the S5 and S6 transmembrane segments as putative pore center, which confer selectivity and conductance. The  $\text{NH}_2$ - and  $\text{COOH}$ -terminals and the interdomain connector are intracellular. Phosphorylation sites were found between I and II as well as between III and IV cytoplasmic interdomain loops. The cytoplasmic connecting segments between domains I and II and between II and III are long, and that between domains III and IV is much shorter (Fozzard and Hanck, 1996).

At resting membrane potentials, cardiac  $\text{Na}^+$  channels are in closed-available resting states. The sudden but short-lived depolarization of a region of the plasma membrane during an action potential is caused by a sudden massive, but transient, influx of  $\text{Na}^+$  ions through the opened voltage-gated  $\text{Na}^+$  channels in that region. The depolarization of the membrane changes the conformation of channel proteins, which then leads to the opening of the channels and allowing  $\text{Na}^+$  influx through them. Once opened, the channels stay open for about 1 ms, during which time about 6000  $\text{Na}^+$  ions pass through. Further  $\text{Na}^+$  influx is prevented by movement of the channel-inactivating segment into the channel opening. As long as the membrane remains depolarized, the channel is inactivated and cannot be reopened. This refractory period of  $\text{Na}^+$  channel is important in determining the unidirectionality of the action potential. A few milliseconds after the resting potential is reestablished, the channels return to the closed resting state and are available for a subsequent depolarization. Compared to the resting state of the channel, inactivation is a process by which the  $\text{Na}^+$  channel becomes unavailable for reopening until after membrane repolarization. Several types of  $\text{Na}^+$  current inactivation can be distinguished: (a) fast inactivation occurring over tens of milliseconds that recovers rapidly at negative membrane potentials; (b) intermediate inactivation accumulates after fast inactivation and occurs over hundreds of milliseconds recovering more slowly; (c) slow inactivation occurs in the range of tens of seconds (Bers, 2001). It has been proposed that the cytoplasmic linker connecting domain III and IV of  $\text{Na}^+$  channel acts as the inactivation gate (Stühmer

et al., 1989). The most important residues for inactivation in this cytoplasmic linker are a triplet of the consecutive amino acids IFM: isoleucine-phenylalanine-methionine. The interaction of the linker between domain III and IV with the carboxy terminus is required for stabilization of the closed gate (Motoike et al., 2004).

### ***1.6.2 Regulation of Na<sup>+</sup> channel by protein kinases***

The regulation of Na<sup>+</sup> channels by protein kinases is isoform-specific. Murphy and colleagues (Murphy et al., 1996) showed that the cardiac Na<sup>+</sup> channel  $\alpha$  subunit is phosphorylated by PKA at two sites in the I-II cytoplasmic linker (Ser-526 and Ser-529) in a cAMP-dependent manner. They also suggested that Ser-526 and Ser-529 play a role in the cAMP-dependent regulation of cardiac Na<sup>+</sup> channel activity. Upon phosphorylation by PKA, cardiac Na<sup>+</sup> channel gating remains unchanged, but whole-cell conductance increases (Frohnwieser et al., 1997). Single channel studies demonstrated that the resulting increase in whole-cell conductance was due to an increase in the number of functional Na<sup>+</sup> channels but neither due to increased single channel current amplitude nor altered mean opening or closing time (Lu et al., 1999). However,  $\beta$ -adrenergic modulation of the cardiac Na<sup>+</sup> channel seems to be more complex. It has been reported that  $\beta$ -adrenergic receptor modulation of cardiac Na<sup>+</sup> current involves two different G protein-dependent mechanisms, one via PKA and the other via a direct modulation of Na<sup>+</sup> current by G protein stimulatory  $\alpha$ -subunit (G $\alpha_s$ ), which is independent of second messengers (Lu et al., 1999). Other studies have revealed that the Na<sup>+</sup> current is decreased via stimulation of  $\beta$ -adrenergic receptors, and that the effect is secondary to the increased levels of intracellular cAMP, with acceleration of cAMP-dependent phosphorylation of the channel. This is in conflict with the hypothesis that PKA-dependent phosphorylation activates the Na<sup>+</sup> current. It was also shown that a cAMP-dependent shift of Na<sup>+</sup> inactivation curve in the hyperpolarizing direction, which is consistent with the reduced function (Ono et al., 1989). Ca<sup>2+</sup>-dependent protein kinase (PKC) phosphorylates a serine residue in the III-IV linker (Ser-1505) of the cardiac Na<sup>+</sup> channel  $\alpha$  subunit, and this phosphorylation reduces current through the cardiac Na<sup>+</sup> channels and is associated with a negative shift in the voltage dependence of channel inactivation, resulting in stronger inhibition of the current at more depolarized holding potentials (Qu et al., 1996). Furthermore, PKC-dependent phosphorylation of the cardiac Na<sup>+</sup> channel is partially responsible for the modulatory action of lysophosphatidylcholine that has been implicated in the arrhythmogenesis during ischemia (Watson and Gold, 1997).

### ***1.6.3 Na<sup>+</sup> channel involvement in arrhythmias***

Mutations in the cardiac voltage-gated Na<sup>+</sup> channel underlie several arrhythmogenic disorders: the long-QT syndrome 3 (LQT3, linked to chromosome 3) (Bennett et al., 1995), the Brugada syndrome (Wang et al., 2000) and isolated cardiac conduction defects predisposing to life-threatening ventricular tachyarrhythmias (VT). These disorders cause distinct molecular effects, but all herald an exceptional risk for sudden death due to life-threatening cardiac arrhythmias. Patients with the congenital long QT syndrome exhibit a delay in cardiac repolarization manifest as a prolonged QT interval in the electrocardiogram, increasing the risk of early and delayed afterdepolarizations. Mutations in long QT syndrome 3 alter amino acid residues in the inactivation gate and in the inactivation gate receptor region and thereby impair inactivation of Na<sup>+</sup> channels. The syndrome is associated with potentially lethal ventricular arrhythmias (Bennett et al., 1995).

Unlike the gain of function mutations leading to the long QT syndrome, loss of Na<sup>+</sup> channel function has been causally linked to the Brugada syndrome. Brugada syndrome is an arrhythmogenic syndrome electrocardiographically characterized by coved ST-segment elevations and negative T waves that reflect electrical forces in the right ventricle but is not associated with QT-interval prolongation (Brugada and Brugada, 1992). The syndrome is associated with life-threatening ventricular tachyarrhythmias. Several mechanisms as consequences of the underlying mutations have been shown to reduce the current through Na<sup>+</sup> channels including the expression of nonfunctional channels, a reduced rate of recovery from inactivation, a faster open-state inactivation, an enhanced intermediate or slow inactivation, and protein trafficking defects (Viswanathan and Balsler, 2004).

Isolated cardiac conduction disease is characterized in the electrocardiogram by a widening of the QRS complex consistent with the delayed ventricular excitation. The observed depolarizing shift of the Na<sup>+</sup> channel activation curve would reduce Na<sup>+</sup> channel current. The mutation results in bradycardia and causes syncope and sudden death. However, these mutations of the cardiac Na<sup>+</sup> channel are relatively rare. These arrhythmias are underlain more often by heart failure associated with an increased risk of sudden death mainly caused by VT and fibrillation and altered Na<sup>+</sup> channel function.

Beside the described mutations in cardiac Na<sup>+</sup> channel there are mutations in cardiac RyR2 which also can lead to arrhythmias.

## **1.7 Mutations in cardiac RyR2 gene as a cause for cardiac arrhythmias**

### ***1.7.1 RyR2 regulates cardiac contraction and rhythm***

Ca<sup>2+</sup> release from the sarcoplasmic reticulum mediated by the cardiac ryanodine receptor is a fundamental event in cardiac muscle contraction. The RyR2 is primarily involved in cardiac contractile function and is a key element in the control of cardiac output. RyR2 are large homotetrameric complexes that are organized into functional Ca<sup>2+</sup> release units via interaction with a multitude of accessory proteins, regulating the duration and amplitude of Ca<sup>2+</sup> efflux from the SR (Marx et al., 2001). The large central protein RyR2 interacts with multiple accessory proteins to form a macromolecular complex. These regulatory proteins are located in the intracytoplasmic region (junction, triadin and calsequestrin) or in the cytosolic portion of RyR2 (calmodulin, PKA, CaMKII, PKC, protein phosphatase 1, protein phosphatase 2A, calcineurin) (Meissner, 2002). Defective regulation of RyR2 that leads to abnormal cellular Ca<sup>2+</sup> handling has been implicated in heart failure, hypertrophy and arrhythmias (Marx et al., 2000; Wehrens et al., 2003; Jiang et al., 2002). RyR2 mutations suggested to cause defective Ca<sup>2+</sup> channel function have recently been identified in a disease termed catecholaminergic polymorphic ventricular tachycardia (CPVT).

### ***1.7.2 Catecholaminergic polymorphic ventricular tachycardia***

The clinical presentation of CPVT is similar to that of LQT3 and is characterized by the occurrence of syncopal episodes in patients triggered by physical exercise or psychological stress. CPVT is an inherited arrhythmogenic disorder characterized by adrenergically mediated bidirectional or polymorphic ventricular tachycardia. It is a main cause of syncope and sudden cardiac death in individuals with a structurally normal heart. CPVT is a highly malignant cardiac disease manifesting in childhood and adolescence (Leenhardt et al., 1995; Priori et al., 2002). The autosomal dominant form of CPVT is caused by mutation in the RyR2 gene encoding the cardiac isoform of the ryanodine receptor (Priori et al., 2001). The nature of CPVT would suggest that these mutations alter the normal physiological response of the channel to an increased catecholaminergic drive during exercise. Bidirectional ventricular tachycardia is a rare and unusual arrhythmia being the most distinguishing characteristics of CPVT patients. To date, more than 70 RyR2 mutations have been reported in the “Gene Connection for the Heart” database for inherited arrhythmogenic diseases. The first family in which a RyR2 mutation was identified was affected by a highly malignant form of the disease that was resistant to beta

blockers; the mutation present in the family (R4497C) is a hot spot that was subsequently identified in other CPVT patients unrelated to the first family members (Priori et al., 2002). Because this mutation was associated with a highly malignant phenotype it has been selected by several authors for their in vitro studies aimed at the functional characterization of RyR2 mutants. Cerrone and colleagues (Cerrone et al., 2005) have been the first developed a conditional knock-in mouse model carrier of the R4496C mutation (RyR2<sup>R4496C+/-</sup>) that is the mouse equivalent of the human mutation R4497C and demonstrated that the RyR2<sup>R4496C+/-</sup> mutation predisposes the murine heart to ventricular tachycardia and fibrillation in response caffeine and/or adrenergic stimulation, that closely mimics the clinical presentation of CPVT. Therefore, this knock-in mouse model is likely to become extremely useful to investigate RyR2-related arrhythmogenesis and the pathophysiology of CPVT.

Inherited genetic diseases have proven to be powerful models for studying complex syndromes. Hence it has been reasoned that inherited VT may provide an alternative approach to understanding VT in heart failure.

## 1.8 Aim of study

Increased CaMKII activity has been linked to heart failure and ventricular arrhythmias. The latter can be caused by an altered Na<sup>+</sup> channel function. Therefore there might be a link between CaMKII and Na<sup>+</sup> channel function. Considering these, the aim of this study was to investigate:

1. whether CaMKII $\delta_C$  associates with Na<sup>+</sup> channels in isolated ventricular rabbit myocytes and mouse heart tissue;
2. whether this association results in Na<sup>+</sup> channel phosphorylation.

The R4496C mutation in cardiac RyR2 does not produce a phenotype under basal conditions (Cerrone et al., 2005). However, it remains unknown so far whether there are changes on the cellular level and whether it might become relevant under pathophysiological conditions. Therefore this study has aimed to investigate also:

1. intracellular Ca<sup>2+</sup> handling in myocytes isolated from RyR2<sup>R4496C/+</sup> knock-in mice;
2. possible alterations of E-C coupling and arrhythmogenic effects due to overexpression of CaMKII $\delta_C$  in mouse hearts carrying the R4496C mutation in cardiac RyR2.

## 2 Materials

### 2.1 Animals

Female Chinchilla bastard rabbits (with body weight of 1.5-2 kg) obtained from Charles River Laboratories (Sulzfeld) were used.

CaMKII $\delta_C$  transgenic mice (Black Swiss), 3-month-old having a 3-fold increase in CaMKII activity and compared to their age- and sex-matched wild-type (WT) littermates were provided by Dr. Tong Zhang and Dr. Joan Heller Brown (USA). Knock-in mice (C57BL/6) harboring the R4496C mutation (RyR2<sup>R4496C+/-</sup>) were provided by Dr. Silvia G. Priori (Molecular Cardiology, Fondazione Salvatore Maugeri, Pavia, Italy). CaMKII $\delta_C$ /RyR2<sup>R4496C</sup> mice were generated by crossbreeding RyR2<sup>R4496C+/-</sup> mice with CaMKII $\delta_C$  transgenic mice. CaMKII $\delta_C$ , RyR<sup>R4496C+/-</sup>, CaMKII $\delta_C$ /RyR2<sup>R4496C</sup> mice and respective WT controls, 8-14 weeks old, of either sex were used. All animals received humane care in accordance with the institution's guidelines, the German Convention for Protection of Animals and the National Institutes' of Health guidelines.

### 2.2 Adenovirus constructs

For the overexpression experiments the following adenoviral constructs were used:

- recombinant adenoviral vector encoding for hemagglutinin-tagged (HA-tagged) CaMKII (Ad-CaMKII $\delta_C$ ) that was kindly provided by T. Zhang (Kohlhaas et al., 2006; Zhu et al., 2003);
- recombinant adenovirus encoding for  $\beta$ -galactosidase (Ad-LacZ) which was generated in our laboratory and used before (Kohlhaas et al., 2006).

### 2.3 Oligonucleotides for polymerase chain reaction

Oligonucleotides of HPLC grade purity for polymerase chain reaction were obtained from MWG-Biotech (Munich):

PCR-primer	Gene	Size of amplified DNA-fragment, bp
Forward: 5'-TTGAAGGGTGCCATCTTGACA-3'	Mouse-CaMKII $\delta_C$	1000



Reverse: 5'-GGTCATGCATGCCTGGAATC-3'		
Forward: 5'-GCCTTCGCCATCAATTCATCC-3'	Mouse-RyR2	800,1000
Reverse: 5'-CACTTTAGCAGTATCGCTGGAG-3'		

## 2.4 Antibodies

### Anti-Calsequestrin Ab (PA1-913)

For the detection of calsequestrin using immunoblotting, affinity purified rabbit polyclonal antibody raised against purified canine cardiac calsequestrin was used (Affinity Bioreagents). Species reactivity: PA1-913 detects cardiac and skeletal muscle calsequestrin from canine, human, mouse, rabbit, rat, and sheep tissues.

### Anti-CaMKII Ab (M-176)

For immunoprecipitation of CaMKII, rabbit polyclonal antibody raised against the recombinant protein corresponding to the amino acids 303-478 mapping at carboxy terminus of protein kinase II (CaMKII $\alpha$ ) of mouse origin was used (Santa Cruze Biotechnology, Inc.). Species reactivity: mouse, rat, human origin.

### Anti-GAPDH Ab (clone 6G5)

For detection of GAPDH using immunoblotting, mouse monoclonal antibody (clone 6G5) was used (Biotrend Chemikalien GmbH). Species cross-reactivity: chicken, mouse, human, fish.

### Anti-HA Ab (clone 12CA5)

For the detection of HA-tagged CaMKII $\delta_C$  isoform using coimmunocytochemical staining, mouse monoclonal antibody (clone 12CA5) raised against peptide sequence derived from the human-influenza hemagglutinin protein was used (Roche Applied Science).

### Anti-Na<sup>+</sup>/Ca<sup>2+</sup>-exchanger Ab (R3F1)

For detection of  $\text{Na}^+/\text{Ca}^{2+}$ -exchanger using immunoblotting, mouse monoclonal antibody raised against the canine  $\text{Na}^+/\text{Ca}^{2+}$ -exchanger was used (Swant, Switzerland). Species reactivity: monkey, horse, dog, rat, bovine and mouse tissue.

Anti- $\text{Na}_v1.5$  Ab (SKM2, SCN5A)

For the detection of cardiac voltage-gated  $\text{Na}^+$  channel using immunoblotting and co-immunocytochemical staining, rabbit polyclonal antibody raised against the peptide corresponding to the residues 493-511 of rH1 was used after affinity purification via immobilized antigen column (Alomone Labs Ltd, Israel). Species reactivity: rat.

Anti-Pan  $\text{Na}_v$  Ab (SP19, Pan  $\text{Na}^+$  Channel)

For the detection of voltage-gated  $\text{Na}^+$  channel using immunoblotting and immunoprecipitation, rabbit polyclonal antibody raised against the purified peptide corresponding to the residues 1500-1518 of rat  $\text{Na}_v1.1$  and affinity purified on immobilized antigen was used (Alomone Labs Ltd, Israel). Species reactivity: rat, mouse.

Anti-Phospholamban Ab (clone A1)

For the detection of phosphorylated and non-phosphorylated forms of phospholamban using immunoblotting, mouse monoclonal antibody raised against bovine phospholamban purified from bovine cardiac sarcoplasmic reticulum was used (Upstate). Species cross-reactivity: canine, bovine, rat, mouse and porcine.

Anti-SERCA2 ATPase Ab (MA3-919)

For the detection of sarcoplasmic reticulum calcium 2 ATPase using immunoblotting, mouse monoclonal antibody raised against purified canine cardiac sarcoplasmic reticulum vesicles was used (Affinity Bioreagents). Species reactivity: human, mouse, rabbit, rat.

Secondary Ab (horse radish peroxidase conjugated):

donkey anti-rabbit whole IgG, Amersham/Freiburg;  
sheep anti-mouse whole IgG, Amersham/Freiburg.

Secondary Ab (dye conjugated):

goat anti-mouse Texas Red-conjugated affinity purified IgG, Jackson ImmunoResearch Laboratories, Inc.;

goat anti-rabbit Fluorescein-conjugated affinity purified IgG, Jackson ImmunoResearch Laboratories, Inc.;

goat anti-rabbit Alexa Fluor 488 IgG, Molecular Probes, Inc.;

goat anti-mouse Alexa Fluor 555 IgG, Molecular Probes, Inc.

## 2.5 Enzymes and nucleotides

CaMKII BioLabs/New England

dNTP Invitrogen/USA

GoTaq® *DNA* polymerase Promega/Mannheim

Liberase Blendzyme 1 Roche/Mannheim

Trypsin, 2,5% liquid Gibco/Invitrogen

## 2.6 Detection, purification and synthesis systems (kits)

BCA Protein Assay, Pierce/Bonn

DNeasy® Blood & Tissue Kit (50), Qiagen GmbH/Hilden

SuperSignal® West Pico Chemiluminescent Substrate, Pierce/Bonn

## 2.7 Inhibitors

Autocamtide 2-related inhibitory peptide (AIP), Sigma /Munich

KN-93, Seikagaku Corporation/Japan

Okadaic acid, Calbiochem/Merck

PKA/PKC inhibitor cocktail, Upstate/USA

Protein kinase A inhibitor, Sigma/Munich

Protease inhibitor cocktail tablets, EDTA-free, Roche/Mannheim

## 2.8 Stock solutions

The stock solutions were prepared using ddH<sub>2</sub>O, the pH values were adjusted at room temperature.

### APS 10%

	For 10 ml	Final concentration
APS	1 g	10%

The solution was dispensed into 100 µl aliquots and stored at -20°C.

### CHAPS stock

	For 100 ml	Final concentration
CHAPS	10 g	10%
ddH <sub>2</sub> O	to 100 ml	

The solution was stored at room temperature.

### DTT stock

	For 3 ml	Final concentration
DTT	46.3 mg	0.1 M
ddH <sub>2</sub> O	to 3 ml	

The solution was dispensed into 100 µl aliquots and stored at -20°C

### EGTA 100 mM

	For 100 ml	Final concentration
EGTA	3.804 g	100 mM

pH was adjusted with KOH to 8.0. The solution was stored at 4°C.

### HEPES 100 mM

	For 1 l	Final concentration
HEPES	23.8 g	100 mM

pH was adjusted with KOH to 7. The solution was stored at 4°C.

Magnesium chloride 1 M

	For 100 ml	Final concentration
MgCl <sub>2</sub> ×6H <sub>2</sub> O	20.33 g	1 M

The solution was stored at 4°C.

PBS 10X

	For 1 l	Final concentration
NaCl	81.82 g	1.4 M
KCl	2 g	27 mM
Na <sub>2</sub> HPO <sub>4</sub>	14.2 g	100 mM
KH <sub>2</sub> PO <sub>4</sub>	2.45 g	18 mM

pH was adjusted with HCl to 7.3. The solution was sterile filtered and stored at room temperature.

Potassium aspartate 2 M

	For 100 ml	Final concentration
C <sub>4</sub> H <sub>6</sub> NO <sub>4</sub> K	34.2 g	2 M

The solution was sterile filtered and stored at room temperature.

SDS 10%

	For 100 ml	Final concentration
SDS	10 g	10%

In the case of precipitation of SDS, the solution was warmed until clear.

Sodium chloride 4 M

	For 1 l	Final concentration
NaCl	233.76 g	4 M

The solution was sterile filtered and stored at room temperature.

Sodium fluoride 200 mM

	For 100 ml	Final concentration
NaF	0.84 g	200 mM

The solution was stored in the dark at 4°C.

Sodium orthovanadate 100 mM

	For 100 ml	Final concentration
Na <sub>3</sub> VO <sub>4</sub>	1.84 g	100 mM

Titration of the solution with HCl and sequential heating were repeated several times to adjust pH to 10.0. The solution was stored in the dark at 4°C.

Tris-HCl 2 M

	For 1 l	Final concentration
Tris-HCl	315.2 g	2 M

pH value was adjusted to pH 7.4. The solutions were sterile filtered and stored at 4°C.

## 2.9 Chemicals

All chemicals used were at least p. a. quality.

Invitrogen/Karlsruhe

agarose

250 bp DNA ladder

Kodak/Paris, France

Developer

Merck/Darmstadt

All usual laboratory chemicals, glucose, ethanol, methanol, HPLC grade water, β-propanol, TEMED, disodium hydrogen phosphate-dihydrate (Na<sub>2</sub>HPO<sub>4</sub>·2H<sub>2</sub>O), potassium dihydrogen phosphate (KH<sub>2</sub>PO<sub>4</sub>), magnesium chloride

## Roth/Karlsruhe

Rotiphorese Gel 30 (30% acrylamide stock solution with 0.8% bisacrylamide in proportion 37.5:1), glycine, D-glucose, milk powder

## Sigma/Munich

All usual laboratory chemicals, adenosine triphosphate (disodium salt), ammonium hydrocarbonate, avertin, DTT, calcium chloride solution, creatine phosphokinase, ethidium bromide, L-glutathione reduced, glycerol,  $\beta$ -glycerophosphate, HEPES, medium M199,  $\beta$ -mercaptoethanol, paraformaldehyde, phosphocreatine, Ponceau S (ready to use solution), saponin, sodium fluoride, sodium orthovanadate, potassium chloride, potassium bicarbonate, sodium bicarbonate, sodium chloride, magnesium sulfate heptahydrate ( $\text{MgSO}_4 \cdot 7\text{H}_2\text{O}$ ), phenol red sodium salt, taurine, 2,3-butanedione monoxime (BDM), caffeine, pluronic F-127, DMSO

## Tetanal photowerk/Germany

Fixer solution

## 2.10 Detergents

CHAPS	Roche/Mannheim
SDS	BioRad/Munich
Triton X-100	Sigma/ Munich
Tween 20	BioRad Munich

## 2.11 Proteins and protein standards

BCS (bovine calf serum)	HyClone/USA
BSA-V (bovine serum Albumine fraction V)	Sigma/Munich
Bromphenol blue, precision plus protein <sup>TM</sup> standards	BioRad/Munich
Calmodulin (CaM)	Upstate/USA
Laminin	Sigma/Munich
Protein G-sepharose FF	Amersham/Freiburg

## 2.12 Fluorescent dyes

Fluo-3 AM, Molecular Probes/USA

Fluo-4 AM, Molecular Probes/USA

Fura-2 AM, Sigma/Munich

## 2.13 Other materials

Chamber Slide, 4 well glass slide, Nunc/USA

Culture dishes (35 and 100 mm), serological pipettes (2, 5, 10, 25 ml), transfer pipettes, Sarstedt/Germany

Nitrocellulose Transfer Membrane, 0.45  $\mu\text{m}$ , PROTRAN<sup>®</sup>, Whatman 3MM paper, Schleicher and Schuell/Dassel

Pipette tips, Brand/Wertheim

Sterile filter pipette tips, Biozym/Oldendorf

Sterile filter, 0.2  $\mu\text{m}$ , Centricon<sup>®</sup> concentrators (MWCO 30000 and 100000 Da), Millipore/Eschborn

Safe-Lock tubes (0.2, 0.5, 1.5 and 2 ml), Eppendorf/Hamburg

X-ray films, Fuji/Düsseldorf

## 2.14 Instruments

Automatic pipettes, type Reference<sup>®</sup>, Eppendorf/Hamburg

Automatic pipettes, type PreCision, Biozym/Oldendorf

Automatic pipettes, type Pipetman, Gilson/Bad Camberg



## Centrifuges:

Eppendorf bench-top centrifuge, type MiniSpin 5415R Eppendorf centrifuge 5810R	Eppendorf/Hamburg
Laborcentrifuge 3 K12	Sigma/Munich
Megafuge 2.0R	Heraeus Instruments/Hanau

Easy-Cast™ Electrophoresis system for DNA electrophoresis, model #B1, peqlab/Erlangen

Electrophoresis apparatus, type Mini-Protean® 3, BioRad/Munich

Electroblotting apparatus, type Mini Trans-Blot®, BioRad/Munich

End-over-end rotator, Heto Lab Equipment/Denmark

Eppendorf BioPhotometer, Eppendorf/Hamburg

Gas controlled incubators “Function Line”, Heraeus/Hanau

Homogenizer Micra D-1, DS-5/K1 ART-Labortechnik/Germany

Ice machine, Ziegra/Isernhagen

Laser scanning confocal microscope LSM 5 Pascal, Zeiss/Germany

Magnetic mixer with warming, type M21/1 Framo-Gerätetechnik/Germany

Microscope, Nikon Eclipse TE300/Japan

Microwave oven, Siemens/Germany

MultiImage Light Cabinet with built-in ultraviolet emitter and video camera, Alpha Innotech Corporation. The instrument is used for documentation of X-ray films and gels

Optical setup, IonWizard/Netherlands

pH-Meter Basic Meter PB-20 Sartorius/Göttingen

Plate reader KC4, BIO-TEK<sup>®</sup> Instruments, inc./USA

PowerPac<sup>™</sup> universal power supply, BioRad/Munich

Shaker Duomax 1030 Heidolph/Germany

Sterile bench, class II, Clean Air/Hilden

Thermocycler, type Mastercycler<sup>®</sup> gradient, Eppendorf/Hamburg

Thermomixer 5436, Eppendorf/Hamburg

UV/Visible spectrophotometer, Ultrospec 3000, Amersham Biosciences/Freiburg

Ultraviolet emitter, 312 nm, Bachofer/Reutlingen

Vortex, Genie 2<sup>™</sup>, Bender and Hobein AG/Zurich

Water bath 1083, GFL/Burgwedel

X-ray film cassettes 10×18, Siemens/Germany

## 3 Methods

### 3.1 Polymerase chain reaction (PCR)

The mice used in the experiments originate from two mouse lines with different genetic backgrounds (Black Swiss and C57BL/6). The former mouse line overexpressed cytoplasmic CaMKII $\delta_C$  in the heart, the latter mouse line was the carrier of the R4496C mutation in the heart. The DNA from the pieces of mouse ears was isolated and the genotype was verified using polymerase chain reaction (PCR). PCR allows amplification of DNA fragments due to repetitive cycles of DNA synthesis.

The DNA from the mouse ear punch was purified using DNeasy Tissue Kit from Qiagen. For this, the ear punch tissue from each mouse was placed into 1.5 ml tube containing 180  $\mu$ l of ATL buffer supplemented with 20  $\mu$ l of proteinase K. The samples were incubated in the thermomixer at 55°C with shaking for 15 sec after every 1 min of the rest until the tissue was completely lysed. The samples were subsequently vortexed for 15 sec and 400  $\mu$ l of buffer AL-ethanol mixture was added and mixed vigorously by vortexing to yield a homogeneous solution. The mixture was pipetted into the DNeasy spin column placed in a new 2 ml collection tube and centrifuged at 6000 x g for 1 min. The DNeasy spin column was placed in a new 2 ml collection tube and loaded with 500  $\mu$ l of AW1 buffer. The column was centrifuged for 1 min at 6000 x g. The DNeasy spin column was again placed in a new 2 ml collection tube, washed with 500  $\mu$ l of AW1 buffer and centrifuged for 3 min at full speed to dry the DNeasy membrane. Flow-through and collection tube were discarded after every centrifugation step. The DNeasy spin column was placed in a clean 1.5 ml tube, 100  $\mu$ l of AE buffer were pipetted directly onto the DNeasy membrane and incubated at room temperature for 1 min. After this the sample was eluted from the membrane by centrifugation for 1 min at 6000 x g. The DNA concentration in the samples was measured using Eppendorf BioPhotometer.

The PCR reaction was performed with CaMKII $\delta_C$ - and RyR2-specific primers. The PCR lasted for 35 cycles in the case of CaMKII $\delta_C$  and 34 cycles in the case of RyR2 under the following conditions:

1. 5 min denaturation at 94°C
2. 1 min annealing at 60°C or 30 seconds at 55°C for CaMKII $\delta_C$  or RyR2, respectively
3. 2 min or 90 seconds DNA synthesis at 72°C for CaMKII $\delta_C$  or RyR2, respectively

The denaturation step at 95°C before the first cycle was extended for 5 minutes. After the last cycle, the synthesis step was prolonged for 7 minutes to finish synthesis of incompletely synthesized DNA strands.

The PCR was performed with the GoTaq® DNA polymerase (Promega). The specific buffers and solutions were received with the polymerase. dNTP master mix from Invitrogen was used.

PCR reaction mixture:

5 µl 10X PCR buffer (500 mM Tris-HCl pH 9.1, 140 mM (NH<sub>4</sub>)<sub>2</sub>SO<sub>4</sub>)

3 µl MgCl<sub>2</sub> (25 mM)

1 µl 100 mM dNTP mix (25 mM of each dATP, dCTP, dGTP, dTTP)

2 µl template (cDNA) obtained as described above

1 µl forward primer

1 µl reverse primer

0.4 µl Taq polymerase

36.6 µl volume was adjusted with sterile DEPC ddH<sub>2</sub>O

To check the size of the PCR product, a 7 µl aliquot of the PCR reaction was electrophoretically analyzed in a 1% agarose gel.

### ***3.1.1 Electrophoresis conditions***

For preparation of a 1% gel, 0.8 g of agarose was dissolved by heating in 40 ml of 1X TBE buffer. For visualization of the bands, 1.6 µl of ethidium bromide (Invitrogen) was added to the mixture. After mixing, the gel was poured into the prepared gel tray. In the mean time of the polymerization, the samples were prepared for loading by mixing of 7 µl of DNA probe with 3.5 µl of 5X loading buffer.

After polymerization, the gel was placed into an electrophoresis chamber filled with 1X TBE buffer, the samples were loaded, and the electrophoresis was performed at 100 V for 60 min.

### ***3.1.2 Visualization of DNA in the gel***

Ethidium bromide is a fluorescent dye which contains a planar group that intercalates between the stacked bases of the DNA. The fixed position of this group and its close proximity to the bases cause dye, bound to DNA, to display an increased fluorescence

yield compared to that of the dye in free solution. Ultraviolet radiation at 254 nm is absorbed by the DNA and transmitted to the dye; radiation at 302 nm and 366 nm is absorbed by the bound dye itself. In both cases, the energy is reemitted at 590 nm in the red orange region of the visible spectrum. Hence, DNA can be visualized under a UV transilluminator. The gel was photographed using a video camera built in the MultiImage Light Cabinet.

### 10X TBE

	For 1 l	Final concentration
Tris base	54 g	450 mM
Borate	27.5 g	450 mM
EDTA	4.15 g	10 mM

### 1X TBE

	For 1 l
10X TBE	100 ml
ddH <sub>2</sub> O	to 1 l

### 5X loading buffer

	For 10 ml	Final concentration
Bromphenol Blue	20 mg	0.2%
Glycerol	5 ml	50%
5X TBE	1 ml	0.5X

The buffer was stored at 4°C.

## **3.2 Adenoviral transfection and culture of adult rabbit ventricular cardiomyocytes**

Ventricular cardiomyocytes were isolated from rabbit hearts using the well established standard protocol (Animal experiment announcement T 9.02, “Killing of animals for scientific purposes” submitted by Dr. med. Harald Kögler) that was kindly provided by the group of Prof. Dr. med. Hasenfuß (Schillinger et al., 2000; Wagner et al., 2003).

### 3.2.1 Preparation of laminin culture dishes

Prior to plating the cells, culture dishes (100 mm) were covered with M 199/laminin mixture (3 ml/30  $\mu$ l) to provide better attachment of the cells to the bottom and incubated at 37°C for 1 h before use.

For transfection of cardiomyocytes, adenovirus-mediated gene transfer was used. The replication of DNA-containing adenoviruses occurs epichromosomally, which makes them a system of choice to study gene expression in primary non-replicative cells, which the cardiomyocytes are. The recombinant adenoviruses coding for HA-tagged CaMKII $\delta_C$  and  $\beta$ -galactosidase as control were amplified in our laboratory.

The cells were transfected immediately after preparation directly in the suspension ( $5 \times 10^5$  cells per dish in the 5 ml of M199) and plated on laminin-coated culture dishes. After the attachment phase of 3 hours, the medium was replaced with fresh M199 (10 ml per dish) and the cells were cultured for 24 hours. The incubation of the cardiomyocytes was performed in a gas-controlled incubator in water vapor saturated air containing 5% CO<sub>2</sub> at 37°C.

### 3.2.2 Calculation of virus quantity taken for transfection

The amount of virus taken for experiments is expressed as a multiplicity of infection (MOI), which is the number of active viral particles per cell. MOI of used viruses was calculated based on the virus concentration estimated in plaque test assays and measured in plaque forming units per ml (pfu/ml). The amount of virus corresponding to MOI 100 was used in experiments of transgene overexpression.

For the calculation of the amount of virus corresponding to the desired MOI, the following formula was used:

$$V_{stock} = \frac{MOI \times a_{ct}}{C_{stock}}, \text{ where}$$

$a_{ct}$  – total amount of cells to be infected with the virus

$V_{stock}$  – volume of virus stock to be added

$C_{stock}$  – concentration of virus in pfu/ $\mu$ l

### 3.3 Total protein homogenate preparation

#### 3.3.1 Protein lysate preparation from rabbit ventricular cardiomyocytes

All steps were performed at 4°C to prevent proteolytic degradation of the proteins. The cells, harvested and pelleted as described above (see section 3.2), were homogenized in 300 µl of lysis buffer. For better solubilization of the proteins, the samples were kept on ice for 20 minutes with occasional vortexing. Obtained primary lysates were passed through a 21 G needle 5 times. To pellet the nuclei and cell debris, crude homogenates were centrifuged for 8 minutes at 3000x g (4°C). The protein concentration of supernatants was determined by the BCA method using the kit from Pierce (Pierce Chemical Co). The samples were used as a starting material for immunoprecipitation and co-immunoprecipitation experiments. For Western blot measurements, aliquots of the prepared lysates corresponding to 25 µg of total protein were denatured in sample buffer containing 2% β-mercaptoethanol by warming at 37°C for 30 minutes and subjected to SDS-polyacrylamide gel electrophoresis (SDS-PAGE).

#### Lysis buffer

	For 10 ml	Final concentration
2 M Tris-HCl, pH 7.4	100 µl	20 mM
4 M NaCl	500 µl	200 mM
200 mM NaF	1 ml	20 mM
100 mM Na <sub>3</sub> VO <sub>4</sub>	100 µl	1 mM
100 mM DTT	100 µl	1 mM
10% CHAPS	200 µl	2 %
ddH <sub>2</sub> O	to 10 ml	

Prior to use the complete protease inhibitor cocktail (Roche) was added.

#### 5X sample buffer

	For 20 ml	Final concentration
Tris-HCl	0.79 g	250 mM
SDS	2 g	10%
Glycerol	10 ml	50 %

The components were dissolved in ddH<sub>2</sub>O (up to 18 ml), pH was adjusted with HCl to 6.8 and finally the following components were added:

	For 20 ml	Final concentration
Bromphenol Blue	5 mg	250 µg/ml
β-mercaptoethanol	2 ml	10%

The solution was aliquoted and stored at -20°C. Protein samples were mixed with the sample buffer in the proportion of 4:1, respectively.

### ***3.3.2 Protein homogenate preparation from mouse heart tissue***

All steps of the procedure were performed at 4°C to prevent proteolytic degradation of the proteins. The whole mouse heart was immersed in homogenization buffer, trimmed of fat and connective tissue and minced with scissors to pieces as small as possible. Minced tissue was homogenized in 1 volume of homogenization buffer using homogenizer Micra D-1, DS-5/K1 ART-(Labortechnik) at maximum speed 4 times for 5 seconds each time. The homogenate was centrifuged for 10 minutes at 3000x g to pellet the nuclei and particular matter. The supernatant from this centrifugation was removed in a fresh safe-lock tube and the pellet was re-homogenized by hand homogenization (8 strokes) in 1.5 safe-lock tube with a tightly fitted teflon pestle in initial volume of homogenization buffer. Afterwards, the suspension was kept on ice for better solubilization of the proteins for 30 minutes with following centrifugation as describe above. The supernatants from 2 centrifugation steps were pooled and the protein concentration was determined by the BCA method using the kit from Pierce. This supernatant was used as a starting material for immunoprecipitation and co-immunoprecipitation experiments. For Western blot aliquots of the prepared homogenate were denatured in sample buffer containing 2% β-mercaptoethanol by warming at 37°C for 30 minutes and 50 µg of total protein was subjected to SDS-polyacrylamide gel electrophoresis (SDS-PAGE).

#### Homogenization buffer

	For 10 ml	Final concentration
2 M Tris-HCl, pH 7.4	100 µl	20 mM
4 M NaCl	500 µl	200 mM
200 mM NaF	1 ml	20 mM
100 mM Na <sub>3</sub> VO <sub>4</sub>	100 µl	1 mM



100 mM DTT	100 $\mu$ l	1 mM
Triton X-100	100 $\mu$ l	1 %
ddH <sub>2</sub> O	to 10 ml	

Prior to use the complete protease inhibitor cocktail (Roche) was added.

### 3.4 Co-immunoprecipitation

#### 3.4.1 Formation of the antigen-antibody complex

Cardiac homogenates (1 mg of protein in each sample), prepared from TG CaMKII $\delta_C$  and WT mouse hearts as described in 3.3.2, or lysates (0.5 mg of protein in each sample), prepared from rabbit ventricular myocytes transfected with CaMKII $\delta_C$  and LacZ using a MOI of 100 as described in 3.3.1, were suspended in dilution medium to bring the volume of each sample up to 500  $\mu$ l. The samples were kept on ice for 30 minutes with occasional vortexing. 3  $\mu$ g of rabbit polyclonal anti-CaMKII antibody (M-176, Santa Cruz Biotechnology Inc.) were added to the samples. Samples were incubated using an end-over-end rotator set at low speed at 4°C overnight. Rabbit polyclonal anti-Cav1.2a antibody (Alomone Labs) added to one sample at a quantity of 3  $\mu$ g served as a control antibody. One sample was incubated with protein G-sepharose beads only.

#### 3.4.2 Precipitation of immune complexes

Protein G-sepharose Fast Flow (Amersham Biosciences) was prepared as follows: per each ml of bed volume, 1.33 ml of 75% slurry in 20% ethanol is needed; based on this ratio, a sufficient amount of 75% slurry was transferred to a 15 ml tube and the matrix was sedimented by centrifugation at 500x  $g_{max}$  for 5 minutes. The supernatant was carefully aspirated with a pipette. Next, protein G-sepharose was washed with 10 bed volumes of dilution medium and sedimented as described above. The supernatant was discarded and for each 1.33 ml of the original slurry of protein G-sepharose 1 ml of dilution media was added. This procedure produced 50% slurry. 100  $\mu$ l of this slurry was added to each sample with preformed antigen-antibody complexes. The mixture was gently mixed for 2 hours at 4°C using an end-over-end rotator set at low speed. After the end of the incubation time, the matrix was sedimented by centrifugation for 30 seconds at 14000x  $g$  in Eppendorf

bench-top MiniSpin centrifuge. The supernatants were discarded with a 29 G cannula connected to a syringe and the pellets were washed 3 times with 500  $\mu$ l (for cardiac homogenates) and 250  $\mu$ l (for cell lysates) of RIPA buffer. The tubes were inverted carefully 5 times to mix. After each washing step, the immunoprecipitates were recovered by centrifugation as described above.

### 3.4.3 Analysis

The immunoprecipitated proteins were eluted in 60  $\mu$ l (for cardiac homogenates) and in 40  $\mu$ l (for cell lysates) of 2X sampler buffer, warmed at 37°C for 30 minutes and centrifuged for 2 minutes at 14000x g. The supernatants were carefully transferred into a fresh safe-lock tube and analyzed by immunoblotting.

#### Dilution medium (prepared just prior to use)

		Final concentration
Modified RIPA buffer	5 ml	
200 mM NaF	25 $\mu$ l	1 mM
100 mM Na <sub>3</sub> VO <sub>4</sub>	50 $\mu$ l	1 mM
100 mM DTT	50 $\mu$ l	1 mM

The complete protease inhibitor cocktail (Roche) were added

#### Modified RIPA buffer

	For 50 ml	Final concentration
2 M Tris-HCl, pH 7.4	1.25 ml	50 mM
4 M NaCl	1.93 ml	154 mM
Triton X-100	125 $\mu$ l	0.25%
ddH <sub>2</sub> O	to 50 ml	

#### 2X sample buffer

	For 20 ml	Final concentration
Tris-HCl	0.32 g	100 mM
SDS	0.8 g	4%
Glycerol	4 ml	20%

The components were dissolved in ddH<sub>2</sub>O (up to 19.2 ml), pH was adjusted with HCl to 6.8 and finally the following components were added:

	For 20 ml	Final concentration
Bromphenol Blue	2 mg	100 µg/ml
β-Mercaptoethanol	0.8 ml	4 %

Solution was aliquoted and stored at -20°C.

### 3.5 Immunoblotting

Samples for loading, obtained as described in the previous chapters, were mixed with sample buffer and warmed for 30 minutes at 37°C.

#### 3.5.1 Casting of SDS-polyacrylamide gel

For hand casting of the gels for vertical electrophoresis, a Mini-PROTEAN™ III Electrophoresis Cell (BioRad) was used. Solutions for the separating gels of the desired percentage and for the 5% stacking gel were prepared as described below. The casting of the gels was performed according to manufacturer's instructions.

The separation gel (7.5 ml for 1.5 mm gel thickness) was poured between the inner (7.3×10.2 cm) and outer (8.3×10.2 cm) glass plates. The gel was carefully overlaid with 2-propanol to create a barrier to oxygen, which inhibits the polymerization. After the gel has set (about 20 min at RT), the overlay was poured off and the top of the separating gel was washed with distilled water. The solution of stacking gel was poured directly onto the polymerized separating gel. The slots were formed by placing an appropriate comb into the gel solution. The polymerization took approximately 10 min.

#### 3.5.2 SDS-polyacrylamide gel electrophoresis (SDS-PAGE) and electrophoretic transfer

The samples were loaded onto the bottom of the wells. Electrophoresis was run at a constant current of 30 mA per gel. The Dual Color protein marker (Bio-Rad) was used as molecular weight standards. Western blotting was carried out by electrophoretic transfer essentially as described by Towbin (Towbin et al., 1979). Prior to stopping the gel running,

fiber pads, filter paper and nitrocellulose transfer membrane (0.45  $\mu\text{m}$  pore size) were soaked in transfer buffer. After electrophoresis, the gel was plated apart and immersed in transfer buffer. For electrophoretic transfer of proteins from the gel to a membrane, a Mini-Trans-Blot<sup>®</sup> Cell (BioRad), compatible with the described system for electrophoresis, was utilized. The transblot sandwich was assembled according to the manufacturer's instructions in the following order starting from the anode side: sponge, 2 sheets of filter paper, nitrocellulose membrane, gel, 2 sheets of filter paper, sponge. The assembled transblot sandwich was inserted into the transblot cell filled with the transfer buffer. An ice-cooling unit was set behind the cathode side of transblot cell. The transfer was performed for 2 hours at 400 mA with one change of the ice-cooling unit after the first hour.

### ***3.5.3 Staining the membrane with Ponceau S***

Ponceau S can be used routinely to verify quality of protein transfer from SDS-PAAG to nitrocellulose membrane. It is applied in acidic aqueous solution. Staining is rapid but not permanent; the red stain is washed away in subsequent processing. Since the binding is reversible, the stain is compatible with most antigen visualization techniques.

The membrane was immersed in freshly diluted Ponceau S solution and incubated for 1 min at room temperature with gentle agitation on the rocking platform. Afterwards, the membrane was destained for 1-2 min with several changes of 1X washing buffer.

### ***3.5.4 Immunovisualization***

After transfer, the membrane was incubated on a rocking platform with blocking solution overnight at 4°C (or alternatively, for 60 minutes at room temperature). Next, the membrane was incubated with primary antibody diluted in the antibody dilution buffer for 2 hours at room temperature. After washing (six times five minutes each), the membrane was incubated with HRP-conjugated secondary antibody diluted in the antibody dilution buffer for 1 hour at room temperature. Afterwards the membrane was washed as before. For the chemiluminescent detection, SuperSignal<sup>®</sup> West Pico Chemiluminescent Substrate (Pierce) was used. Substrate working solution was prepared by mixing of equal volumes of two substrate components. The membrane was incubated with substrate working solution for 5 minutes at room temperature, laid between sheets of transparent plastic protector and

exposed to X-ray film, which was developed afterwards according to manufacturer's instructions.

#### Separating gel

Components	7.5% gel		10% gel		15% gel	
	10 ml	20 ml	10 ml	20 ml	10 ml	20 ml
Rotiphorese Gel 30	2.5 ml	5 ml	3.33 ml	6.66 ml	4.45 ml	8.9 ml
4X Tris/SDS, pH8.8	2.5 ml	5 ml	2.5 ml	5 ml	2.5 ml	5 ml
ddH <sub>2</sub> O	4.9 ml	9.8 ml	4.1 ml	8.2 ml	2.45 ml	4.9 ml
10% APS	100 µl	200 µl	100 µl	200 µl	100 µl	200 µl
TEMED	10 µl	20 µl	10 µl	20 µl	10 µl	20 µl

#### 5% stacking gel

Component	Amount
Rotiphorese Gel 30	0.83 ml
4X Tris/SDS, pH 6.8	1.25 ml
ddH <sub>2</sub> O	2.86 ml
10% APS	50 µl
TEMED	5 µl

#### 4X Tris/SDS, pH 6.8

	For 100 ml
Tris base	6.05 g
SDS	0.4 g
ddH <sub>2</sub> O	to 100 ml

pH was adjusted with 37% HCl to 6.8; the solution was stored at room temperature.

4X Tris/SDS, pH 8.8

	For 250 ml
Tris base	45.5 g
SDS	1 g
ddH <sub>2</sub> O	to 250 ml

pH was adjusted with 37% HCl to 6.8; the solution was stored at room temperature.

5X SDS-PAGE running buffer

	For 2 l
Tris base	30.2 g
Glycine	144 g
SDS	10 g
ddH <sub>2</sub> O	to 2 l

pH was adjusted with 37% HCl to 8.3; the solution was stored at room temperature.

1X SDS-PAGE running buffer

	For 2 l
5X stock	400 ml
ddH <sub>2</sub> O	to 2 l

5X transfer buffer

	For 2 l
Tris base	39.4 g
Glycine	144 g
ddH <sub>2</sub> O	to 2 l

pH was adjusted with 37% HCl to 8.3; the solution was stored at room temperature.

1X SDS-PAGE transfer buffer

	For 2 l	Final concentration
5X stock	400 ml	1X
100% methanol	400 ml	20%
10% SDS	2 ml	0.01%

ddH<sub>2</sub>O to 2 l

10X washing buffer

	For 2 l
Tris base	48.4 g
NaCl	58.48 g
ddH <sub>2</sub> O	to 2 l

pH was adjusted with HCl to 7.5; the solution was stored at room temperature

1X washing buffer

	For 5 l	Final concentration
10X stock	500 ml	1X
Tween 20	5 ml	0.1%
ddH <sub>2</sub> O	to 5 l	

Blocking reagent

	For 50 ml	Final concentration
Nonfat dry milk	2.5 g	5%
1X washing buffer	to 50 ml	

The solution should be prepared freshly and can be stored at 4°C for 1-2 days.

Antibody incubation buffer

	For 50 ml	Final concentration
5% nonfat milk	5 ml	0.5%
1X washing buffer	to 50 ml	

Primary antibodies were used in the following dilutions:

Antibody	Used dilution
Anti-Pan Na <sub>v</sub> Ab	1:500
Anti-Na <sub>v</sub> 1.5 Ab	1:500
Anti-PLB Ab	1:10000
Anti-SERCA2a Ab	1:20000

Anti-NCX Ab	1:2000
Anti-Calsequestrin Ab	1:5000
Anti-GAPDH Ab	1:20000

Secondary HRP-conjugated antibodies were used in the following dilutions:

Antibody	Used dilution
Donkey anti-rabbit whole IgG	1:10000
Sheep anti-mouse whole IgG	1:10000

### **3.6 Co-immunocytochemical analysis**

Immunocytochemical (ICC) staining is a technique used to detect a specific antigen (protein) in live or fixed cell cultures by use of specific primary antibodies which recognize the protein in the cell. A secondary antibody has a fluorescent molecule attached to it so that it can be detected by confocal microscopy.

ICC technique can be divided into four steps, such as cell preparation, fixation, antibody binding and detection.

#### ***3.6.1 Preparation and fixation of cells***

Prior to plating the cells, chamber slides (4 well glass slide, Nunc/USA) were covered with M199/laminin mixture (3 ml/30  $\mu$ l) to ensure a better attachment of the cells to the bottom and incubated at 37°C for 1 h before use.

Ventricular cardiomyocytes isolated from rabbit were transfected with recombinant adenovirus encoding for HA-tagged CaMKII $\delta_C$  (or  $\beta$ -gal as control) with a MOI of 100 directly in the suspension ( $1 \times 10^5$  cells in 4 ml of M199) and plated on laminin-coated chamber slides. After the attachment phase of 3 hours, the medium was replaced with fresh M199 (4 ml per chamber slide) and cultured for 24 hours. The incubation of the cardiomyocytes was performed in gas-controlled incubator in water vapor saturated air containing 5% CO<sub>2</sub> at 37°C. Ventricular cardiomyocytes isolated from CaMKII $\delta_C$  TG mouse were plated on laminin-coated chamber slides and incubated for 1 hour at room temperature to allow the cells to attach to the bottom. After incubation the rabbit and mouse myocytes were washed with 1X PBS (three times five minutes) and fixed. Fixation



is needed to preserve cells in a reproducible and live-like manner. The rabbit myocytes were fixed with 4% paraformaldehyde for 30 minutes at room temperature. The mouse myocytes were fixed in ice-cold 100% ethanol for 20 minutes at -20°C. After fixation the cells were washed with 1X PBS (three times five minutes) and blocked with blocking solution overnight at 4°C to minimize nonspecific staining.

### ***3.6.2 Incubation with antibodies***

After blocking the myocytes were washed with 1X PBS (three times five minutes). Next, the cells were incubated with primary antibody diluted with the antibody dilution buffer for 1 hour at 37°C (for rabbit myocytes) and overnight at 4°C (for mouse myocytes). After washing with 1X PBS (six times five minutes), the cells were incubated with dye conjugated secondary antibody diluted in antibody dilution buffer for 2 hour at room temperature in darkness. Afterwards the cells were washed as before, covered with VECTASHIELD HardSet Mounting Medium (Vector Laboratories) and analyzed using an LSM 5 Pascal confocal microscope (Zeiss). For control, no primary antibody was used.

#### 4% paraformaldehyde

	For 100 ml	Final concentration
Paraformaldehyde	4 g	4%
1X PBS	to 100 ml	

#### Blocking reagent

	For 10 ml	Final concentration
BSA-V	100 mg	1%
1X PBS	to 10 ml	

The solution should be prepared freshly and can be stored at 4°C for 1-2 days.

#### Incubation buffer for primary antibody

	For 10 ml	Final concentration
BSA-V	50 mg	0.5%
Triton X-100	75 µl	0.75%
1X PBS	to 10 ml	

Incubation buffer for secondary antibody

	For 10 ml	Final concentration
BSA-V	50 mg	0.5%
1X PBS	to 10 ml	

Primary antibodies were used in the following dilutions:

Antibody	Used dilution
Anti-HA	1:100
Anti-Na <sub>v</sub> 1.5	1:60

Secondary dye conjugated antibodies were used in the following dilutions:

Antibody	Used dilution
goat anti-mouse Texas Red-conjugated	1:200
goat anti-rabbit Fluorescein-conjugated	1:200
goat anti-rabbit Alexa Fluor 488	1:200
goat anti-mouse Alexa Fluor 555	1:200

**3.7 Back-phosphorylation*****3.7.1 Immunoprecipitation of Na<sup>+</sup> channel from mouse cardiac homogenates***

Cardiac homogenate, prepared from WT mouse heart as described in 3.3.2, was split in 3 tubes with 1 mg of total protein in each and suspended in the dilution media to bring the volume of each sample up to 500  $\mu$ l. The samples were kept on ice for 30 minutes with occasional vortexing. After adding, 5  $\mu$ g of rabbit polyclonal anti-Pan Na<sub>v</sub> antibody (Pan Na<sup>+</sup> Channel, Alomone Labs), the samples were incubated using an end-over-end rotator set at low speed for 2 hours at 4°C. Protein G-sepharose Fast Flow (Amersham Biosciences) was prepared as described in 3.4.2 and 100  $\mu$ l of the slurry was added to each sample. The mixture was gently mixed for 2 hours at 4°C using an end-over-end rotator set at low speed. Subsequently, the matrix was sedimented by centrifugation for 30 seconds at 14000x g in an Eppendorf bench-top MiniSpin centrifuge. The supernatants were removed with a 29 G cannula connected to a syringe and the pellets were washed 3 times with 500  $\mu$ l of RIPA buffer. The tubes were inverted carefully 5 times to mix. After each washing step, the immunoprecipitates were recovered by centrifugation as described above.

Immunoprecipitated Na<sup>+</sup> channels were resuspended in 1X CaMKII reaction buffer contained 50 mM Tris-HCl, 10 mM MgCl<sub>2</sub>, 2 mM dithiothreitol, 0.1 mM Na<sub>2</sub> EDTA, pH 7.5.

### ***3.7.2 Preactivation of endogenous CaMKII and immunoprecipitation of Na<sup>+</sup> channels from rabbit myocytes***

Ventricular cardiomyocytes isolated from a rabbit were transfected with either CaMKII $\delta_C$  or LacZ using a MOI of 100 as described in 3.2.1. Transfected myocytes were superfused with the relaxation solution for 5 minutes at room temperature. Afterwards, saponin (50  $\mu$ l/ml) was added for 30 seconds to permeabilize the sarcolemma. After permeabilization, the myocytes were exposed to the internal solution. To prevent possible basal PKA activity, the PKA inhibitory peptide PKI (15  $\mu$ M, Sigma) was included in all bath solutions. After 5 minute equilibration, okadaic acid (2  $\mu$ M) was added to prevent dephosphorylation. To activate an endogenous CaMKII, the myocytes were incubated for 5 more minutes in the presence of 50 nM or 500 nM free Ca<sup>2+</sup> in the latter case, CaCl<sub>2</sub> concentration was raised with simultaneous addition of CaM (Upstate). Then myocytes were harvested and lysed in 500  $\mu$ l of dilution medium. Immunoprecipitation of Na<sup>+</sup> channels were carried out as describe above.

### ***3.7.3 Preactivation of exogenous CaMKII and back-phosphorylation***

CaMKII (30 U, New England Biolabs Inc.) was preactivated either in the presence or absence of CaMKII inhibitors KN-93 (Seikagaku Corporation), AIP (Sigma), or PKA/PKC inhibitor cocktail (Upstate). Immunoprecipitated Na<sup>+</sup> channels from mouse and rabbit samples were phosphorylated with CaMKII for 30 minutes at 30°C in the presence of [ $\gamma$ -<sup>32</sup>P]-ATP with a specific activity of 5.7 Ci/mmol. After washing the beads with 500  $\mu$ l of RIPA buffer, proteins were eluted by heating for 30 min at 37°C in 65  $\mu$ l of 2X sampler buffer and separated from the beads by centrifugation. The supernatants were resolved by SDS-7.5% polyacrylamide gel, and phosphorylated proteins were visualized using a phosphoimager.

Dilution medium (prepared just prior to use)

	For 5 ml	Final concentration
Modified RIPA buffer	5 ml	
200 mM NaF	500 $\mu$ l	20 mM
100 mM Na <sub>3</sub> VO <sub>4</sub>	50 $\mu$ l	1 mM
100 mM DTT	50 $\mu$ l	1 mM
10% CHAPS	50 $\mu$ l	1%

The complete protease inhibitor cocktail (Roche) was added.

Modified RIPA buffer

	For 50 ml	Final concentration
2 M Tris-HCl, pH 7.4	1.25 ml	50 mM
4 M NaCl	2.5 ml	200 mM
ddH <sub>2</sub> O	to 50 ml	

Relaxation solution (prepared just prior to use)

	For 50 ml	Final concentration
100 mM HEPES, pH 7.4	5 ml	10 mM
100 mM EGTA	50 $\mu$ l	0.1 mM
2 M potassium aspartate	3.75 ml	150 mM
1 M MgCl <sub>2</sub>	12.5 $\mu$ l	0.25 mM
100 mM Na <sub>3</sub> -ATP	2.5 ml	5 mM
Reduced glutathione	150 mg	10 mM

Internal solution (prepared just prior to use)

	For 50 ml	Final concentration
100 mM HEPES, pH 7.2	5 ml	10 mM
100 mM EGTA	0.5 ml	1 mM
2 M potassium aspartate	3 ml	120 mM
1 M MgCl <sub>2</sub>	285 $\mu$ l	5.7 mM (1mM free [Mg])
100 mM Na <sub>3</sub> -ATP	2.5 ml	5 mM
1 M CaCl <sub>2</sub>	12.5 $\mu$ l	0.25 mM (50 nM free [Ca <sup>2+</sup> ])
0.5 mM PKI inhibitory peptide	1.5 ml	15 $\mu$ M

Reduced glutathione	150 mg	10 mM
Creatine phosphokinase	5 mg	5 U/ml
Phosphocreatine	138.9 mg	10 mM
Dextran (Mr. 40000)	2 mg	4%

### 2X sampler buffer

	For 20 ml	Final concentration
Tris-HCl	0.32 g	100 mM
SDS	0.8 g	4%
Glycerol	4 ml	20%

### **3.8 Isolation of mouse ventricular myocytes**

The isolation of mouse ventricular cardiomyocytes was performed using Langendorff perfusion apparatus. Before isolation, perfusion apparatus was washed two times with distilled water and then with perfusion buffer through the system for at least 5 min.

Mice were anesthetized in a gas chamber with 800  $\mu$ l of halothane (Eurime-Pharm GmbH). A cannula was inserted into the aorta and perfusion started with a flow rate of 3 ml/min for 4 minutes. Afterwards, the heart perfusion was continued with myocyte digestion buffer for 8 to 10 minutes at 3 ml/min. After enzymatic digestion, the heart was cut from the cannula and placed in a 60-mm dish containing 2.5 ml of myocyte digestion buffer. The heart was cut in half and the ventricles were gently teased with fine forceps into several small pieces. These were then pipetted gently several times with a sterile plastic transfer pipette (2 mm opening). The cell suspension was transferred into a 15 ml tube, 2.5 ml of myocyte stopping buffer 1 was added and the heart tissue were continued to dissociate gently, using sterile plastic transfer pipettes with different size of openings (2 mm, 1.5 mm, and then 1 mm diameters) until all the large pieces of heart tissue were dispersed in the cell suspension. Next, the myocytes were sedimented by gravity for 8 to 10 min in the 15 ml tube; the supernatant was transferred to a new 15 ml tube and centrifuged for 1 min at 180x g. The pellet was resuspended in 5 ml of myocyte stopping buffer 2, combined with the gravity-sedimented myocytes and diluted with myocyte stopping buffer 2 to bring the total volume up to 10 ml. Other cell types and dead myocytes were removed by numerous steps of selective sedimentation under gravity (for about 10 minutes) in washing solution.

Each portion of washing solution used for every subsequent sedimentation-resuspension cycle contained  $\text{Ca}^{2+}$  at gradually rising concentrations, reaching the concentration of 0.8 mM in the final washing, which is close to that in the medium (1 mM) used for further cell measurements.

#### 10X Perfusion buffer

	For 1 L	Final concentration
NaCl	65.992 g	1.13 M
KCl	3.506 g	47 mM
$\text{KH}_2\text{PO}_4$	816.6 mg	6 mM
$\text{Na}_2\text{HPO}_4 \cdot 2\text{H}_2\text{O}$	1067.9 mg	6 mM
$\text{MgSO}_4 \cdot 7\text{H}_2\text{O}$	2958.0 mg	12 mM
Phenol-red	120.4 mg	0.32 mM
$\text{NaHCO}_3$	10.080 g	120 mM
$\text{KHCO}_3$	10.100 g	100 mM
HEPES	23.831 g	100 mM
Taurine	37.530 g	300 mM

The buffer was stored +4°C

#### BDM

	For 1 L	Final concentration
BDM (2,3-butanedione monoxime)	50.5 mg	500 mM
ddH <sub>2</sub> O	to 1 L	

The solution was stored +4°C

#### 1X Perfusion buffer

	For 1 L	Final concentration
10X Perfusion buffer	100 ml	1X
BDM	20 ml	10 mM
Glucose	0.991g	5.5 mM

pH was adjusted with NaOH to 7.46 at 37 °C. The buffer was stored +4°C

Myocyte digestion buffer

	For 18 ml	Final concentration
1X Perfusion buffer	18 ml	
Liberase Blendzyme 1	4.5 mg	
Trypsin	100.08 $\mu$ l	
10 mM CaCl <sub>2</sub>	22.5 $\mu$ l	1.25 mM

Myocyte stopping buffer 1

	For 2.5 ml	Final concentration
1X Perfusion buffer	2.25 ml	
BCS (Bovine calf serum)	0.25 ml	10%
10 mM CaCl <sub>2</sub>	3.125 $\mu$ l	1.25 mM

Myocyte stopping buffer 2

	For 20 ml	Final concentration
1X Perfusion buffer	19 ml	
BCS (Bovine calf serum)	1 ml	5%
10 mM CaCl <sub>2</sub>	25 ml	1.25 mM

Washing solution

	#1	#2	#3	#4
1X Perfusion buffer (with 5% BCS)	5 ml	5 ml	10 ml	10 ml
100 mM CaCl <sub>2</sub>	5 $\mu$ l (0.1 mM)	10 $\mu$ l (0.2 mM)	40 $\mu$ l (0.4 mM)	80 $\mu$ l (0.8 mM)

### 3.9 Measurement of cell shortening and Ca<sup>2+</sup> transients using an epifluorescence microscope

Evaluation of global excitation–contraction coupling was performed in isolated single ventricular cardiac myocytes. These were obtained by enzymatic digestion of the explanted hearts via Langendorff perfusion apparatus using a digestion buffer as described in Methods 3.8.

Experiments to evaluate E-C coupling was performed to determine whether increased stimulation rates lead to changes in fractional shortening of myocytes (i.e. force-frequency relationship) and whether this may be due to altered intracellular  $\text{Ca}^{2+}$ . Therefore, cell shortening was measured in parallel with estimation of the intracellular  $\text{Ca}^{2+}$  concentration by a  $\text{Ca}^{2+}$ -fluorescent dye at different stimulation frequencies. Application of caffeine is one of the most useful methods to assess SR  $\text{Ca}^{2+}$  load. Rapid application of caffeine opens the RyR2 channels thereby releasing all calcium ions, which are stored in the SR. The amplitude of the caffeine induced  $\text{Ca}^{2+}$  transient was used to calculate total SR  $\text{Ca}^{2+}$  content.

Isolated cardiomyocytes were plated on laminin-coated IonOptix chamber for 15 minutes to allow the cells to attach. The washing solution was removed and replaced with 200  $\mu\text{l}$  of  $\text{Ca}^{2+}$ -fluorescent dye Fluo-3 by incubation with 10  $\mu\text{M}$  of the acetoxymethyl ester (AM) form of the dye (Molecular Probes) for 15 min at room temperature in darkness. The chamber was placed into the microscope holder. After loading, the cells were washed with normal 1X Tyrode solution containing 1 mM  $\text{Ca}^{2+}$  at 37°C at a flow rate of 80 ml/h for 5 minutes using the superfusion system. This also allows for deesterification of the dye. The image of the myocytes was recorded using a camera (MyoCam) and displayed on a monitor. The dye was excited with a wavelength at  $480\pm 15$  nm using a 75 W xenon arc lamp (Ushio, Japan) on the stage of a Nikon Eclipse TE200-U inverted microscope. Emitted fluorescence was measured using a photomultiplier (at  $535\pm 20$  nm; IonOptix Corp, Milton, Mass). From the raw fluorescence,  $F/F_0$  was calculated by dividing it by the baseline fluorescence ( $F_0$ ), after subtraction of background fluorescence. Myocytes were field-stimulated (voltage 25% above the threshold) at 1 Hz and 37°C until steady-state was achieved and only those cells exhibiting stable steady-state contractions were included in the study. Cells were transilluminated by red light ( $>650$  nm, to avoid interference with Fluo-3 epifluorescence measurement), and shortening was measured using a sarcomere length detection system (IonOptix Corp, Milton, Mass). After steady-state conditions were achieved, stimulation frequency was increased stepwise from 1 Hz to 2, 4 and 8 Hz. SR  $\text{Ca}^{2+}$  content was estimated by rapid application of a 10 mM caffeine pulse to cause SR  $\text{Ca}^{2+}$  release. Diastolic  $\text{Ca}^{2+}$  was measured in cardiomyocytes loaded with 10  $\mu\text{M}$  Fura-2 AM (Sigma): excitation was performed at 340 nm as well as 380 nm and emission was recorded at 510 nm. The obtained values were used to calculate  $\text{Ca}^{2+}$  transient amplitude in Fluo-3 experiments as described before (Maier et al., 2003).



10X Tyrode

	For 1 L	Final concentration
KCl	2.982 g	40 mM
NaCl	81.816 g	1.4 M
MgCl <sub>2</sub>	0.952 g	10 mM
HEPES	11.916 g	50 mM

pH was adjusted with NaOH to 7.00. The tyrode was stored +4°C

1X Tyrode supplemented with 1 mM Ca<sup>2+</sup>

	For 1 L	Final concentration
10X Tyrode	100 ml	
Glucose	1.802 g	10 mM
1 M CaCl <sub>2</sub>	1 ml	1 mM

pH was adjusted with NaOH to 7.54 at room temperature. The tyrode was stored +4°C

1X Tyrode with caffeine

	For 100 ml	Final concentration
1X Tyrode	100 ml	
Caffeine	194 mg	10 mM

Fluo-3 AM

	For 5 ml	Final concentration
1X Tyrode	5 ml	
1 mM Fluo-3 AM	50 µl	10 mM
Pluronic F-127	5 µl	2 %

The solution was dispensed into 200 µl aliquots and stored at -20°C in darkness.

Fura-2 AM

	For 5 ml	Final concentration
1X Tyrode	5 ml	
1 mM Fura-2 AM	50 µl	10 mM
Pluronic F-127	5 µl	2 %

The solution was dispensed into 200  $\mu\text{l}$  aliquots and stored at  $-20^{\circ}\text{C}$  in darkness.

### 3.10 Measurement of the $\text{Ca}^{2+}$ sparks using confocal microscope

Isolated mouse cardiomyocytes were plated on laminin-coated chamber for 15 minutes to allow the cells to attach. The washing solution was removed and replaced with 200  $\mu\text{l}$  of  $\text{Ca}^{2+}$ -fluorescent dye Fluo-4 by incubation with 10  $\mu\text{M}$  of the acetoxymethyl ester (AM) form of the dye (Molecular Probes) for 15 min at room temperature in darkness. After 15 minutes the loading buffer was exchanged for normal 1X Tyrode solution containing 3 mM  $\text{Ca}^{2+}$  at room temperature to deesterify Fluo-4 AM before recording the fluorescence.  $\text{Ca}^{2+}$  sparks were recorded using a laser scanning confocal microscope (LSM 5 Pascal, Zeiss) with a 40 $\times$ oil-immersion objective. During the recording, the intact myocytes were continuously perfused with experimental solution. Fluo-4 AM was excited via an argon laser at 488 nm and emitted fluorescence was collected through a 515 nm long-pass emission filter. Fluorescence images were recorded in line-scan mode with 512 pixels per line, pixel time 0,64  $\mu\text{s}$ , pixel size 0,07  $\mu\text{m}\times 0,07 \mu\text{m}$ , width of the scan 38,4  $\mu\text{m}$ .  $\text{Ca}^{2+}$  spark frequency (CaSpF) was measured during 0.5 Hz stimulation and normalized to cell volume and scan rate as sparks ( $\text{pl}^{-1}\cdot\text{s}^{-1}$ ). Peak of  $\text{Ca}^{2+}$  sparks were normalized as  $F/F_0$  ( $F/F_0$  was calculated by dividing by the baseline fluorescence  $F_0$ , after subtraction of the background fluorescence), and duration was taken from the full-duration half-maximum (FDHM).

#### 10X Tyrode

	For 1 L	Final concentration
KCl	2.982 g	40 mM
NaCl	81.816 g	1.4 M
MgCl <sub>2</sub>	0.952 g	10 mM
HEPES	11.916 g	50 mM

pH was adjusted with NaOH to 7.00. The tyrode was stored  $+4^{\circ}\text{C}$

1X Tyrode supplemented with 3 mM Ca<sup>2+</sup>

	For 1 L	Final concentration
10X Tyrode	100 ml	
Glucose	1.802 g	10 mM
1 M CaCl <sub>2</sub>	3 ml	3 mM

pH was adjusted with NaOH to 7.4 at room temperature. The tyrode was stored +4

Fluo-4 AM

	For 5 ml	Final concentration
1X Tyrode	4.56 ml	
1 mM Fluo-3 AM	45.6 µl	10 mM
Pluronic F-127	4.56 µl	2 %

The solution was dispensed into 200 µl aliquots and stored at -20°C in darkness

**3.11 Echocardiographic measurements**

Echocardiography was performed using a Visual Sonic 770 system with a 30 MHz transducer. Mice were anesthetized by intraperitoneal injection of 2.5 % Avertin (5 µl per gram of body weight). M-mode was recorded at a sweep speed of 150 mm/sec with the cursor placed in the middle of the LV cavity. Measurements were obtained by an examiner blinded to the genotype of the animals.

**3.12 Statistical analysis**

All data are presented as mean±SEM. Statistical analyses were performed using Student's *t*-test for unpaired values or the two-way analysis of variance (ANOVA) for repeated measurements combined with post-hoc (Student-Newman-Keuls or Fisher-LSD) tests where appropriate. Values of P<0.05 were considered as statistically significant.

## 4 Results

### 4.1 Association with and phosphorylation of Na<sup>+</sup> channels by CaMKII

#### 4.1.1 CaMKII associates with Na<sup>+</sup> channels

To determine whether CaMKII $\delta_C$  associates with Na<sup>+</sup> channel, co-immunoprecipitation technique was performed.

As a starting material for co-immunoprecipitation, Triton X-100-solubilized cardiac homogenates, prepared from CaMKII $\delta_C$  TG and WT mouse hearts as well as lysates, prepared from rabbit ventricular myocytes transfected with CaMKII $\delta_C$  using a MOI of 100 for 24 hours were used.

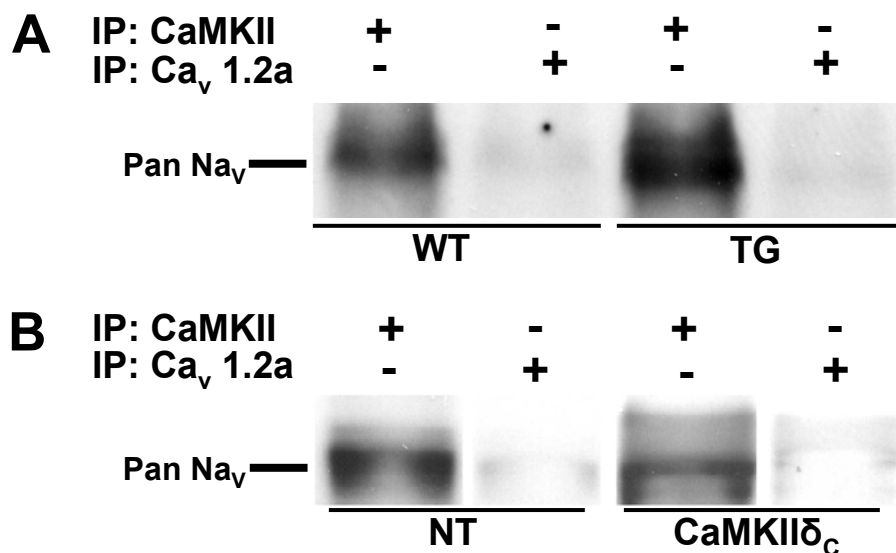


**Figure 7. Association of CaMKII with all Na<sup>+</sup> channel isoforms (Pan Na<sub>v</sub>) in Triton X-100-solubilized cardiac mouse homogenate and rabbit lysates.** The Triton X-100-solubilized (A) homogenate from mouse hearts and (B) lysates from rabbit ventricular myocytes were subjected to immunoprecipitation with either anti-CaMKII or anti-Ca<sub>v</sub>1.2a Ab, the immunoprecipitates were electrophoretically separated on 7.5% gel; detection of Na<sup>+</sup> channel bands was conducted by Western blot analysis with anti-Pan Na<sub>v</sub> Ab. CaMKII immunoprecipitation showed CaMKII association with the Na<sup>+</sup> channel in WT and TG hearts (n=3 and n=3, respectively). No Na<sup>+</sup> channel was co-immunoprecipitated when anti-Ca<sub>v</sub>1.2a antibody was used. Similar results were seen in rabbit myocytes (CaMKII $\delta_C$  and nontransfected cells, n=4 and n=4, respectively).

CaMKII was immunoprecipitated from both cardiac homogenates and lysates using a rabbit polyclonal anti-CaMKII antibody (Santa Cruze Biotechnology). The immunoprecipitates were subjected to Western blotting with rabbit polyclonal anti-Pan Na<sub>v</sub> antibody (Alomone Labs) and revealed an immunoreactive band at ~ 250 kDa (Fig. 7). Anti-Pan Na<sub>v</sub> antibody recognizes all Na<sup>+</sup> channel isoforms, therefore western blotting of the immunoprecipitates was repeated with cardiac-specific anti-Na<sub>v</sub>1.5 antibody, showing similar results (Fig. 8). To confirm the specificity of interaction between CaMKII and Na<sup>+</sup>

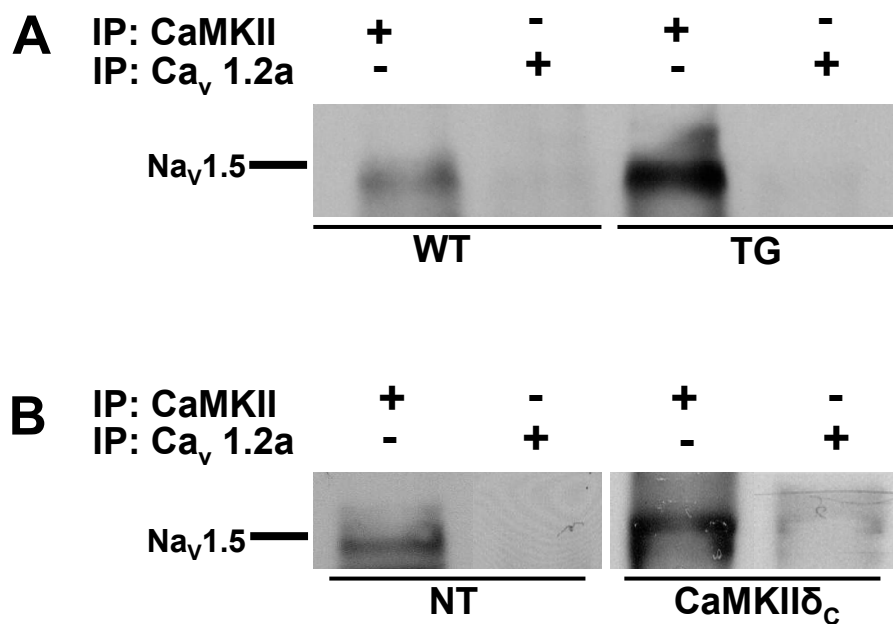


**Figure 8. Association of CaMKII with the cardiac Na<sup>+</sup> channel isoform (Na<sub>v</sub>1.5) in Triton X-100-solubilized cardiac mouse homogenate and rabbit lysates.** The Triton X-100-solubilized (A) homogenate from mouse hearts and (B) lysates from rabbit ventricular myocytes were subjected to immunoprecipitation with either anti-CaMKII or anti-Ca<sub>v</sub>1.2a Ab, the immunoprecipitates were electrophoretically separated on 7.5% gel; detection of Na<sup>+</sup> channel bands was conducted by Western blot analysis with anti-Na<sub>v</sub>1.5 Ab. CaMKII immunoprecipitation showed CaMKII association with the Na<sup>+</sup> channel in WT and TG hearts (n=3 and n=3, respectively), while there was no co-immunoprecipitation of the Na<sup>+</sup> channel in control reactions performed with anti-Ca<sub>v</sub>1.2a antibody. Similar results were seen in rabbit myocytes (CaMKIIδ<sub>c</sub> and nontransfected cells, n=4 and n=4, respectively).

channel, the following negatives controls were included: incubation of the samples with antibody against L-type  $\text{Ca}^{2+}$  channel ( $\text{Ca}_v1.2a$ , Alomone Labs), which is known neither to associate with  $\text{Na}^+$  channel nor does it lead to its precipitation (Fig. 7&8A and 7&8B, lanes 2 and 4); incubation of the samples with protein G-sepharose beads alone. As expected, no-precipitation of the  $\text{Na}^+$  channel was observed under these conditions (data not shown). Thus, co-immunoprecipitation experiments showed an association of CaMKII with  $\text{Na}^+$  channel in WT and CaMKII $\delta_C$  TG mouse hearts as well as in transfected and nontransfected rabbit myocytes.

#### ***4.1.2 Immunocolocalization of CaMKII and $\text{Na}^+$ channels in single cardiomyocytes***

The special relationship between CaMKII $\delta_C$  and the  $\text{Na}^+$  channel was confirmed with double labeling immunocytochemical techniques combined with laser scanning confocal microscopy. For this study ventricular cardiomyocytes from CaMKII $\delta_C$  transgenic mouse hearts as well as ventricular cardiomyocytes from rabbit hearts transfected with recombinant adenovirus carrying CaMKII $\delta_C$  (or  $\beta$ -gal as control) with MOI of 100 for 24 hours were used. Immunofluorescence images of each protein were obtained in the same cell. After fixation, the cardiomyocytes were incubated simultaneously with two different antibodies that recognize overexpressed HA-tagged CaMKII $\delta_C$  (anti-HA, Roche) and the cardiac  $\text{Na}^+$  channel (anti- $\text{Na}_v1.5$ , Alomone Labs) to determine their subcellular localization. Only cardiomyocytes with the normal rod-shaped morphology were analyzed. Cardiac  $\text{Na}^+$  channels was observed at high density in the transverse tubular membrane system (shown in green) in both mouse and rabbit myocytes, whereas CaMKII $\delta_C$  was concentrated in the cytoplasm of the isolated cardiomyocytes (depicted in red) from both species (Fig. 9). Co-localization was established when identical regions contained both proteins. Double labeling of  $\text{Na}_v1.5$  and HA-tag revealed significant co-localization of cardiac  $\text{Na}^+$  channels with the cytosolic isoform of CaMKII $\delta_C$  (yellow) in transverse tubular membrane system in both mouse and rabbit cardiomyocytes. Apart of the membrane-associated CaMKII $\delta_C$ , which overlapped with cardiac  $\text{Na}^+$  channels, free CaMKII $\delta_C$  was also observed in numerous small foci in cytosol. To determine the degree of non-specific binding, negatives controls were included: incubation of the rabbit control-transfected myocytes with anti-HA antibody as well as incubation of the myocytes with secondary antibody alone. In both cases, no signal above background was detected (data not shown).

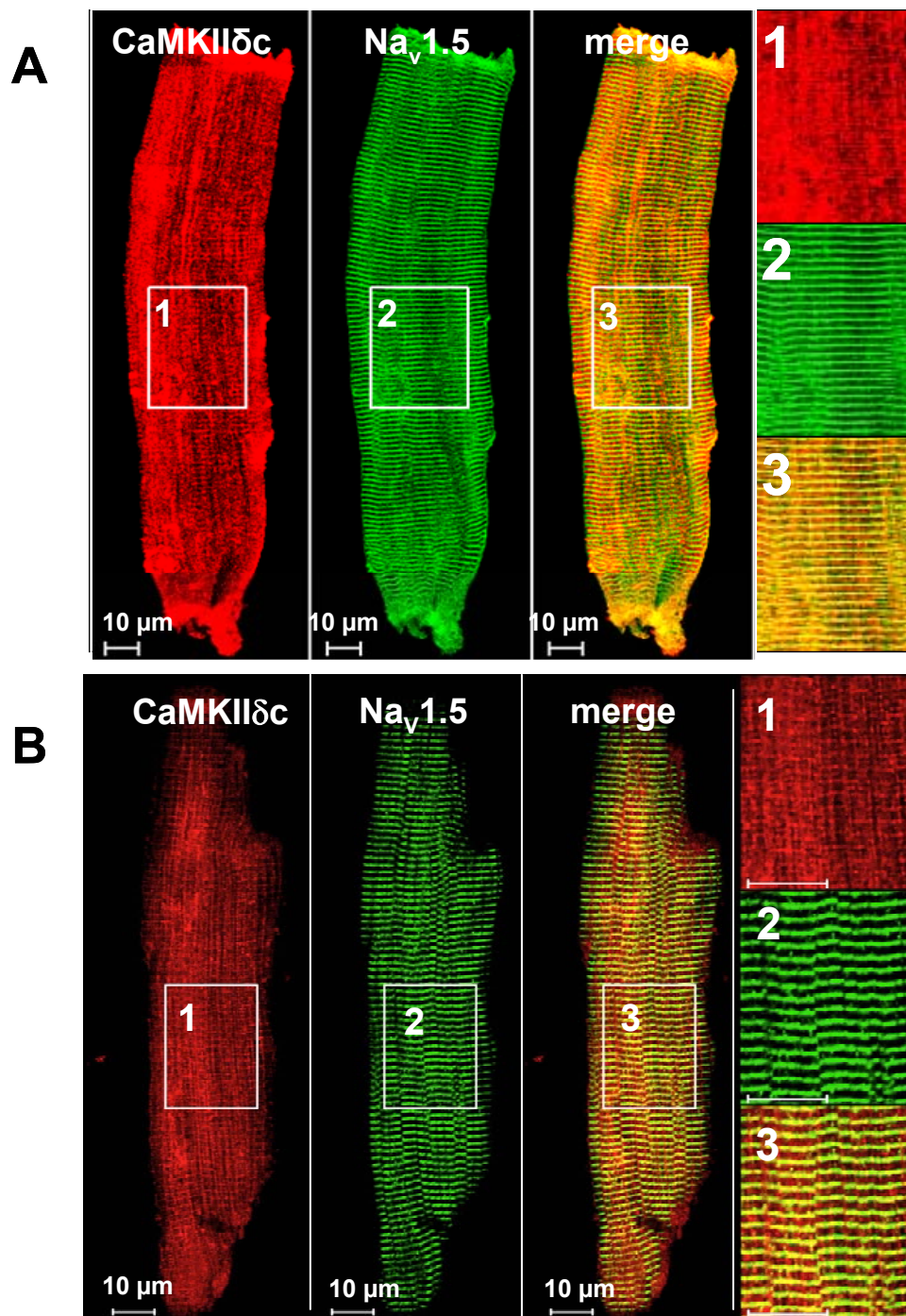


**Figure 9. Co-localization of CaMKII and Na<sup>+</sup> channels in mouse and rabbit cardiomyocytes.** Simultaneous labeling of CaMKII and Na<sup>+</sup> channels in ventricular myocytes from mouse (A) and rabbit (B) with primary anti-HA and anti-Na<sub>v</sub>1.5 antibodies followed by visualization of their localization with dye-conjugated secondary antibodies using laser scanning confocal microscopy. (A and B lane 1) single labeling of CaMKII $\delta$ c (red), concentrated in the cytoplasm of the isolated cardiomyocytes of both species. (A and B lane 2) single labeling of Na<sup>+</sup> channels (green), observed in the transverse tubular membrane system. (A and B lane 3) double staining, illustrating co-localization of CaMKII and Na<sup>+</sup> channels in transverse tubular in both mouse and rabbit cardiomyocytes (yellow).

### 4.1.3 *CaMKII-dependent phosphorylation of Na<sup>+</sup> channels*

Phosphorylation is the most frequent protein post translational modification regulating its function. To assess whether CaMKII phosphorylates Na<sup>+</sup> channels, a back-phosphorylation assay with purified CaMKII and [ $\gamma$ -<sup>32</sup>P]-ATP was utilized.

At first, phosphorylation of Na<sup>+</sup> channels by CaMKII was proven in WT mouse myocardium (Fig. 10A and B), because in CaMKII $\delta_C$  TG mice Na<sup>+</sup> channels might have been already nearly maximally phosphorylated and therefore not available for phosphorylation by exogenous CaMKII during our back-phosphorylation assay. CaMKII activation mix containing buffer supplemented with Ca<sup>2+</sup>/CaM and Mg<sup>2+</sup>/ATP was prepared. To all samples (except tube 2) CaMKII was added and all tubes were incubated for 10 minutes at 30°C to allow activation of the enzyme. Subsequently these mixtures were transferred to the beads containing material immunoprecipitated with anti-Pan Na<sub>v</sub> antibody (Alomone Labs). Radioactive ATP was added and back-phosphorylation was carried out. Exogenous CaMKII clearly phosphorylated Na<sup>+</sup> channels (Fig 10A lane 1), and this effect was inhibited when KN-93 or AIP (known CaMKII inhibitors) were included (Fig. 10A lane 3 and 4), but not when PKA and PKC were blocked (Fig. 10B lane 2). In Figure 10A lane 2 immunoprecipitated materials were treated like other samples in the presence of Ca<sup>2+</sup>/CaM and Mg<sup>2+</sup>/ATP but without exogenous CaMKII. However, no significant incorporation was found. If CaMKII association with the Na<sup>+</sup> channels leads to CaMKII-dependent phosphorylation, then one would expect that addition of Ca<sup>2+</sup>/CaM and Mg<sup>2+</sup>/ATP to the immunoprecipitated Na<sup>+</sup> channels would lead to channel phosphorylation without any need for exogenous CaMKII (since CaMKII should already be part of the complex). There might be several reasons why significant back-phosphorylation with Ca<sup>2+</sup>/CaM and Mg<sup>2+</sup>/ATP alone was never seen in our experiments: a) it is likely that those Na<sup>+</sup> channels to which endogenous CaMKII was attached were already phosphorylated. Since the Na<sup>+</sup> channels were not de-phosphorylated prior to back-phosphorylation, only free, unphosphorylated Na<sup>+</sup> channels were subject to exogenous CaMKII phosphorylation and visible via <sup>32</sup>P incorporation; b) our immunoprecipitation was done in the presence of 20 mM NaF-an unspecific enzyme inhibitor-which was washed away just before adding the exogenous CaMKII (so the activity of endogenous CaMKII might have been decreased dramatically); c) the amount of active endogenous enzyme in our immunoprecipitate was probably too low to allow significant phosphorylation. It is noteworthy that the conditions for immunoprecipitation with anti- Pan Na<sub>v</sub> antibody were different from that used for



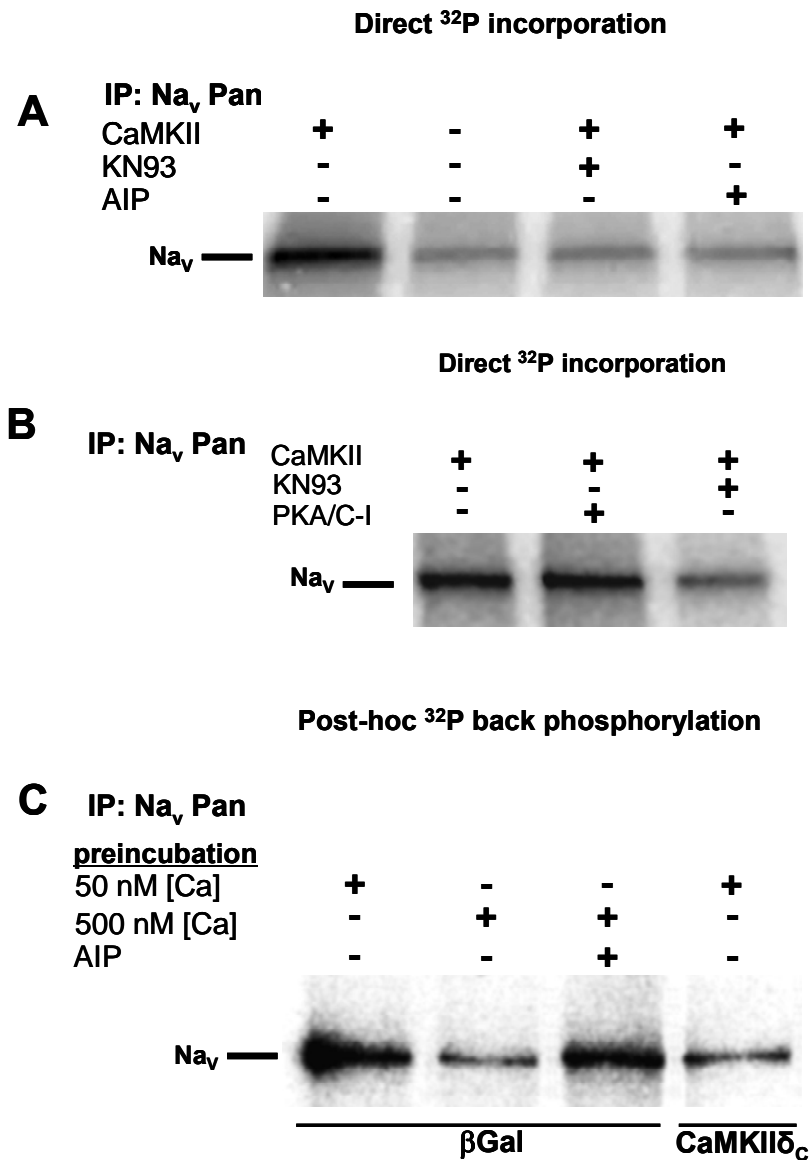


**Figure 10. Phosphorylation of  $\text{Na}^+$  channel in cardiac mouse homogenate and rabbit lysates by either exogenous or endogenous CaMKII.** (A and B)  $\text{Na}^+$  channel was immunoprecipitated from WT mouse hearts ( $n=3$ ) with anti-Pan  $\text{Na}_v$  Ab and directly phosphorylated with or without addition of exogenous CaMKII, KN-93, AIP or PKA/PKC inhibitor cocktail (PKA/C-1). (C) Endogenous CaMKII-dependent  $\text{Na}^+$  channel phosphorylation was activated in permeabilized rabbit myocytes by preincubating them for 5 minutes in internal solutions of 500 nM  $[\text{Ca}^{2+}]$  plus 2  $\mu\text{M}$  CaM (versus 50 nM  $[\text{Ca}^{2+}]$ ). Sites not already phosphorylated were subsequently back-phosphorylated in  $\text{Na}^+$  channel immunoprecipitates from mouse and rabbit samples by exogenous preactivated CaMKII and  $[\gamma\text{-}^{32}\text{P}]\text{-ATP}$ . Phosphorylation of  $\text{Na}^+$  channel was quantified using a phosphoimager.

co-immunoprecipitation with anti-CaMKII antibody and included a higher salt concentration (to gain more pure preparation of Na<sup>+</sup> channels) and two additional washes with CaMKII buffer to bring the immunoprecipitated material into conditions suitable for back-phosphorylation. Since CaMKII is likely to associate with Na<sup>+</sup> channels only transiently, it might have been largely lost during the immunoprecipitation, performed under these more stringent conditions. However, because the amount and activity of CaMKII $\delta_C$  as well as the phosphorylation level of Na<sup>+</sup> channels in immunoprecipitates were difficult to address directly, we cannot discriminate between the above mentioned possibilities.

Since endogenous CaMKII $\delta_C$  associates with the Na<sup>+</sup> channels, it was tested whether endogenous CaMKII can phosphorylate Na<sup>+</sup> channels in the myocytes (Fig. 10C). Saponin-permeabilized rabbit myocytes were exposed for 5 minutes to internal solution at 50 nM Ca<sup>2+</sup> or 500 nM Ca<sup>2+</sup> plus 2  $\mu$ M CaM (to activate endogenous CaMKII). The extent of CaMKII-dependent Na<sup>+</sup> channel phosphorylation was assessed afterwards by Na<sup>+</sup> channel immunoprecipitation and subsequent back-phosphorylation with exogenous preactivated CaMKII and [ $\gamma$ -<sup>32</sup>P]-ATP. Activation of endogenous CaMKII (500 nM Ca<sup>2+</sup>) reduced back-phosphorylation (Fig. 10C lane 2 versus lane 1), indicating increased Na<sup>+</sup> channel phosphorylation upon activation of cellular CaMKII. Inclusion of AIP during preincubation of the myocyte prevented the increased phosphorylation (Fig. 10C lane 3). Interestingly, overexpression of CaMKII $\delta_C$  increased the phosphorylation level (decreased back-phosphorylation) of Na<sup>+</sup> channels at 50 nM Ca<sup>2+</sup> to a level comparable to that attained in the control at the 500 nM Ca<sup>2+</sup> incubation. Thus, CaMKII associates with the Na<sup>+</sup> channel and endogenous CaMKII can phosphorylate the Na<sup>+</sup> channel.

#### ***4.1.4 Protein expression level of Na<sup>+</sup> channels***

To test whether Na<sup>+</sup> channel protein expression levels were changed, Western blot analysis was performed. Protein homogenates prepared from WT and CaMKII $\delta_C$  transgenic mouse hearts as well as protein lysates from rabbit cardiomyocytes prepared 24 hours after transfection with CaMKII $\delta_C$  at MOI 100 (or not transfected as control) were denatured in sample buffer containing 2%  $\beta$ -mercaptoethanol by warming at 37°C for 30 minutes and 50  $\mu$ g and 25  $\mu$ g, respectively, of total protein was subjected to SDS-polyacrylamide gel. Western blotting performed with the antibody against Na<sup>+</sup> channels (anti-Pan Na<sub>v</sub>, Alomone Labs) revealed a significantly elevated (1.6-fold) Na<sup>+</sup> channel expression level in hearts from CaMKII $\delta_C$  TG as compared to that of WT mice (Fig. 11A). In contrast, Na<sup>+</sup>

channel expression levels were not altered in rabbit cardiomyocytes acutely overexpressing CaMKII $\delta_C$  for 24 hours (Fig. 11B). For quantification, the Na<sup>+</sup> channel level was normalized to calsequestrin protein expression.

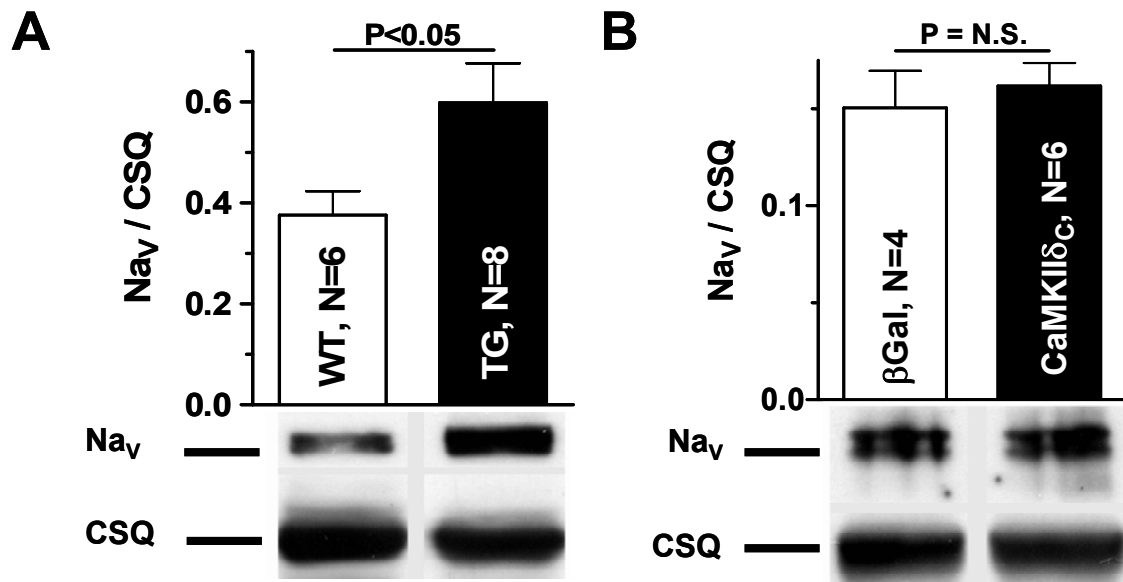


**Figure 11. Protein expression levels of Na<sup>+</sup> channel in mice (CaMKII $\delta_C$  TG versus WT) and in transfected rabbit myocytes (CaMKII $\delta_C$  versus  $\beta$ -gal, MOI of 100, 24 hours).** Cardiac homogenates from (A) WT and CaMKII $\delta_C$  TG mice as well as (B) total lysates from  $\beta$ -gal and CaMKII $\delta_C$  transfected rabbit cardiomyocytes were separated on 7.5% polyacrylamide-SDS gels and transferred to nitrocellulose. Western blots were developed with anti- Pan Na<sub>v</sub> antibody (upper panel) and anti-calsequestrin (CSQ) antibody (bottom panel). The amount of the proteins was determined densitometrically.

## 4.2 Generation and identification of mutant mice

### 4.2.1 PCR-mediated verification of genotypes of mutant mice

CaMKII $\delta_C$  transgenic mice exhibiting a 3-fold increase in CaMKII activity were provided by Dr. Tong Zhang and Dr. Joan Heller Brown (Zhang et al., 2003). Knock-in mice harboring the R4496C mutation (RyR2<sup>R4496C/+</sup>) were kindly provided by Dr. Silvia G. Priori (Cerrone et al., 2005). CaMKII $\delta_C$ /RyR2<sup>R4496C</sup> double mutant mice were generated by crossbreeding of RyR2<sup>R4496C/+</sup> mice with CaMKII $\delta_C$  mice. Mice were born to the expected

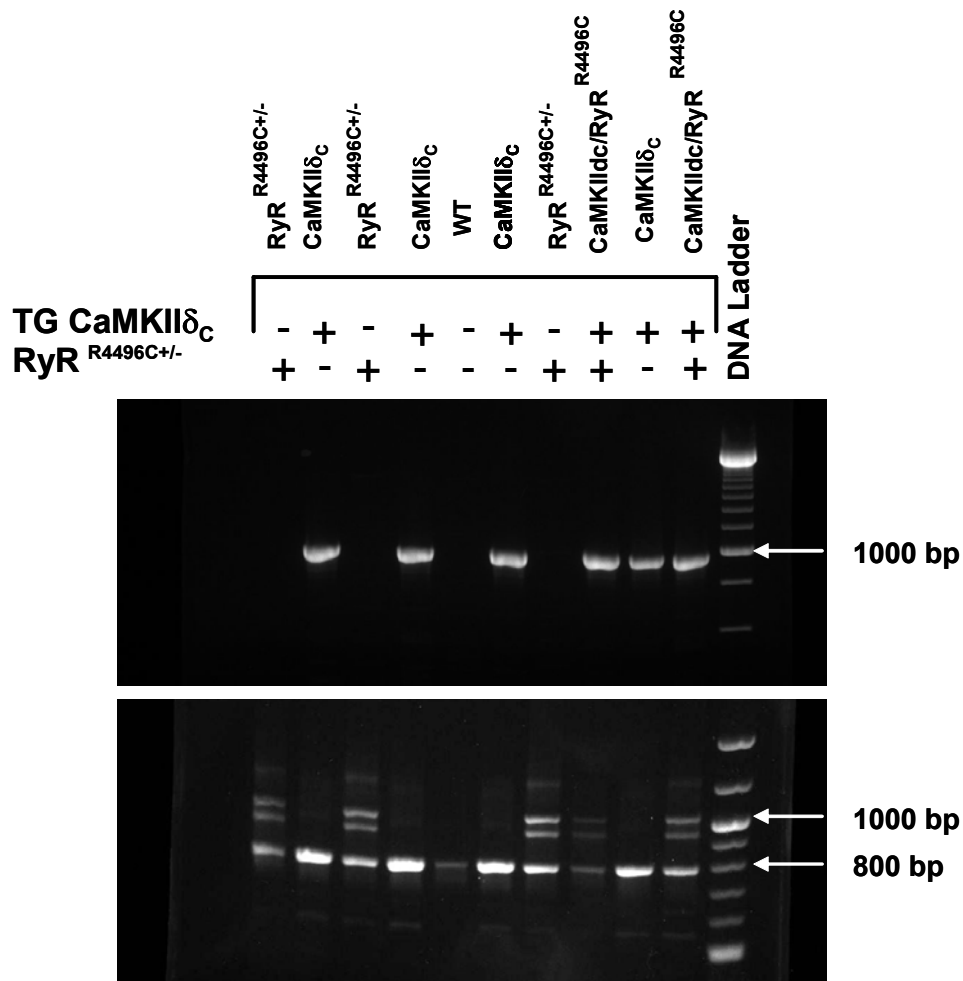


**Figure 12. PCR confirmation of CaMKII $\delta_C$  TG, RyR2<sup>R4496C/+</sup> knock-in and WT mouse genotypes.** The 1000-bp bands on the upper gel indicate the CaMKII $\delta_C$  TG and no bands show WT mice. The 800-bp and 1000-bp bands on the bottom gel indicate the heterozygous RyR2<sup>R4496C/+</sup> and the 800-bp point to WT mice. The CaMKII $\delta_C$ /RyR2<sup>R4496C</sup> were double heterozygous mice that have both the CaMKII $\delta_C$  transgene and the RyR2<sup>R4496C</sup> mutation.

mendelian ratios. CaMKII $\delta_C$ , RyR2<sup>R4496C+/-</sup>, CaMKII $\delta_C$ /RyR2<sup>R4496C</sup> mice and respective WT controls, 8-14 weeks old, of either sex were used.

PCR using DNA from ear biopsy was performed as described in the Methods (3.1) with CaMKII $\delta_C$ - and RyR2-specific primers to determine the genotype of the mutant mice (Fig.12). CaMKII $\delta_C$  transgenic mice displayed a band on the 2% agarose gel at 1000-bp, whereas WT mice showed no band. RyR2<sup>R4496C+/-</sup> heterozygous mice display 2 bands on the 1% agarose gel at 800-bp and 1000-bp, while WT have 1 band of 800-bp. The generation of CaMKII $\delta_C$ /RyR2<sup>R4496C</sup> double mutant mice was confirmed by the presence of the PCR products characteristic for CaMKII $\delta_C$  transgene and RyR2 gene harboring the R4496C mutation.

#### ***4.2.2 Cardiac overexpression of CaMKII $\delta_C$ in CaMKII $\delta_C$ TG and RyR2<sup>R4496C+/-</sup> mice induces cardiac hypertrophy and mortality***

No difference between WT versus RyR2<sup>R4496C+/-</sup> mice was present in the duration of the pregnancy, development, size, weight, survival and behavior. Whereas CaMKII $\delta_C$  overexpression alone as well as crossbreeding of RyR2<sup>R4496C+/-</sup> knock-in mutant with CaMKII $\delta_C$  transgenic mice induced hypertrophy, ventricular dilation and increased mortality. There was a significant enlargement of hearts and single myocytes from CaMKII $\delta_C$ /RyR2<sup>R4496C</sup> double mutant and CaMKII $\delta_C$  transgenic mice by age of 8 to 14 weeks. However, the hearts and single myocytes of RyR2<sup>R4496C+/-</sup> mice did not show any abnormalities (Fig. 13A). After cardiectomy, when the heart was carefully separated from other tissues the heart as well as body weight was assessed. Heart weight/body weight ratio in CaMKII $\delta_C$ /RyR2<sup>R4496C</sup> double mutant (19.57 $\pm$ 0.72 mg/g; n=34) and CaMKII $\delta_C$  transgenic (20.78 $\pm$ 1.25 mg/g; n=29) mice was significantly increased about 3-fold versus RyR2<sup>R4496C+/-</sup> (7.33 $\pm$ 0.23 mg/g; n=25; P<0.05) and WT mice (7.17 $\pm$ 0.15 mg/g; n=29; P<0.05) (Fig. 13B). In all cases the increase in ventricular mass is paralleled by myocyte hypertrophy (Bers, 2001). Quantitative analysis of cardiomyocyte cell volume from 12-week-old mice gave values of 42.57 $\pm$ 1.95 pl for CaMKII $\delta_C$ /RyR2<sup>R4496C</sup> (n=76), 36.71 $\pm$ 1.76 pl for CaMKII $\delta_C$  (n=110) versus 21.02 $\pm$ 1.15 pl for RyR2<sup>R4496C+/-</sup> (n=88; P<0.05) and 23.00 $\pm$ 1.26 pl for WT (n=91; P<0.05). The myocytes were enlarged (as judged length/width ratio) in CaMKII $\delta_C$ /RyR2<sup>R4496C</sup> (8.34 $\pm$ 0.26; n=76) and CaMKII $\delta_C$  (8.15 $\pm$ 0.19; n=110) mice versus RyR2<sup>R4496C+/-</sup> (5.25 $\pm$ 0.09; n=88; P<0.05) and WT (5.33 $\pm$ 0.12; n=90; P<0.05) (Fig. 13A).

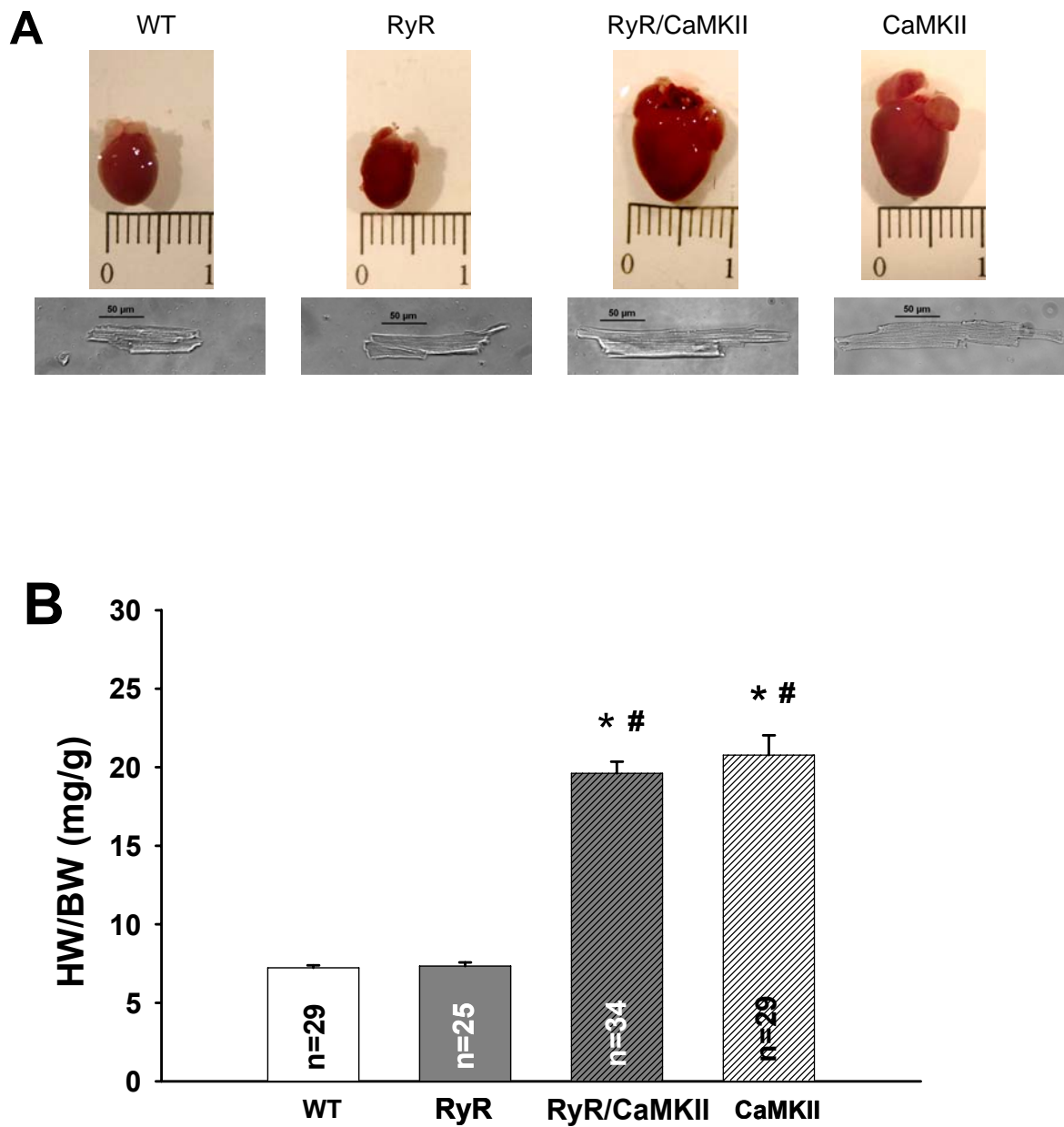


**Figure 13. CaMKII $\delta_C$  overexpression in mouse hearts induced cardiac hypertrophy. (A)** Representative images of whole hearts and ventricular myocytes isolated from WT, RyR2<sup>R4496C/+</sup>, CaMKII $\delta_C$ /RyR2<sup>R4496C</sup> and CaMKII $\delta_C$  mice at 13 weeks of age showing heart hypertrophy in CaMKII $\delta_C$ /RyR2<sup>R4496C</sup> and CaMKII $\delta_C$  mice. **(B)** Average ratios of heart weight/body weight in WT, RyR2<sup>R4496C/+</sup>, CaMKII $\delta_C$ /RyR2<sup>R4496C</sup> and CaMKII $\delta_C$  mice. \*P<0.05 versus WT. # P<0.05 versus RyR2<sup>R4496C/+</sup>.

Interestingly, while RyR2<sup>R4496C+/-</sup> knock-in mice had a normal life span and CaMKII $\delta_C$  transgenic mice, had a premature mortality rate of only 20 % until 10 weeks, CaMKII $\delta_C$ /RyR2<sup>R4496C</sup> double mutant died spontaneously with only 50% survival after 10 weeks ( $P < 0.05$  versus RyR2<sup>R4496C+/-</sup>, CaMKII $\delta_C$ , and WT; Fig. 14).

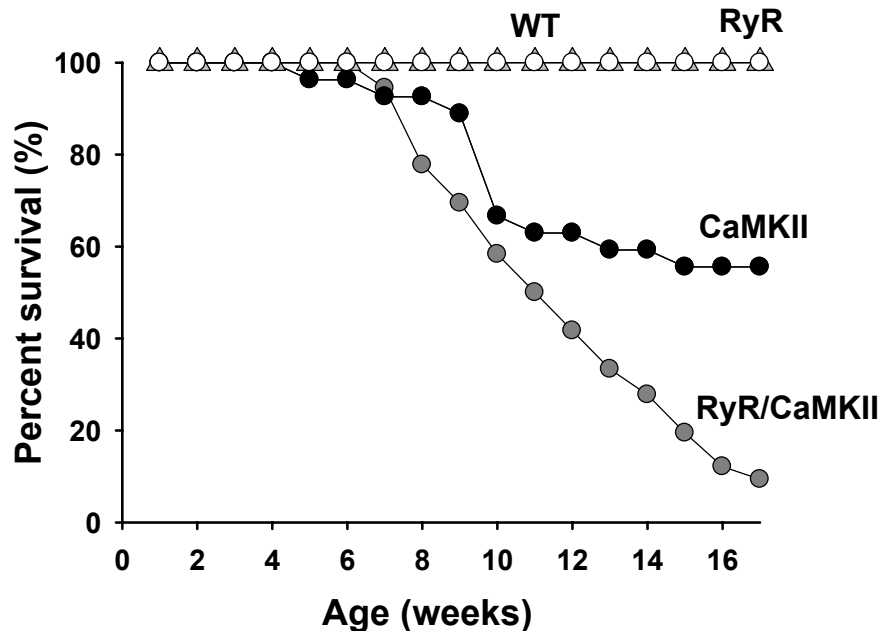


**Figure 14. Overexpression of CaMKII $\delta_C$  led to sudden premature death.** Survival curve for WT (n=37), RyR2<sup>R4496C+/-</sup> (n=28), CaMKII $\delta_C$ /RyR2<sup>R4496C</sup> (n=35) and CaMKII $\delta_C$  (n=22) mice with significantly impaired survival for CaMKII $\delta_C$ /RyR2<sup>R4496C</sup> double mutant mice as compared to the RyR2<sup>R4496C+/-</sup> knock-in mutant, CaMKII $\delta_C$  transgenic, and WT mice.

### 4.3 Echocardiographic analysis of RyR2<sup>R4496C+/-</sup>, CaMKII $\delta_C$ /RyR2<sup>R4496C</sup>, CaMKII $\delta_C$ and WT mice

To analyze the consequences of the R4496C knock-in mutation in vivo, M-mode echocardiography of RyR2<sup>R4496C+/-</sup>, CaMKII $\delta_C$ /RyR2<sup>R4496C</sup>, CaMKII $\delta_C$  and WT mice was performed as described in the Methods (3.11). The hearts of RyR2<sup>R4496C+/-</sup> knock-in mice showed normal dimensions as well as contractile function in the echocardiographic measurements. In stark contrast, CaMKII $\delta_C$ /RyR2<sup>R4496C</sup> double mutant and CaMKII $\delta_C$  transgenic mice exhibited evident cardiac remodeling and systolic dysfunction (Fig. 15). Left ventricular end diastolic diameter (LVEDD; Fig. 16A) in CaMKII $\delta_C$ /RyR2<sup>R4496C</sup>

( $5.45 \pm 0.4$  mm;  $n=6$ ) and  $\text{CaMKII}\delta_C$  ( $5.77 \pm 0.7$  mm;  $n=5$ ) mice was significantly increased as compared to  $\text{RyR2}^{\text{R4496C}/-}$  ( $3.55 \pm 0.2$  mm;  $n=5$ ;  $P < 0.05$ ) or WT ( $3.02 \pm 0.3$  mm;  $n=6$ ;  $P < 0.05$ ).

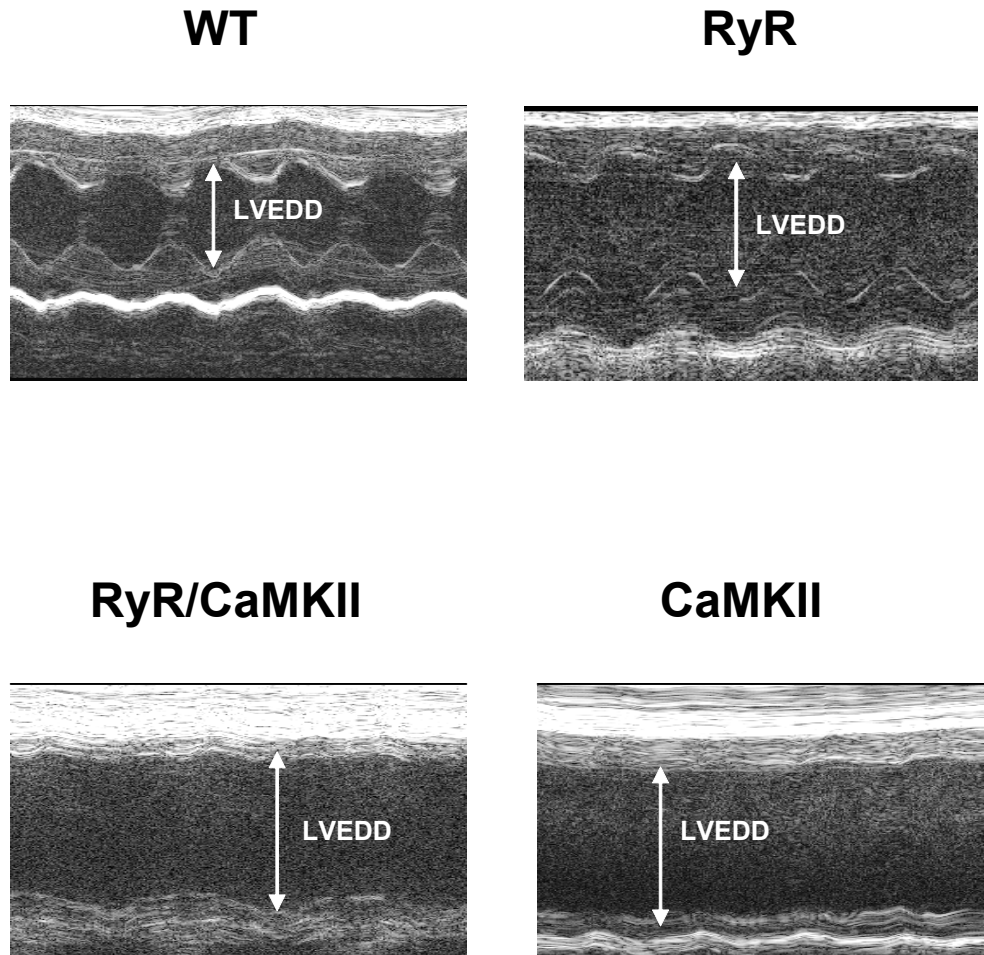


**Figure 15. Dilated cardiomyopathy and cardiac dysfunction at the whole heart level in vivo in  $\text{CaMKII}\delta_C/\text{RyR2}^{\text{R4496C}}$  and  $\text{CaMKII}\delta_C$  mice.** Representative M-mode images of echocardiography in WT,  $\text{RyR2}^{\text{R4496C}/-}$ ,  $\text{CaMKII}\delta_C/\text{RyR2}^{\text{R4496C}}$  and  $\text{CaMKII}\delta_C$  mice at 10-13 weeks of age.

In parallel, left ventricular posterior wall thickness (LVPW; Fig. 16B) decreased significantly in both  $\text{CaMKII}\delta_C/\text{RyR2}^{\text{R4496C}}$  double mutant ( $0.59 \pm 0.03$  mm;  $n=6$ ) and  $\text{CaMKII}\delta_C$  transgenic mice ( $0.52 \pm 0.04$  mm;  $n=5$ ) versus  $\text{RyR2}^{\text{R4496C}/-}$  ( $0.77 \pm 0.06$  mm;  $n=5$ ;  $P < 0.05$ ) and WT ( $0.96 \pm 0.06$  mm;  $n=6$ ;  $P < 0.05$ ).



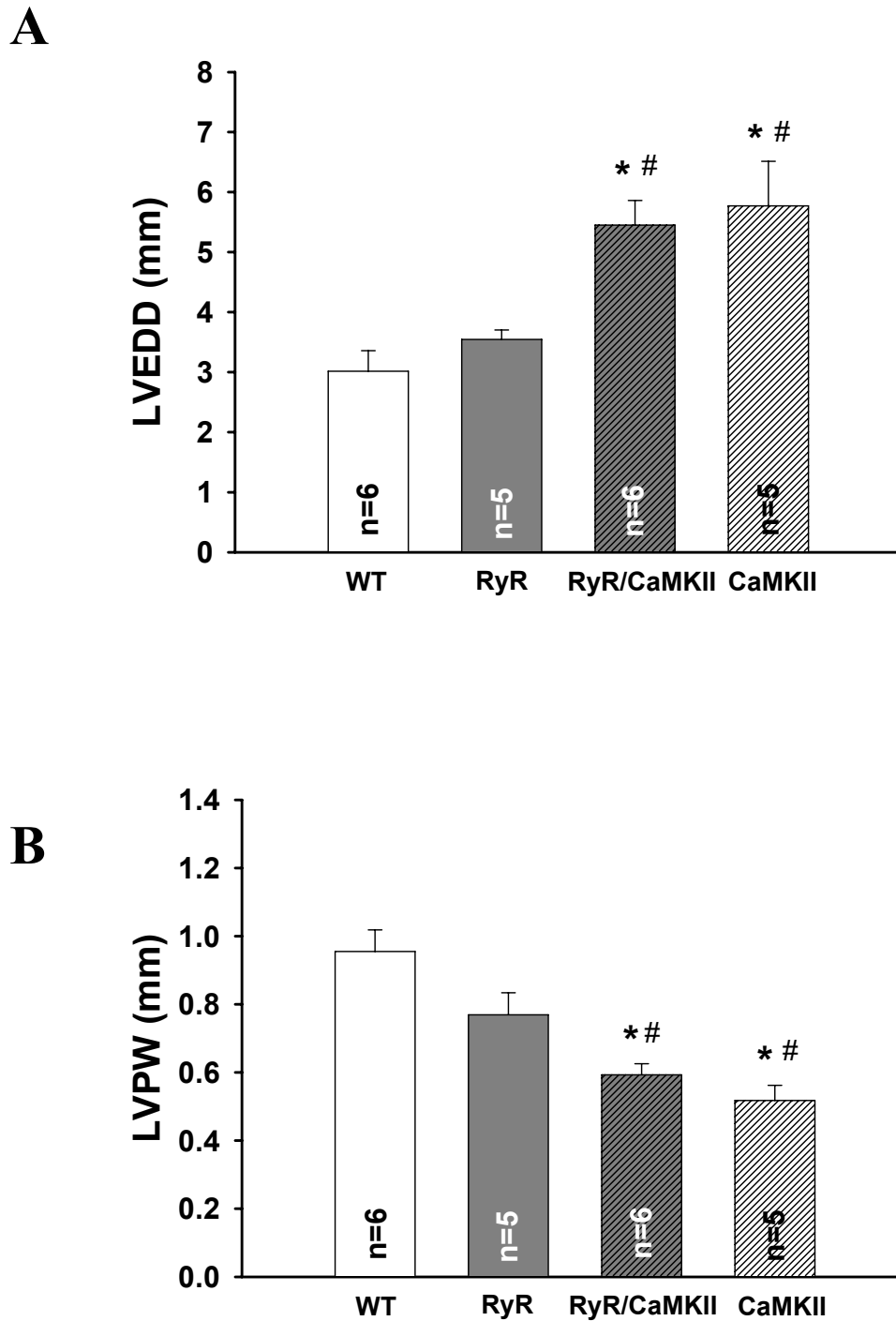


**Figure 16.** Averaged structural echocardiographic parameters for WT, RyR<sup>R4496C+/-</sup>, CaMKII $\delta$ <sub>C</sub>/RyR<sup>R4496C</sup> and CaMKII $\delta$ <sub>C</sub> mice. Data are presented for left ventricular end diastolic diameter (LVEDD) and left ventricular posterior wall thickness (LVPW). Ventricular dilation and wall thinning in CaMKII $\delta$ <sub>C</sub>/RyR<sup>R4496C</sup> and CaMKII $\delta$ <sub>C</sub> mice can be seen. \*P<0.05 versus WT. # P<0.05 versus RyR<sup>R4496C+/-</sup>.

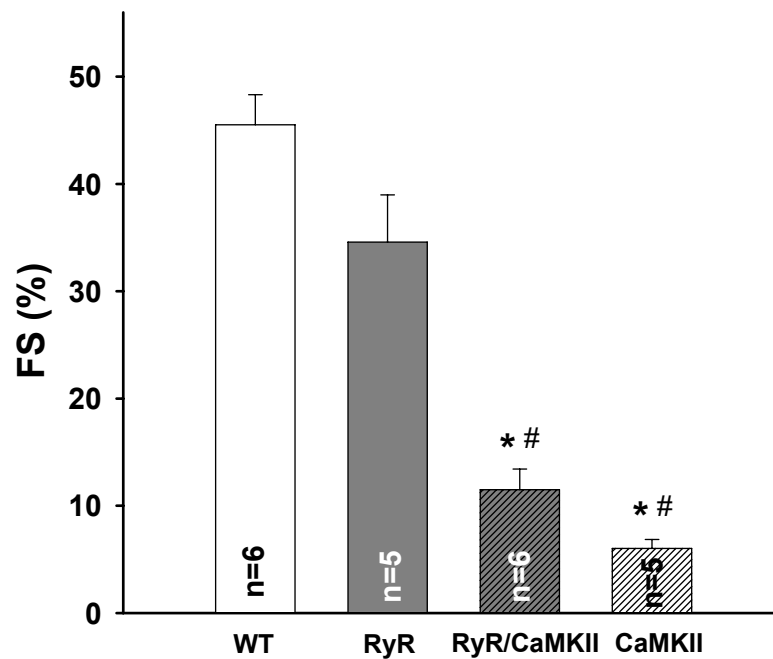


**Figure 17. Averaged functional echocardiographic parameter for WT, RyR2<sup>R4496C/+</sup>, CaMKII $\delta_C$ /RyR2<sup>R4496C</sup> and CaMKII $\delta_C$  mice.** Data are presented for fractional shortening (FS). Percentage of fractional shortening calculated as  $100 \times ((LVEDD - LVESD) / LVEDD)$ . LVEDD indicates left ventricular end diastolic diameter; LVESD indicates left ventricular end systolic diameter. Impaired fractional shortening indicated contractile dysfunction pointing to heart failure in CaMKII $\delta_C$ /RyR2<sup>R4496C</sup> and CaMKII $\delta_C$  mice. \*P<0.05 versus WT. # P<0.05 versus RyR2<sup>R4496C/+</sup>.

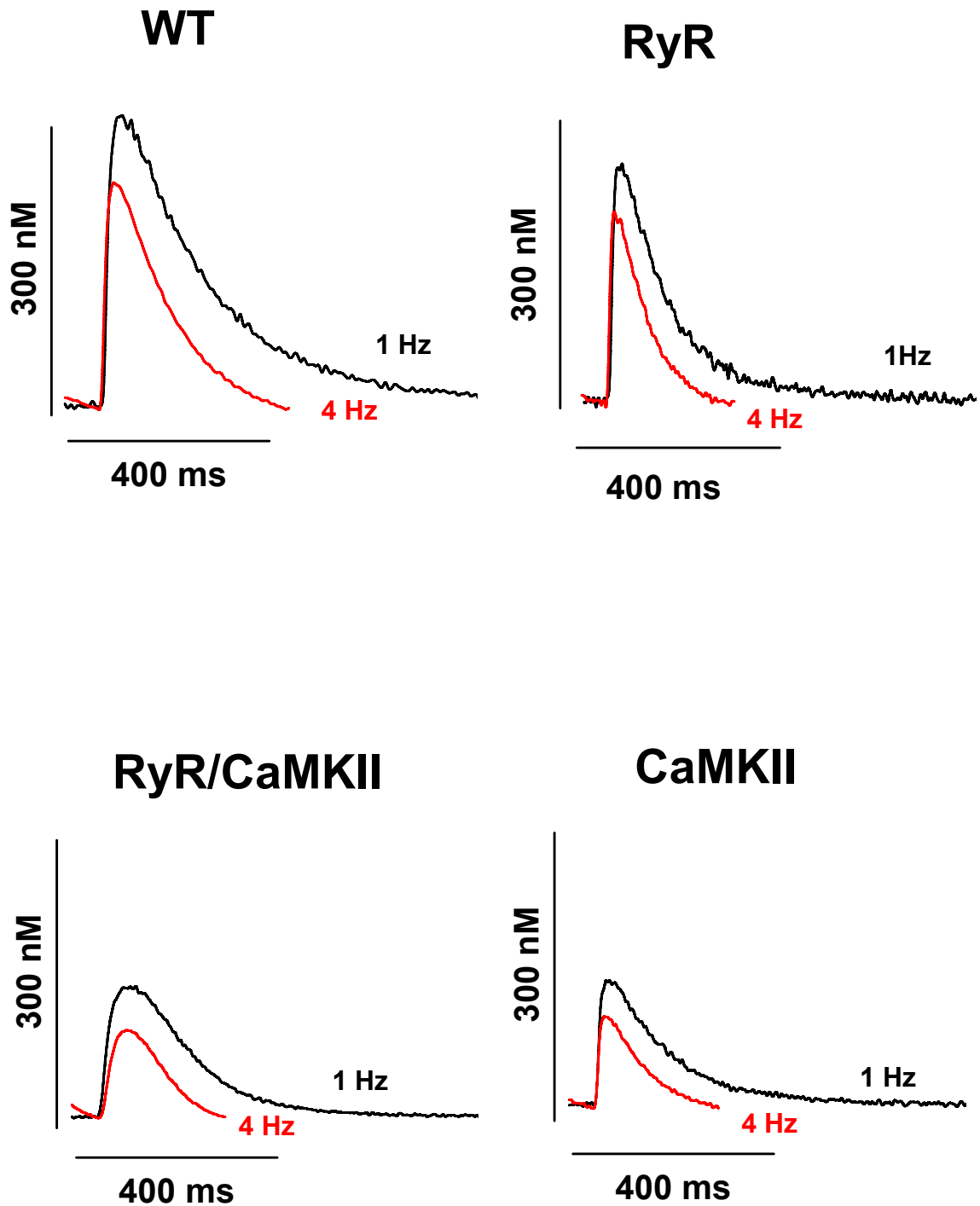
Most importantly, fractional shortening was dramatically reduced in CaMKII $\delta_C$ /RyR2<sup>R4496C</sup> (11.50±1.9%; n=6) and CaMKII $\delta_C$  (5.85±1%; n=5) in contrast to RyR2<sup>R4496C/+</sup> (34.58±4.4%; n=5; P<0.05) and WT (45.52±2.8%; n=6; P<0.05; Fig. 17). Alteration of these parameters indicates development of contractile dysfunction in a heart failure phenotype in CaMKII $\delta_C$ /RyR2<sup>R4496C</sup> double mutant very similar to CaMKII $\delta_C$  transgenic mice. It should be noted that none of these parameters was significantly altered in RyR2<sup>R4496C/+</sup> knock-in mice as compared to WT.

## 4.4 Analysis of cardiomyocyte shortening and $\text{Ca}^{2+}$ transients using an epifluorescence microscope

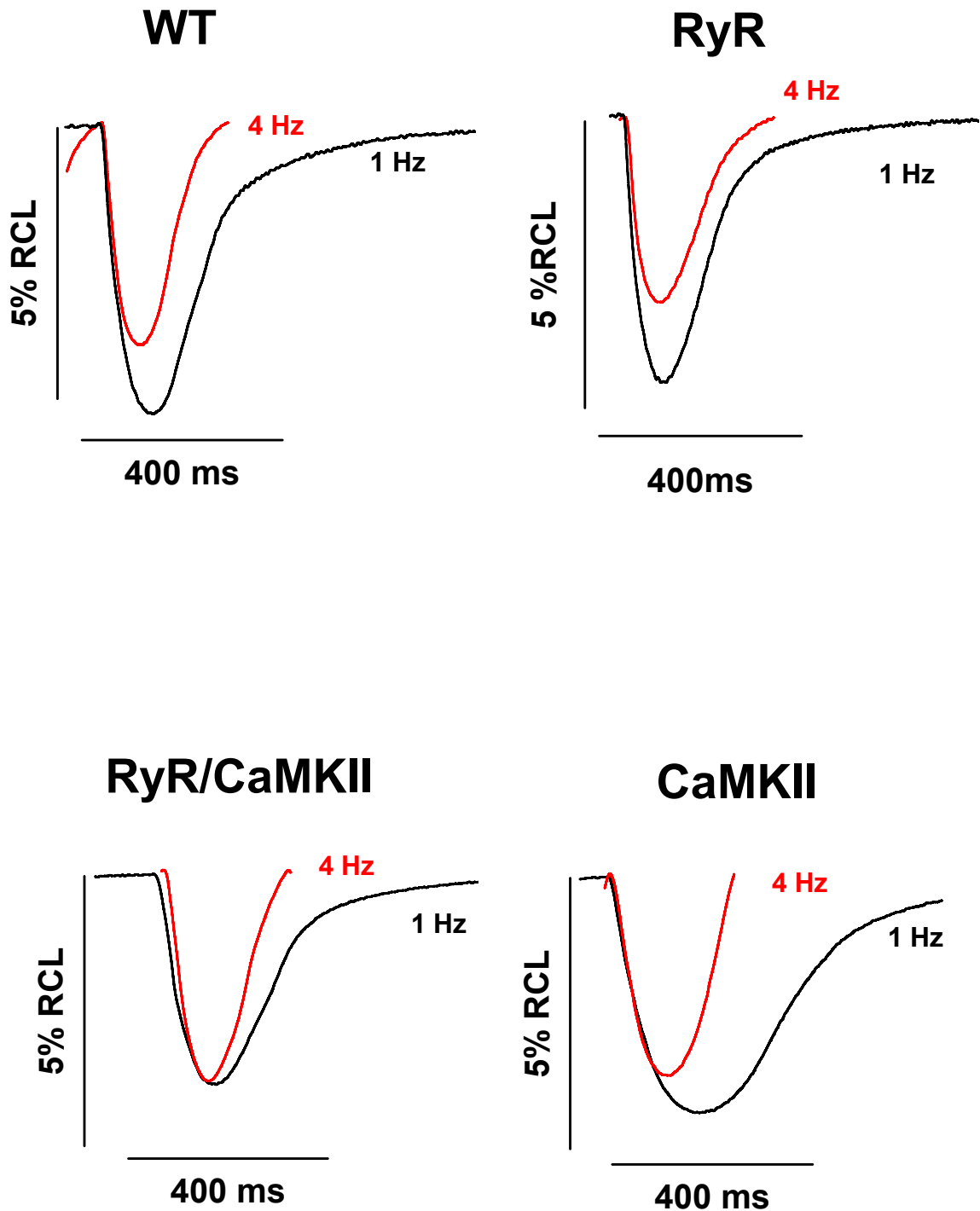
### 4.4.1 Fractional shortening and intracellular $\text{Ca}^{2+}$ transients

The functional effect of the RyR2<sup>R4496C/+</sup> knock-in mutation and CaMKII $\delta$ <sub>C</sub>/RyR2<sup>R4496C</sup> cross-bred models as well as CaMKII $\delta$ <sub>C</sub> transgenic overexpression, was probed by measuring intracellular  $\text{Ca}^{2+}$  transients in vitro using a  $\text{Ca}^{2+}$ -fluorescent dye in Fluo-3-loaded isolated ventricular myocytes. Fractional shortening was simultaneously assessed. Isolation of mouse ventricular myocytes was performed using enzymatic digestion as described in the Methods (3.8). The images of the myocytes were recorded using a camera (MyoCam) and displayed on a monitor. The fluorescent dye was excited by a 75 W xenon arc lamp at 480±15 nm on the stage of a Nikon Eclipse TE200-U inverted microscope as described in the Methods (3.9). Myocytes were field-stimulated at 1 Hz and 37°C until steady-state was achieved and shortening was measured using a sarcomere length detection system. After steady-state conditions were achieved, stimulation frequency was increased stepwise from 1 Hz to 2, 4 and 8 Hz. The cells selected for data analysis had clear striation, rod-shaped form and stable diastolic length.

In cardiac muscle,  $\text{Ca}^{2+}$  directly contributes to electrical and contractile activity and is central to E-C coupling (Bers, 2001; Bers, 2002). Alterations in intracellular  $\text{Ca}^{2+}$  could also result in hypertrophy and heart failure. The amplitude of the  $\text{Ca}^{2+}$  transient is generated mainly by SR  $\text{Ca}^{2+}$  release in the murine heart and directly determines the extent of contractile force in cardiomyocytes. As shown by the original traces in Figures 18&19, both twitch  $\text{Ca}^{2+}$  transient amplitude and shortening were significantly decreased in CaMKII $\delta$ <sub>C</sub>/RyR2<sup>R4496C</sup> and CaMKII $\delta$ <sub>C</sub> as compared to RyR2<sup>R4496C/+</sup> and WT myocytes. Average data (Fig. 20) show that  $\text{Ca}^{2+}$  transient amplitudes were only 215.27±7.73 nM in CaMKII $\delta$ <sub>C</sub>/RyR2<sup>R4496C</sup> (n=46) and 194.54±9.25 nM in CaMKII $\delta$ <sub>C</sub> (n=36) compared to RyR2<sup>R4496C/+</sup> with 435.58±20.16 nM (n=51; P<0.05) and WT with 466.68±23.65 nM (n=61; P<0.05) at a baseline frequency of 1 Hz. Accordingly, fractional shortening of isolated cardiomyocytes at 1 Hz was also significantly impaired in CaMKII $\delta$ <sub>C</sub>/RyR2<sup>R4496C</sup> (3.32±0.19% resting cell length; n=46) and CaMKII $\delta$ <sub>C</sub> (3.34±0.24% resting cell length; n=36) mice versus RyR2<sup>R4496C/+</sup> (3.92±0.21% resting cell length, n=51; P<0.05) and WT (4.42±0.23% resting cell length; n=61; P<0.05). Reduction in twitch contraction in CaMKII $\delta$ <sub>C</sub>/RyR2<sup>R4496C</sup> and CaMKII $\delta$ <sub>C</sub> mice was expected, because this is seen in almost all heart failure models.



**Figure 18.** Frequency-dependent changes in  $\text{Ca}^{2+}$  transient amplitude in isolated cardiomyocytes measured using Fluo-3. Original recordings for  $\text{Ca}^{2+}$  transient amplitude at 1 and 4 Hz showing a decrease in intracellular  $\text{Ca}^{2+}$  transients in CaMKII $\delta_C$ /RyR2<sup>R4496C</sup> and CaMKII $\delta_C$  versus RyR2<sup>R4496C/+</sup> and WT. The graphs show the time-course of  $\text{Ca}^{2+}$  transients during a single systole-diastole cycle.

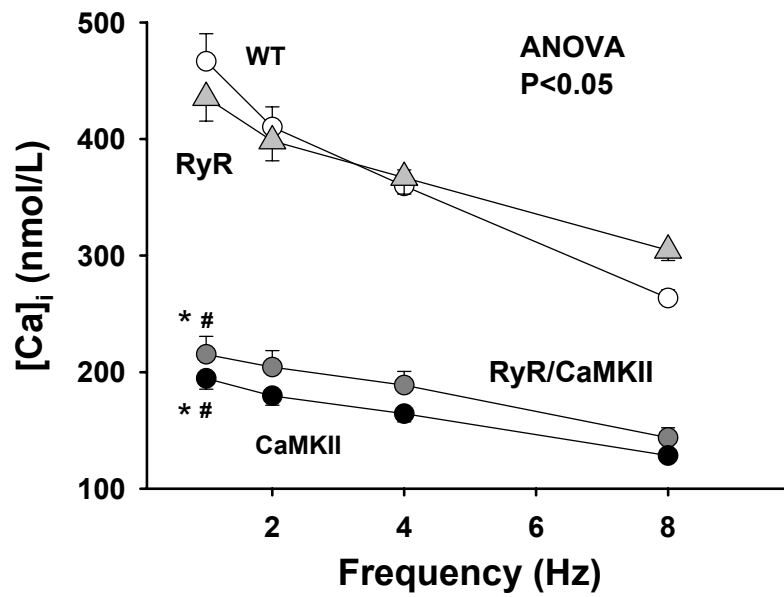
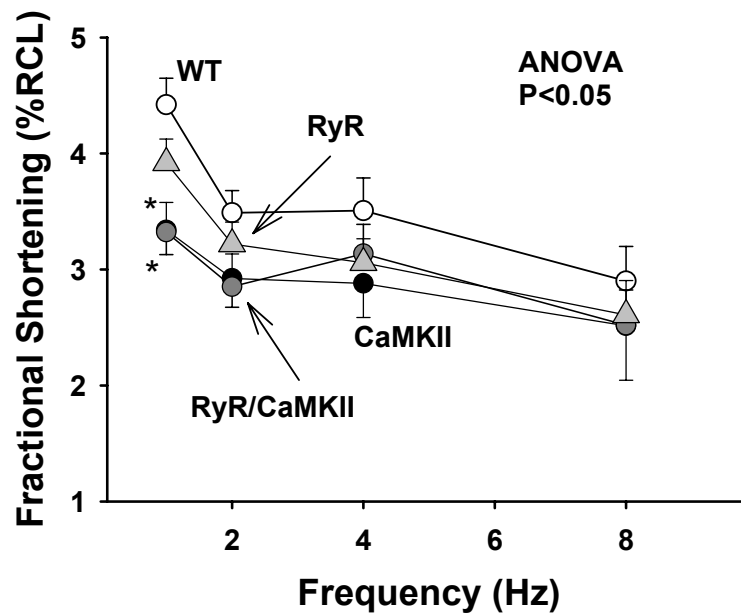


**Figure 19.** Frequency-dependent changes in fractional shortening in isolated cardiomyocytes measured using a sarcomere length detection system. Original recordings for twitch shortening (% RCL=% resting cell length) at 1 and 4 Hz showing impaired fractional shortening in CaMKII $\delta_c$ /RyR2<sup>R4496C</sup> and CaMKII $\delta_c$  versus RyR2<sup>R4496C+/-</sup> and WT. The graphs show the time-course of cell length during a single systole-diastole cycle.

In addition, while diastolic  $\text{Ca}^{2+}$  was only nonsignificantly increased in  $\text{RyR2}^{\text{R4496C}/-}$  ( $162 \pm 23$  nM;  $n=24$ ) versus WT ( $138 \pm 16$  nM;  $n=24$ ), it was dramatically reduced in  $\text{CaMKII}\delta_{\text{C}}/\text{RyR2}^{\text{R4496C}}$  ( $81 \pm 11$  nM;  $n=27$ ) and  $\text{CaMKII}\delta_{\text{C}}$  ( $80 \pm 13$  nM;  $n=18$ ) mice as compared to  $\text{RyR2}^{\text{R4496C}/-}$  ( $P < 0.05$ ) and WT ( $P < 0.05$ ).

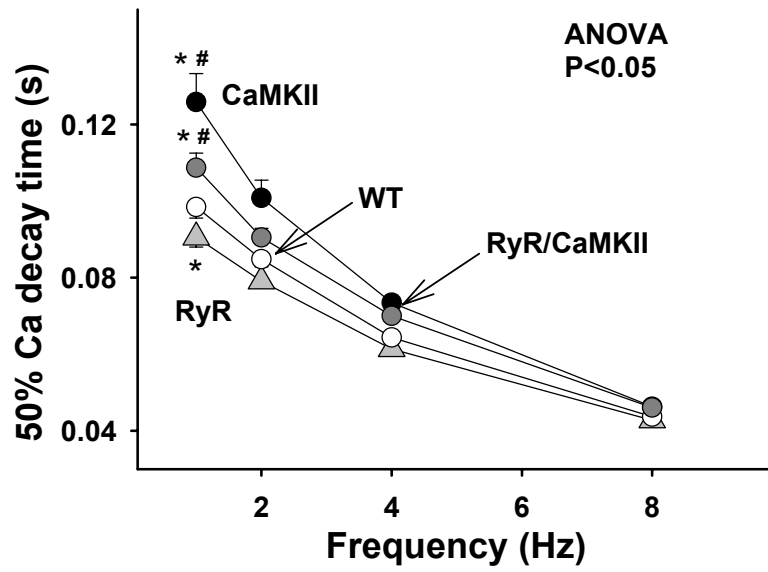
#### ***4.4.2 Frequency-dependence of shortening, intracellular $\text{Ca}^{2+}$ transients and relaxation***

Increasing the stimulation frequency of cardiac muscle not only modifies the amplitude but also the relaxation kinetics of contractile force. A positive or negative force-frequency relationship (staircase) in cardiac muscle depends on the  $\text{Ca}^{2+}$  loading status of the SR and recovery of the RyR2 from inactivation. Mouse myocytes often show a negative force-frequency relationship (Bers, 2001). To determine whether increased stimulation rates lead to changes in fractional shortening of myocytes (i.e. force-frequency relationship) and whether this may be due to altered intracellular  $\text{Ca}^{2+}$ , cell shortening and  $\text{Ca}^{2+}$  transient amplitude at different stimulation frequencies were assessed. Increasing stimulation rates stepwise from 1 Hz to 2, 4 and 8 Hz led to decreased intracellular  $\text{Ca}^{2+}$  transient amplitudes and fractional shortening in myocytes isolated from  $\text{CaMKII}\delta_{\text{C}}/\text{RyR2}^{\text{R4496C}}$  and  $\text{CaMKII}\delta_{\text{C}}$  mice as compared to  $\text{RyR2}^{\text{R4496C}/-}$  and WT with a negative staircase in all groups (Fig. 20). The time course of twitches and  $\text{Ca}^{2+}$  transients is critically dependent on SR  $\text{Ca}^{2+}$  uptake and is physiologically accelerated at high stimulation rates (Bers, 2001). Figure 21 shows time courses of relaxation and  $\text{Ca}^{2+}$  decline during twitches at different stimulation frequencies. Half-relaxation time ( $\text{RT}_{50\%}$ ) for fractional shortening in cardiomyocytes stimulated at the baseline frequency of 1 Hz was significantly prolonged in  $\text{CaMKII}\delta_{\text{C}}/\text{RyR2}^{\text{R4496C}}$  ( $\text{RT}_{50\%}$ :  $110 \pm 6$  ms;  $n=46$ ) and  $\text{CaMKII}\delta_{\text{C}}$  mice ( $\text{RT}_{50\%}$ :  $128 \pm 10$  ms;  $n=36$ ) relative to  $\text{RyR2}^{\text{R4496C}/-}$  ( $\text{RT}_{50\%}$ :  $86 \pm 5$  ms;  $n=51$ ;  $P < 0.05$ ) and WT ( $\text{RT}_{50\%}$ :  $79 \pm 5$  ms;  $n=61$ ;  $P < 0.05$ ). However, there was no difference between  $\text{RyR2}^{\text{R4496C}/-}$  and WT. Half-relaxation time of  $\text{Ca}^{2+}$  decay at 1 Hz was significantly prolonged for  $\text{CaMKII}\delta_{\text{C}}/\text{RyR2}^{\text{R4496C}}$  (50%  $\text{Ca}^{2+}$  decay:  $109 \pm 4$  ms;  $n=46$ ) and  $\text{CaMKII}\delta_{\text{C}}$  ( $\text{RT}_{50\%}$ :  $125 \pm 7$  ms;  $n=36$ ) myocytes as compared to  $\text{RyR2}^{\text{R4496C}/-}$  (50%  $\text{Ca}^{2+}$  decay:  $90 \pm 3$  ms;  $n=51$ ;  $P < 0.05$ ) and WT (50%  $\text{Ca}^{2+}$  decay:  $98 \pm 3$  ms;  $n=61$ ;  $P < 0.05$ ), but showed significantly faster  $\text{Ca}^{2+}$  removal from the cytosol in  $\text{RyR2}^{\text{R4496C}/-}$  versus WT. Prolongation in relaxation parameters which were observed in  $\text{CaMKII}\delta_{\text{C}}/\text{RyR2}^{\text{R4496C}}$  double mutant and  $\text{CaMKII}\delta_{\text{C}}$  transgenic mice indicated an altered basal SR  $\text{Ca}^{2+}$  ATPase function.

**A****B**

**Figure 20. Frequency-dependent changes in  $\text{Ca}^{2+}$  transients and fractional shortening.** Average values for (A)  $\text{Ca}^{2+}$  transients and (B) twitch shortening at increasing stimulation rates stepwise from 1 Hz to 2, 4 and 8 Hz which led to decreased intracellular  $\text{Ca}^{2+}$  transients and fractional shortening in myocytes isolated from  $\text{CaMKII}\delta_{\text{C}}/\text{RyR}2^{\text{R4496C}}$  (n=46) and  $\text{CaMKII}\delta_{\text{C}}$  (n=36) mice compared to  $\text{RyR}2^{\text{R4496C}/-}$  (n=51) and WT (n=61) and showed negative staircase in all mice. \*P<0.05 (ANOVA) versus WT. # P<0.05 (ANOVA) versus  $\text{RyR}2^{\text{R4496C}/-}$ .

A



B

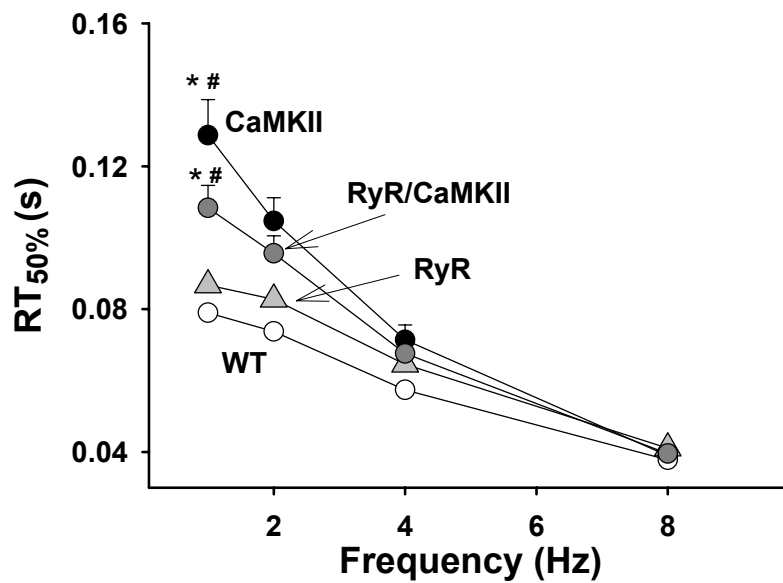


**Figure 21. Frequency-dependent acceleration of relaxation.** Mean data of half-relaxation time for (A)  $\text{Ca}^{2+}$  transient decay and (B) fractional shortening ( $\text{RT}_{50\%}$ ) at increasing stimulation rates stepwise from 1 Hz to 2, 4 and to 8 Hz which were significantly prolonged in  $\text{CaMKII}\delta_{\text{C}}/\text{RyR}2^{\text{R4496C}}$  ( $n=46$ ) and  $\text{CaMKII}\delta_{\text{C}}$  ( $n=36$ ) myocytes versus  $\text{RyR}2^{\text{R4496C}+/}$  ( $n=51$ ) and WT ( $n=61$ ). \* $P<0.05$  (ANOVA) versus WT. #  $P<0.05$  (ANOVA) versus  $\text{RyR}2^{\text{R4496C}+/}$ .



Frequency-dependent acceleration of relaxation (FDAR) is an intrinsic physiological mechanism, which allows more rapid ventricular diastolic filling at higher heart rates possibly due to CaMKII-dependent increased SR  $\text{Ca}^{2+}$  uptake (Maier and Bers, 2002). FDAR for  $\text{Ca}^{2+}$  transient amplitude and twitch shortening (measured in parallel) at 1 Hz to 8 Hz stimulation rates was apparent in all cells, but it was significantly enhanced in CaMKII $\delta_C$ /RyR2<sup>R4496C</sup> and CaMKII $\delta_C$  myocytes versus RyR2<sup>R4496C+/-</sup> and WT. Half-relaxation time in WT twitch shortening decreased from 79 $\pm$ 5 ms at 1 Hz to 38 $\pm$ 1 ms at 8 Hz, in RyR2<sup>R4496C+/-</sup> from 89 $\pm$ 4 ms at 1 Hz to 41 $\pm$ 1 ms at 8 Hz, in CaMKII $\delta_C$ /RyR2<sup>R4496C</sup> from 108 $\pm$ 6 ms at 1 Hz to 40 $\pm$ 1 ms at 8 Hz and in CaMKII $\delta_C$  from 128 $\pm$ 10 ms at 1 Hz to 39 $\pm$ 2 ms at 8 Hz. Half-relaxation time of  $\text{Ca}^{2+}$  decay declined from 98 $\pm$ 3 ms at 1 Hz to 44 $\pm$ 1 ms at 8 Hz in WT, 90 $\pm$ 3 ms at 1 Hz to 43 $\pm$ 1 ms at 8 Hz in RyR2<sup>R4496C+/-</sup>, 109 $\pm$ 4 ms at 1 Hz to 46 $\pm$ 1 ms at 8 Hz in CaMKII $\delta_C$ /RyR2<sup>R4496C</sup> and from 125 $\pm$ 7 ms at 1 Hz to 46 $\pm$ 1 ms at 8 Hz in CaMKII $\delta_C$ . The index of FDAR (as ratio of  $\text{Ca}^{2+}$  decline and twitch shortening at 8 Hz versus 1 Hz) was 0.42 $\pm$ 0.3 in CaMKII $\delta_C$ /RyR2<sup>R4496C</sup> and 0.37 $\pm$ 0.1 in CaMKII $\delta_C$  versus 0.47 $\pm$ 0.3 in RyR2<sup>R4496C+/-</sup> and 0.45 $\pm$ 0.3 in WT cardiac myocytes. However, it was even more dramatic for FDAR of shortening with 0.37 $\pm$ 0.2 in CaMKII $\delta_C$ /RyR2<sup>R4496C</sup> and 0.30 $\pm$ 0.2 versus 0.46 $\pm$ 0.2 in RyR2<sup>R4496C+/-</sup> and 0.48 $\pm$ 0.2 in WT.

#### 4.4.3 SR $\text{Ca}^{2+}$ content and NCX function

To analyze whether altered  $\text{Ca}^{2+}$  transient amplitudes in CaMKII $\delta_C$ /RyR2<sup>R4496C</sup> and CaMKII $\delta_C$  mice result from changes of SR  $\text{Ca}^{2+}$  content, we measured caffeine-induced  $\text{Ca}^{2+}$  transients. Application of caffeine caused a rapid increase in intracellular  $\text{Ca}^{2+}$  concentration as a result of sudden SR  $\text{Ca}^{2+}$  release. As shown by the original traces in Figure 22,  $\text{Ca}^{2+}$  transient amplitude after rapid application of caffeine was significantly decreased in CaMKII $\delta_C$ /RyR2<sup>R4496C</sup> and CaMKII $\delta_C$  versus RyR2<sup>R4496C+/-</sup> and WT myocytes. Average data (Fig. 23) show that the caffeine-induced  $\text{Ca}^{2+}$  transient after 1 Hz stimulation in RyR2<sup>R4496C+/-</sup> (932.60 $\pm$ 89.44 nM; n=31) was not significantly different from WT (1065.44 $\pm$ 46.49 nM; n=24). However, the  $\text{Ca}^{2+}$  transient after caffeine application was significantly smaller by 36% in CaMKII $\delta_C$ /RyR2<sup>R4496C</sup> (383.00 $\pm$ 16.77 nM; n=23) and by 34% in CaMKII $\delta_C$  (361.22 $\pm$ 24.52 nM; n=20) myocytes as compared to RyR2<sup>R4496C+/-</sup> (P<0.05) and WT (P<0.05), suggesting a dramatically decreased SR  $\text{Ca}^{2+}$  content in these double mutant and transgenic mice. This may explain the reduction in  $\text{Ca}^{2+}$  transient amplitude and impairment of contractile function of intact myocytes isolated from CaMKII $\delta_C$ /RyR2<sup>R4496C</sup> and CaMKII $\delta_C$  mice.

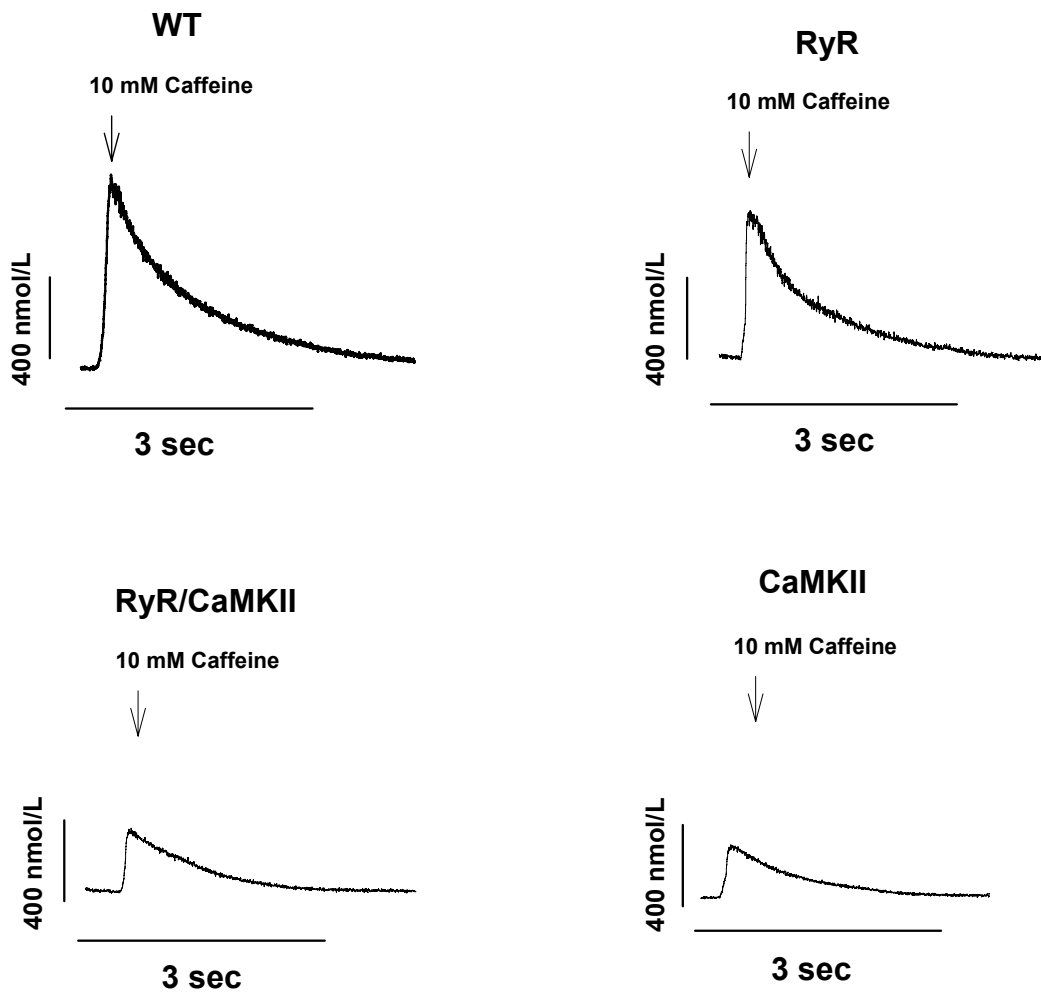


**Figure 22. Caffeine-induced Ca<sup>2+</sup> transients.** Representative Ca<sup>2+</sup> traces after rapid application of 10 mM caffeine at a stimulation frequency of 1 Hz showing decreased SR Ca<sup>2+</sup> content in CaMKII $\delta_C$ /RyR2<sup>R4496C</sup> and CaMKII $\delta_C$  myocytes versus RyR2<sup>R4496C/+</sup> and WT.

The subsequent decline of intracellular Ca<sup>2+</sup> concentration during caffeine application results from extrusion of Ca<sup>2+</sup> across the sarcolemma mainly via NCX and thus allows to assess NCX function by determining the exponential rate time-constant ( $\tau$ ) of Ca<sup>2+</sup> transient amplitude decline (Bers, 2001). There was a tendency for increased NCX function in RyR2<sup>R4496C/+</sup> ( $\tau$  1.01 $\pm$ 0.07 sec; n=31), CaMKII $\delta_C$ /RyR2<sup>R4496C</sup> ( $\tau$  0.99 $\pm$ 0.12 sec; n=23) and CaMKII $\delta_C$  ( $\tau$  1.04 $\pm$ 0.06 sec; n=16) mice versus WT ( $\tau$  1.15 $\pm$ 0.07 sec; n=24), but the data did not reach significant differences (Fig. 24).

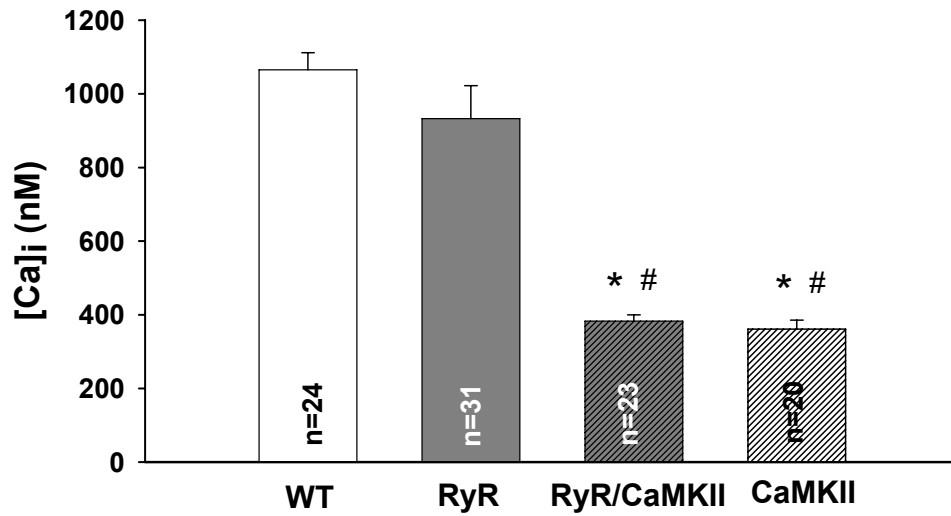


**Figure 23. SR Ca<sup>2+</sup> content in cardiomyocytes.** Average data for caffeine-induced Ca<sup>2+</sup> transients showing a dramatic decrease in SR Ca<sup>2+</sup> content in isolated cardiomyocytes from CaMKII $\delta_C$ /RyR2<sup>R4496C</sup>, CaMKII $\delta_C$  versus RyR2<sup>R4496C+/-</sup> and WT mice. \*P<0.05 versus WT. # P<0.05 versus RyR2<sup>R4496C+/-</sup>.

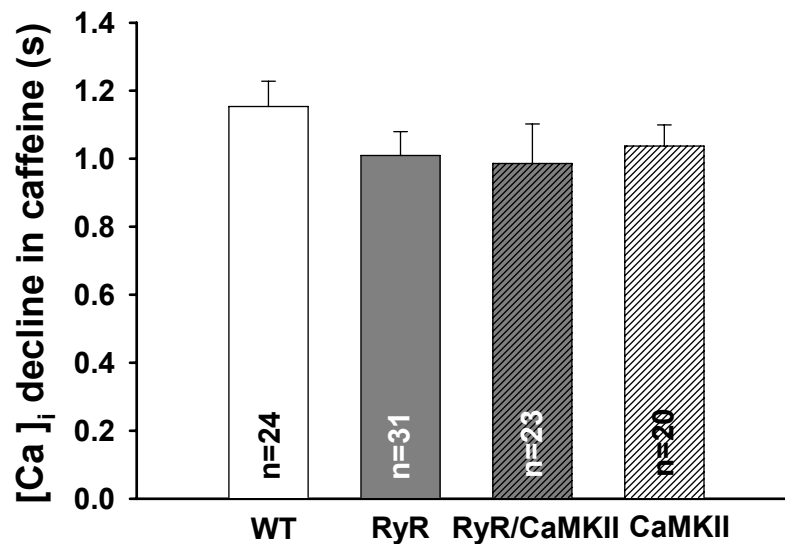


**Figure 24. NCX function.** Mean data for Ca<sup>2+</sup> transient decline during caffeine-induced Ca<sup>2+</sup> transients indicating a slightly increased NCX function in RyR2<sup>R4496C+/-</sup>, CaMKII $\delta_C$ /RyR2<sup>R4496C</sup> and CaMKII $\delta_C$  myocytes.

The ratio of individual twitch  $\text{Ca}^{2+}$  transient amplitude/cafeine-induced  $\text{Ca}^{2+}$  transient (an index of SR fractional  $\text{Ca}^{2+}$  release, or amount of  $\text{Ca}^{2+}$  released during a twitch versus that  $\text{Ca}^{2+}$  stored in the SR) was significantly increased in  $\text{CaMKII}\delta_{\text{C}}/\text{RyR2}^{\text{R4496C}}$  ( $63.21 \pm 2.20$ ;  $n=23$ ) and  $\text{CaMKII}\delta_{\text{C}}$  ( $61.69 \pm 2.24$ ;  $n=17$ ) versus WT cardiomyocytes ( $48.30 \pm 1.63$ ;  $n=24$ ;  $P < 0.05$ ), even though the lower SR  $\text{Ca}^{2+}$  content by itself would tend to greatly reduce fractional SR  $\text{Ca}^{2+}$  release (Fig. 25). This is usually found in  $\text{CaMKII}$  overexpressing cardiomyocytes due to  $\text{CaMKII}$ -dependent RyR2 phosphorylation. Thus, whereas SR  $\text{Ca}^{2+}$  content was reduced in  $\text{CaMKII}\delta_{\text{C}}/\text{RyR2}^{\text{R4496C}}$  and  $\text{CaMKII}\delta_{\text{C}}$  myocytes, the fraction of SR  $\text{Ca}^{2+}$  released during a twitch was increased. Interestingly, the fractional SR  $\text{Ca}^{2+}$  release in  $\text{RyR2}^{\text{R4496C}+/}$  ( $60.94 \pm 2.24$ ;  $n=31$ ) was also dramatically augmented as compared to WT and this abnormal  $\text{Ca}^{2+}$  release could be attributed to R4496C mutation in the gene encoding RyR2.

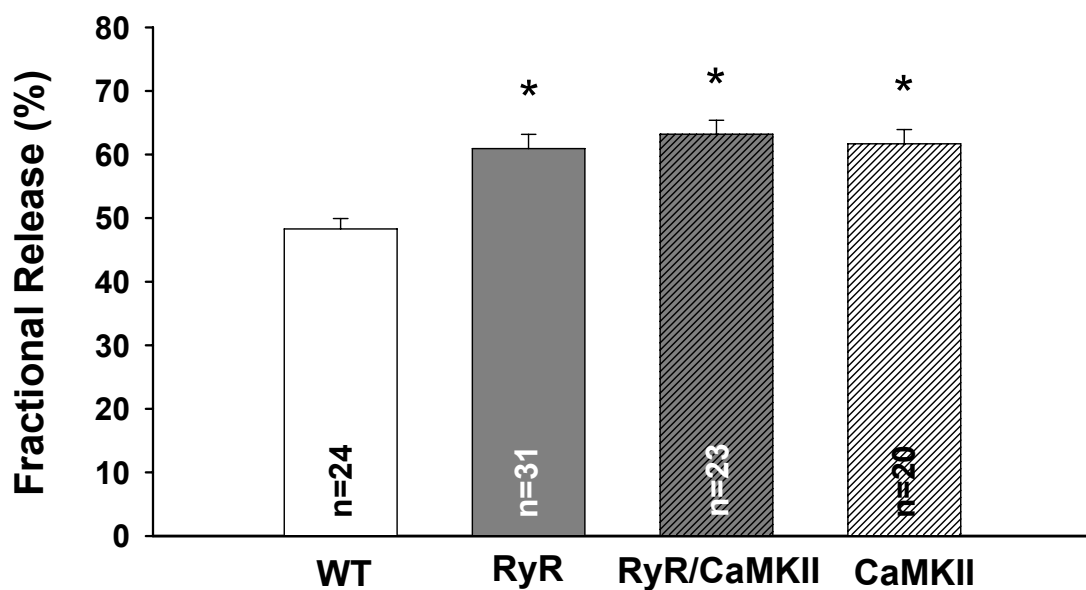
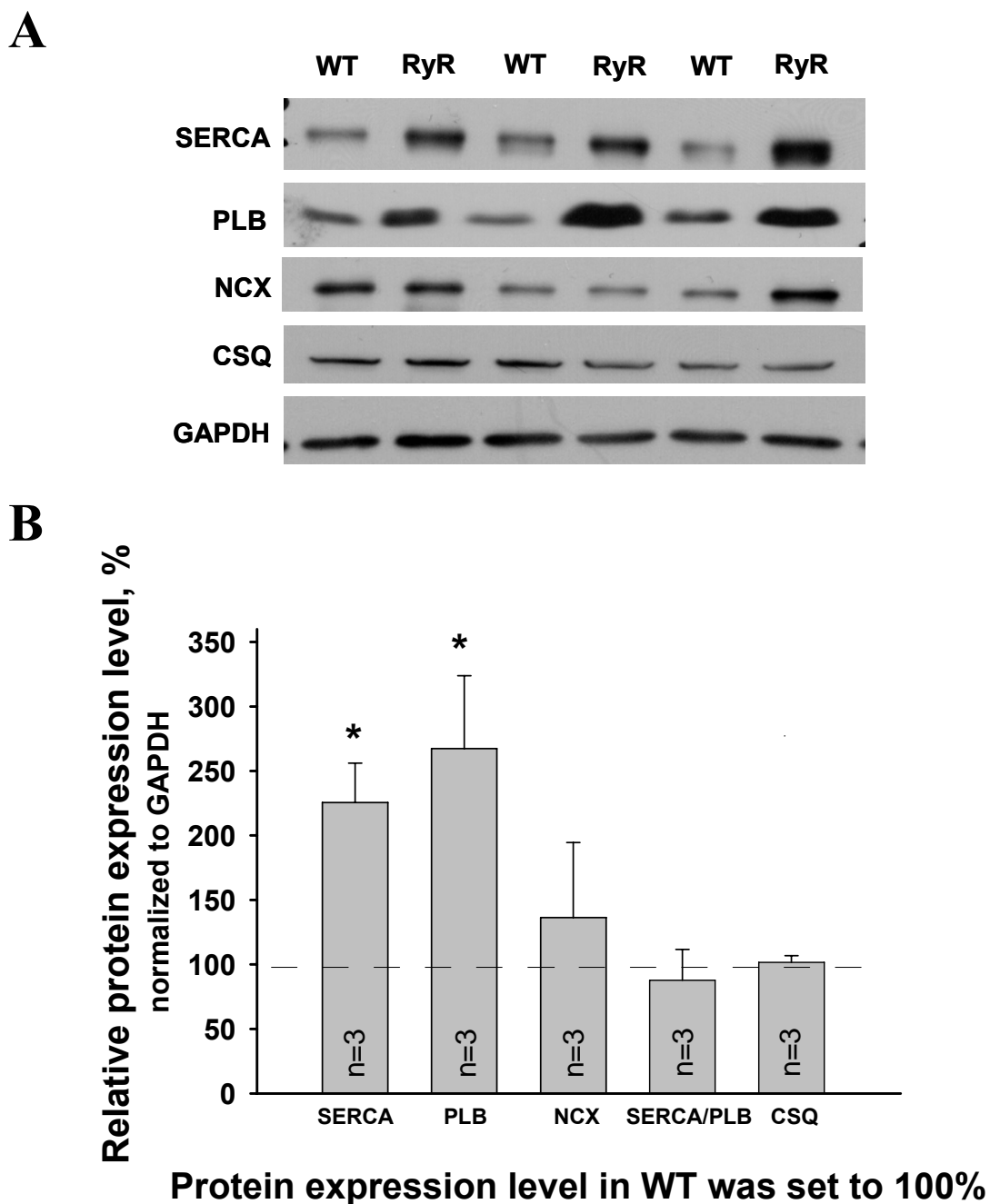


**Figure 25. Fractional SR  $\text{Ca}^{2+}$  release.** Average data for fractional SR  $\text{Ca}^{2+}$  release (ratio of twitch  $\text{Ca}^{2+}$  transient/cafeine-induced  $\text{Ca}^{2+}$  transient) showing an increased fraction of SR  $\text{Ca}^{2+}$  released during a twitch in  $\text{RyR2}^{\text{R4496C}+/}$ ,  $\text{CaMKII}\delta_{\text{C}}/\text{RyR2}^{\text{R4496C}}$  and  $\text{CaMKII}\delta_{\text{C}}$  myocytes versus WT. \* $P < 0.05$  versus WT.

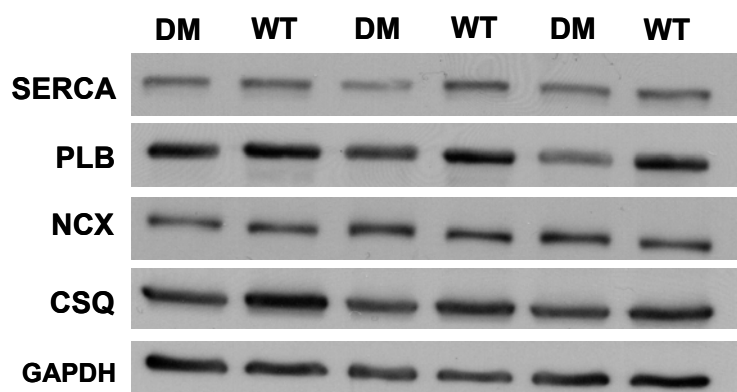
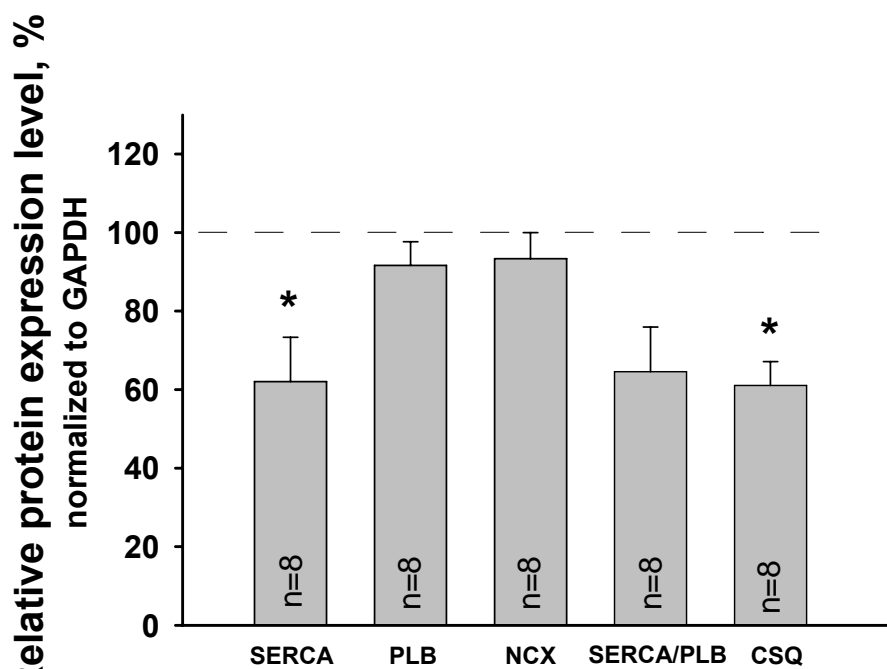
#### 4.5 Expression levels of important Ca<sup>2+</sup> transport proteins in mouse hearts

To investigate whether phenotypic changes as well as functional alterations observed in RyR2<sup>R4496C+/-</sup> and CaMKII $\delta_C$ /RyR2<sup>R4496C</sup> mice could be associated with altered expression levels of important Ca<sup>2+</sup> transport proteins such as SERCA2a, PLB, NCX and CSQ, Western blot measurements were performed. Protein homogenates prepared from RyR2<sup>R4496C+/-</sup> knock-in, CaMKII $\delta_C$ /RyR2<sup>R4496C</sup> double mutant and WT mouse hearts were denatured in sample buffer containing 2%  $\beta$ -mercaptoethanol and subjected to SDS-polyacrylamide gel. Immunoblotting with the antibody against SERCA2a (Affinity Bioreagents), PLB (Upstate), NCX (Swant) and CSQ (Affinity Bioreagents) revealed significantly increased expression levels of SERCA2a by 125% and PLB by 167% (n=5; P<0.05) in homogenates prepared from RyR2<sup>R4496C+/-</sup> knock-in mouse hearts versus WT when normalized to GAPDH. The SERCA2a/PLB ratio remained however unchanged, indicating unaltered SR Ca<sup>2+</sup> uptake function. Expression levels of two other Ca<sup>2+</sup> handling proteins, NCX and CSQ, were also not significantly altered (Fig. 26).

In CaMKII $\delta_C$ /RyR2<sup>R4496C</sup> double mutant mouse hearts a reduced expression of SERCA2a by 37% (n=8; P<0.05) was observed, whereas PLB (n=8) and NCX (n=8) expression levels were unaltered. The SERCA2a/PLB ratio was lower by 36% in the CaMKII $\delta_C$ /RyR2<sup>R4496C</sup> double mutant as well (P=0.08), indicating a slightly greater Ca<sup>2+</sup>-pump inhibition as compared to WT. Interestingly, we also found decreased expression levels of calsequestrin (n=8; by 39%; P<0.05) in CaMKII $\delta_C$ /RyR2<sup>R4496C</sup> mice. GAPDH served as control of equal loading (Fig. 27).



**Figure 26. (A) Representative Western blots of important Ca<sup>2+</sup> cycling proteins from cardiac homogenates prepared from hearts of RyR2<sup>R4496C+/-</sup> and WT mice.** Cardiac homogenates from WT and RyR2<sup>R4496C+/-</sup> mice were warmed in the sample buffer containing 2%  $\beta$ -mercaptoethanol, separated on 10% and 15% polyacrylamide-SDS gels and transferred to nitrocellulose. Western blots were probed with anti-SERCA2a, anti-PLB, anti-NCX, anti-CSQ and anti-GAPDH antibodies. **(B) Quantification of the protein expression level in RyR2<sup>R4496C+/-</sup> versus WT mice.** A significantly increased expression of SERCA2a (by 125%) and PLB (by 167%) was observed in RyR2<sup>R4496C+/-</sup> versus WT. The amount of the proteins was determined densitometrically and normalized to GAPDH. \*P<0.05 versus WT.

**A****B**

**Protein expression level in WT was set to 100%**

**Figure 27. (A) Representative Western blots of important  $\text{Ca}^{2+}$  cycling proteins from cardiac homogenates prepared from hearts of  $\text{CaMKII}\delta_{\text{C}}/\text{RyR2}^{\text{R4496C}}$  and WT mice.** Cardiac homogenates from WT and  $\text{CaMKII}\delta_{\text{C}}/\text{RyR2}^{\text{R4496C}}$  mice were warmed in the sample buffer containing 2%  $\beta$ -mercaptoethanol, separated on 10% and 15% polyacrylamide-SDS gels and transferred to nitrocellulose. Western blots were probed with anti-SERCA2a, anti-PLB, anti-NCX, anti-CSQ and anti-GAPDH antibodies. **(B) Quantification of the protein expression level in  $\text{CaMKII}\delta_{\text{C}}/\text{RyR2}^{\text{R4496C}}$  versus WT mice.** There was a significantly lower expression of SERCA2a (by 37%) and CSQ (by 39%) in  $\text{CaMKII}\delta_{\text{C}}/\text{RyR2}^{\text{R4496C}}$  versus WT. The amount of the proteins was determined densitometrically and normalized to GAPDH. \* $P < 0.05$  versus WT.

#### 4.6 Measurement of Ca<sup>2+</sup> release from the SR using confocal microscopy

The activity of individual RyR2 clusters generates localized Ca<sup>2+</sup> release events termed Ca<sup>2+</sup> sparks. The frequency, amplitude and time course of Ca<sup>2+</sup> sparks contributes to the spontaneous Ca<sup>2+</sup> leak from the SR.

Ca<sup>2+</sup> sparks were recorded on a laser scanning confocal microscope (LSM 5 Pascal, Zeiss) using intact cardiomyocytes loaded with the Ca<sup>2+</sup>-fluorescent dye Fluo-4 AM. The dye was excited by an argon laser at 488 nm and emitted fluorescence was collected through a 515 nm long-pass emission filter. Figure 28A shows representative line scan images from WT, RyR2<sup>R4496C/+</sup>, CaMKII $\delta_C$ /RyR2<sup>R4496C</sup> and CaMKII $\delta_C$  myocytes during perfusion with normal Tyrode solution containing 3 mM Ca<sup>2+</sup>. One would expect that a reduction in SR Ca<sup>2+</sup> load leads to a decrease of spontaneous SR Ca<sup>2+</sup> release events in CaMKII $\delta_C$ /RyR2<sup>R4496C</sup> and CaMKII $\delta_C$  myocytes. Strikingly, the opposite was observed: CaSpF during 0.5 Hz stimulation was significantly increased by  $\approx 50\%$  in CaMKII $\delta_C$ /RyR2<sup>R4496C</sup> ( $2.26 \pm 0.23 \text{ pl}^{-1} \cdot \text{s}^{-1}$ ; n=60) and CaMKII $\delta_C$  ( $2.45 \pm 0.26 \text{ pl}^{-1} \cdot \text{s}^{-1}$ ; n=53) versus WT mice ( $1.14 \pm 0.1 \text{ pl}^{-1} \cdot \text{s}^{-1}$ ; n=46;  $P < 0.05$ ). CaSpF in RyR2<sup>R4496C/+</sup> knock-in mice ( $2.22 \pm 0.20 \text{ pl}^{-1} \cdot \text{s}^{-1}$ ; n=68) was also significantly higher than in WT ( $P < 0.05$ ), probably due to the mutated RyR2 (Fig. 28B). Additionally, significant changes in Ca<sup>2+</sup> spark characteristics were observed. The Ca<sup>2+</sup> spark amplitude (F/F<sub>0</sub>) was increased to the same level in CaMKII $\delta_C$ /RyR2<sup>R4496C</sup> ( $1.70 \pm 0.02$ ; n=178) and RyR2<sup>R4496C/+</sup> ( $1.70 \pm 0.02$ ; n=192) myocytes versus WT ( $1.57 \pm 0.02$ ; n=67;  $P < 0.05$ ). This is expected, because usually Ca<sup>2+</sup> spark frequency and amplitude are altered in the same direction. Nevertheless, in CaMKII $\delta_C$  transgenic mice ( $1.60 \pm 0.02$ ; n=171) the Ca<sup>2+</sup> spark amplitude was not much higher than in WT control. Lower Ca<sup>2+</sup> spark amplitude in these mice is consistent with the lower SR Ca<sup>2+</sup> content (Fig. 29A). The duration of the Ca<sup>2+</sup> sparks was significantly prolonged in RyR2<sup>R4496C/+</sup> knock-in ( $91.78 \pm 3.56 \text{ ms}$ ; n=183), CaMKII $\delta_C$ /RyR2<sup>R4496C</sup> double mutant ( $92.23 \pm 3.66 \text{ ms}$ ; n=175) and CaMKII $\delta_C$  transgenic myocytes ( $106 \pm 4.56 \text{ ms}$ ; n=166) relative to WT ( $75.55 \pm 4.28 \text{ ms}$ ; n=65;  $P < 0.05$ ), suggesting longer RyR2 openings (Fig. 29B). These increases in frequency, amplitude and duration of Ca<sup>2+</sup> sparks suggest a severely altered diastolic RyR2 function. The much higher frequency of long Ca<sup>2+</sup> sparks with increased spark amplitude may reflect a higher propensity for the initiation of delayed afterdepolarizations and consequent triggered arrhythmias in CaMKII $\delta_C$ /RyR2<sup>R4496C</sup> double mutant mice.



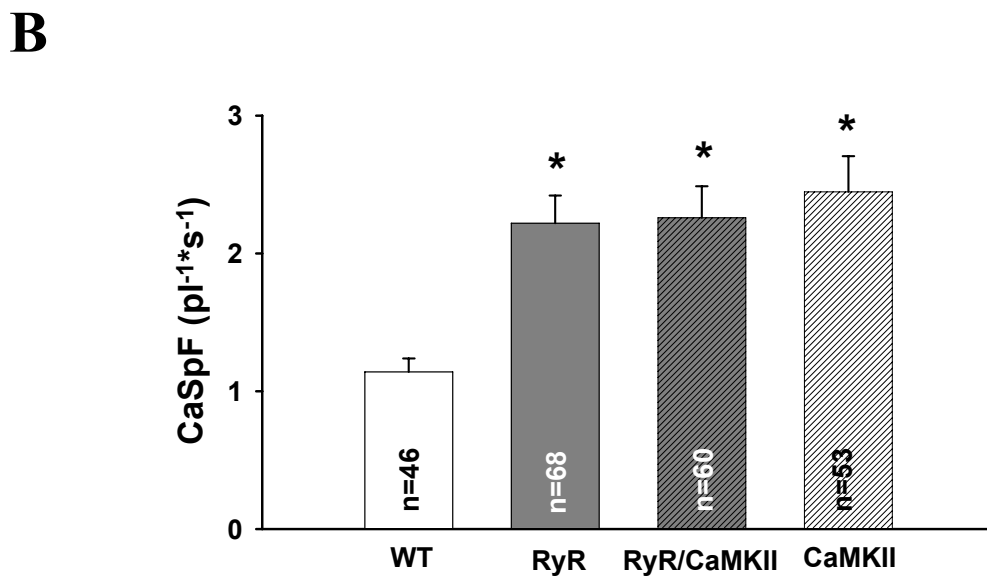
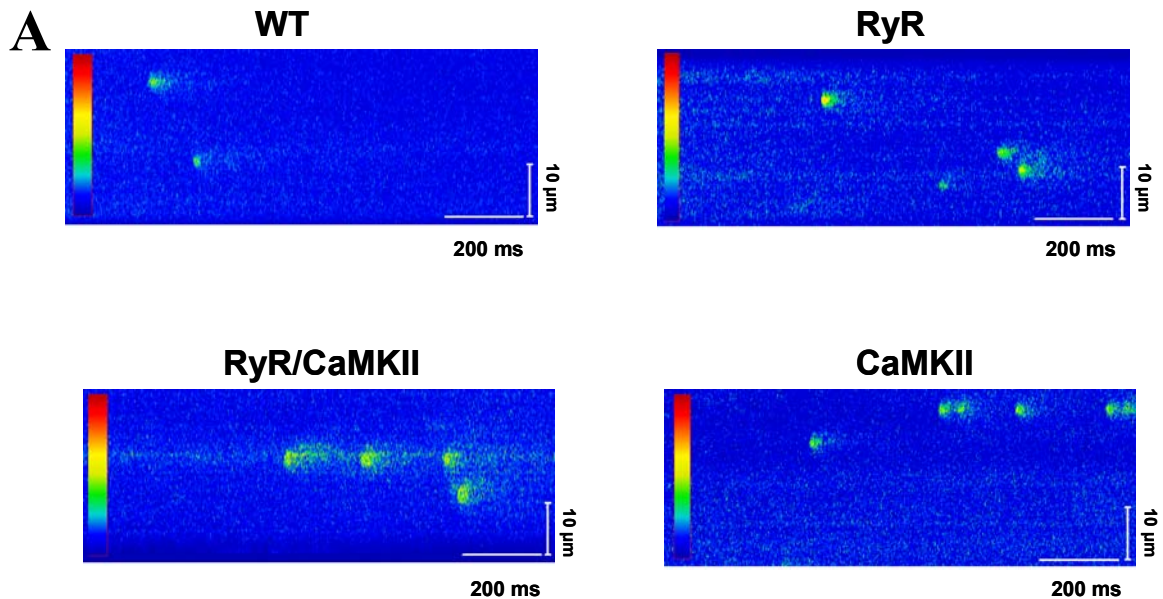


**Figure 28.** Ca<sup>2+</sup> sparks in mouse ventricular myocytes measured using Fluo-4. (A) Confocal line scan images of spontaneous Ca<sup>2+</sup> sparks in WT, RyR<sup>R4496C/+</sup>, CaMKII $\delta_c$ /RyR<sup>R4496C</sup> and CaMKII $\delta_c$  myocytes, as a measure of diastolic RyR2 activity (Ca<sup>2+</sup> leak). (B) Average data for Ca<sup>2+</sup> spark frequency (CaSpF) showing dramatically increased spontaneous SR Ca<sup>2+</sup> release in cardiomyocytes isolated from RyR<sup>R4496C/+</sup>, CaMKII $\delta_c$ /RyR<sup>R4496C</sup> and CaMKII $\delta_c$  mice compared to WT. \*P<0.05 versus WT.

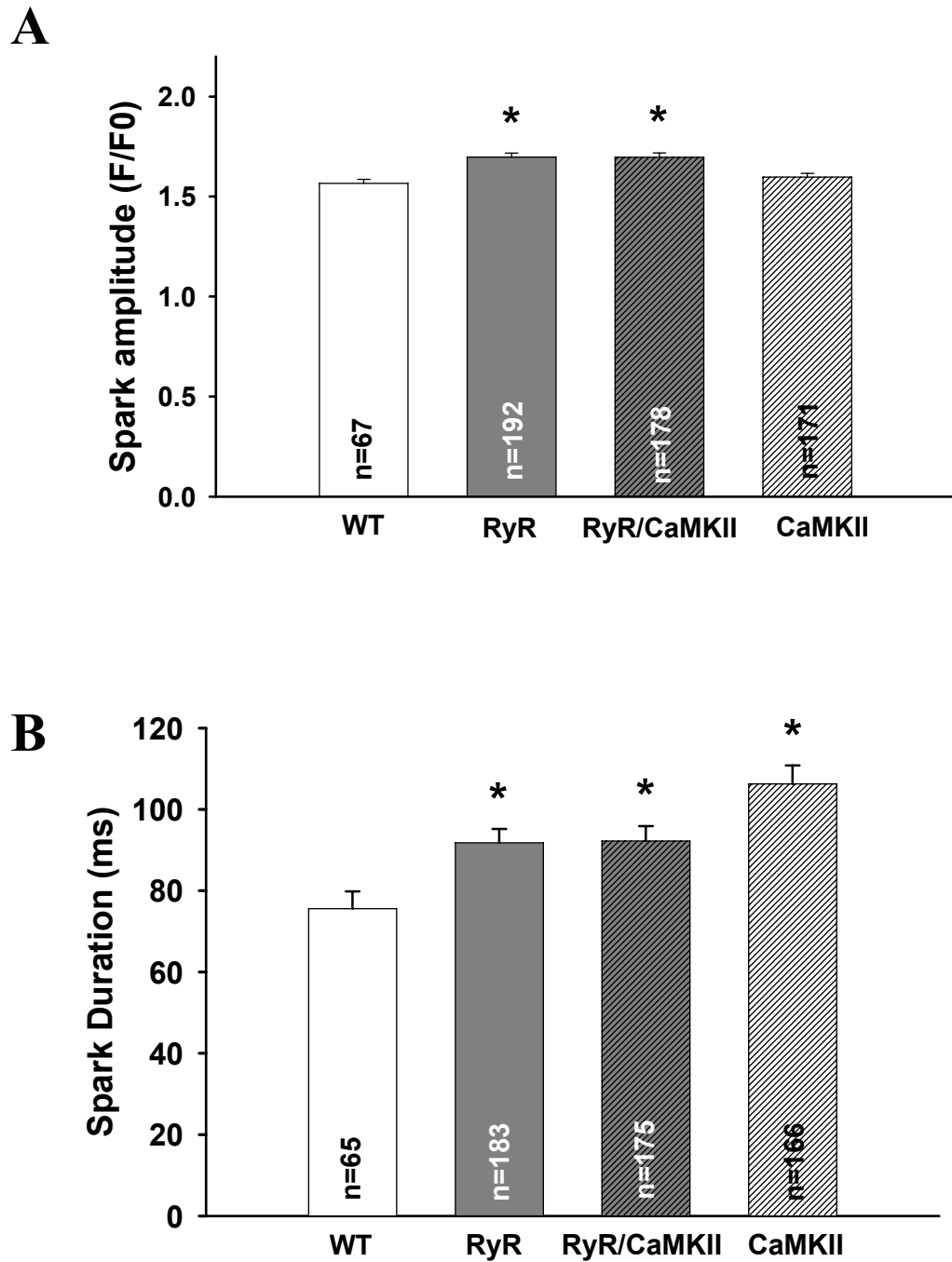


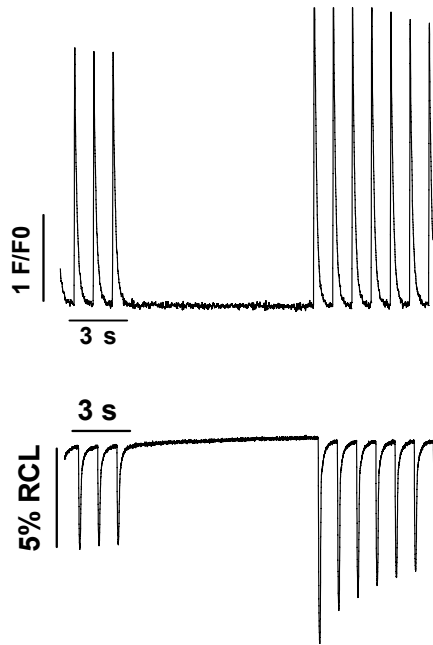
**Figure 29. Ca<sup>2+</sup> spark characteristics.** (A) Mean data for the Ca<sup>2+</sup> spark amplitude (F/F<sub>0</sub>) representing increased amplitude in RyR2<sup>R4496C+/-</sup>, CaMKII $\delta_c$ /RyR2<sup>R4496C</sup> myocytes, but not in CaMKII $\delta_c$  versus WT. \*P<0.05 versus WT. (B) Mean data of Ca<sup>2+</sup> spark duration showing larger duration in RyR2<sup>R4496C+/-</sup>, CaMKII $\delta_c$ /RyR2<sup>R4496C</sup> and CaMKII $\delta_c$  myocytes compare to WT, which suggests longer RyR2 openings. \*P<0.05 versus WT.

#### 4.7 Increased arrhythmogenic events in RyR2<sup>R4496C+/-</sup>, CaMKII $\delta_C$ /RyR2<sup>R4496C</sup> and CaMKII $\delta_C$ mice

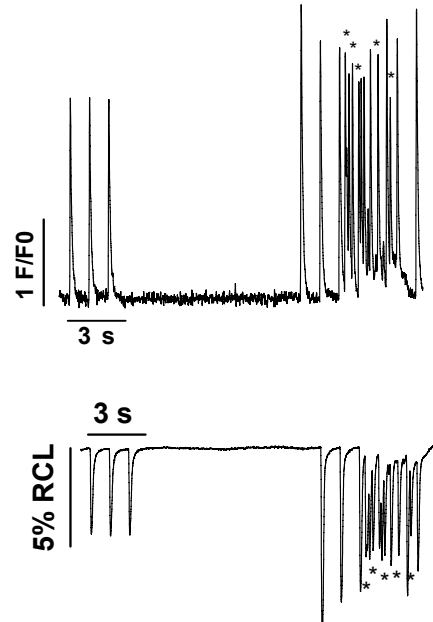
To test whether RyR2<sup>R4496C+/-</sup>, CaMKII $\delta_C$ /RyR2<sup>R4496C</sup> and CaMKII $\delta_C$  mice have increased cellular arrhythmias at baseline, the incidence of proarrhythmogenic events (non-stimulated events) in electrically paced isolated ventricular myocytes from RyR2<sup>R4496C+/-</sup> knock-in, CaMKII $\delta_C$ /RyR2<sup>R4496C</sup> double mutant, and CaMKII $\delta_C$  transgenic mouse hearts relative to WT was assessed. These proarrhythmogenic events were observed during the measurement of cell shortening and Ca<sup>2+</sup> transients using epifluorescence experiments when stimulation was paused (Fig. 30A) as well as during steady-state stimulation at 1 Hz (Fig. 30B). A previously published non-stimulated events classification differentiated between early-spike non-stimulated events and late-spike non-stimulated events. The late-spike non-stimulated events occur as single events or can sustain if they outlast electric field stimulation (Wu et al., 2002). In every mouse genotype tested in this study all classes of non-stimulated events occurred. However, cellular arrhythmias were significantly more common in RyR2<sup>R4496C+/-</sup>, CaMKII $\delta_C$ /RyR2<sup>R4496C</sup> and CaMKII $\delta_C$  myocytes as compared to WT control myocytes, which might indicate their predisposition to triggered arrhythmias in vivo. Non-stimulated events were present in 27 out 96 myocytes in RyR2<sup>R4496C+/-</sup>, in 31 out 105 in CaMKII $\delta_C$ /RyR2<sup>R4496C</sup>, and in 18 out 77 in CaMKII $\delta_C$ , whereas WT myocytes showed non-stimulated events only in 10 out 136 ( $P < 0.05$ ). Compared to WT myocytes, which showed mainly early-spike non-stimulated events, RyR2<sup>R4496C+/-</sup>, CaMKII $\delta_C$ /RyR2<sup>R4496C</sup> and CaMKII $\delta_C$  myocytes exhibited more frequently cellular arrhythmias characterized by sustained late-spike non-stimulated events. Most importantly, arrhythmias were observed in isolated myocytes from ~50% of RyR2<sup>R4496C+/-</sup>, from ~80% of CaMKII $\delta_C$ /RyR2<sup>R4496C</sup> but only from ~30% of CaMKII $\delta_C$  mice, as compared to less than 10% in WT control (Fig. 30C). Therefore, enhanced cellular arrhythmias at baseline in CaMKII $\delta_C$ /RyR2<sup>R4496C</sup> mice might be due to an increased SR Ca<sup>2+</sup> leak. This could explain the high mortality in CaMKII $\delta_C$ /RyR2<sup>R4496C</sup> double mutant mice as compared to WT and RyR2<sup>R4496C+/-</sup> mice and even when compared to CaMKII $\delta_C$  mice.

**A**

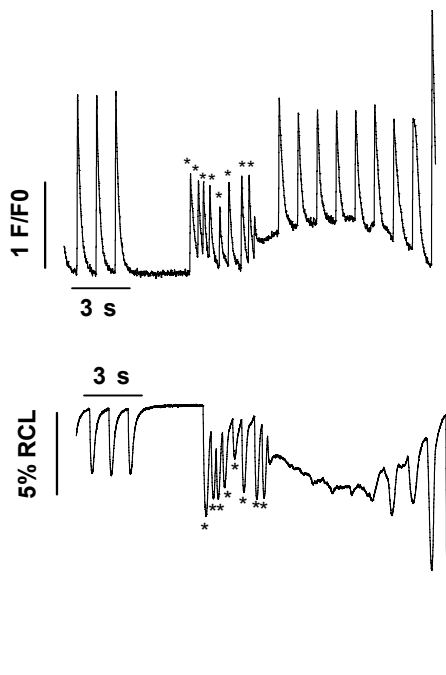
**WT**



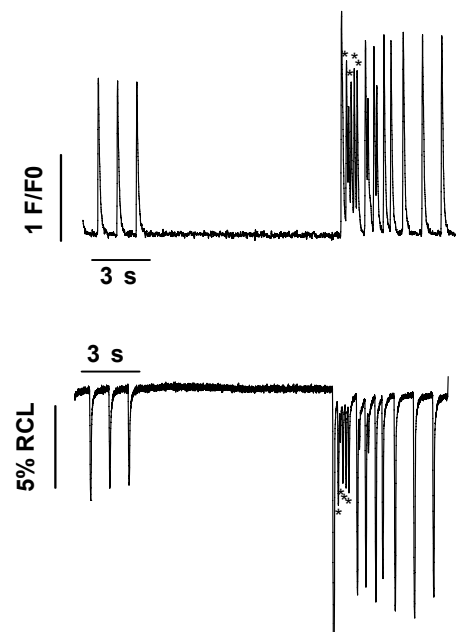
**RyR**



**RyR/CaMKII**



**CaMKII**



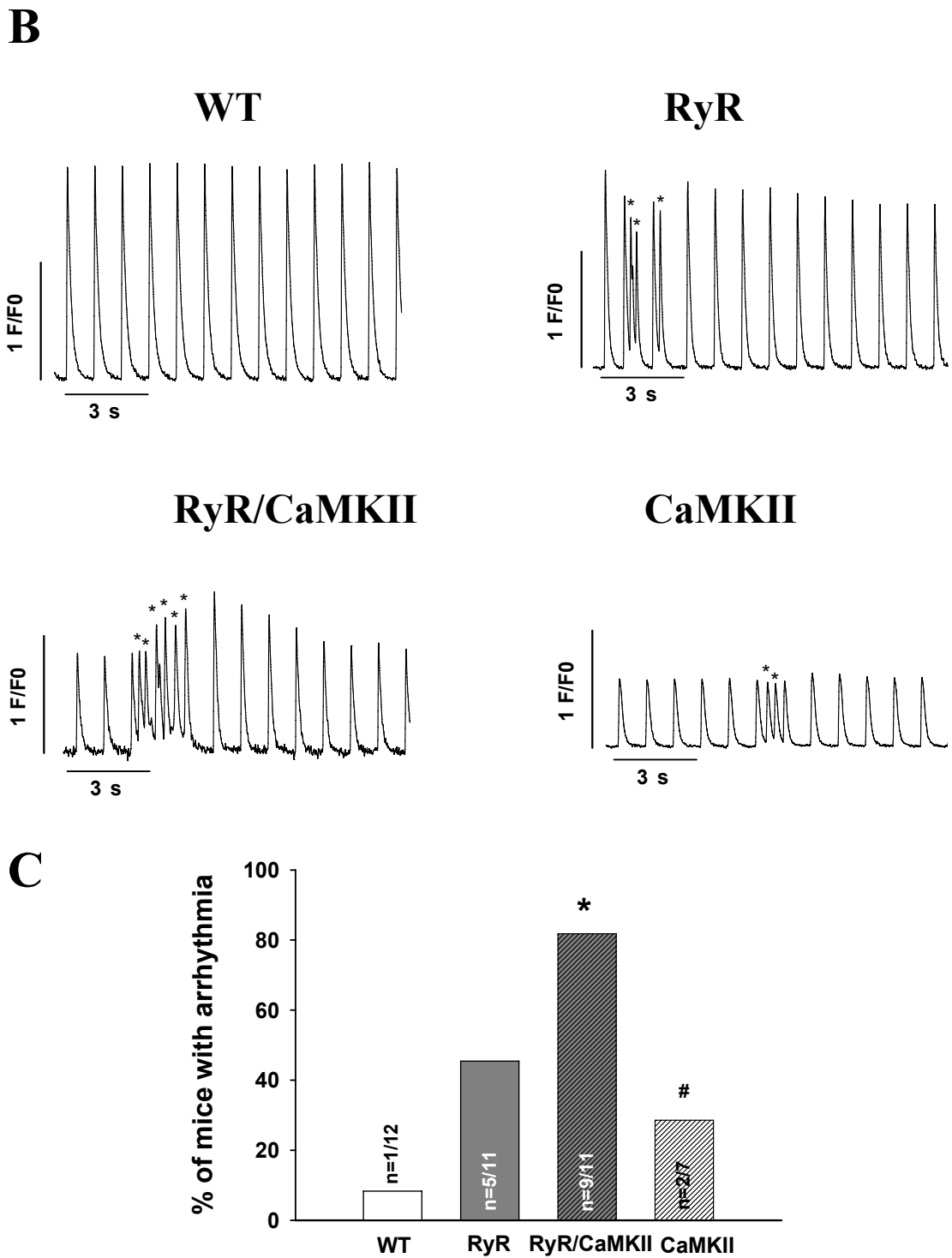


**Figure 30. Cellular arrhythmias recorded in electrically paced isolated ventricular myocytes from  $RyR2^{R4496C/+}$ ,  $CaMKII\delta_C/RyR2^{R4496C}$  and  $CaMKII\delta_C$  mouse hearts. (A) Original  $Ca^{2+}$  and shortening traces showing spontaneous cellular arrhythmias (depicted by \*) in myocytes isolated from  $RyR2^{R4496C/+}$ ,  $CaMKII\delta_C/RyR2^{R4496C}$  and  $CaMKII\delta_C$  mice during 10 sec rest but no arrhythmias in WT. (B) Original  $Ca^{2+}$  traces with increased non-stimulated events during 1 Hz stimulation. (C) The number of mice with arrhythmias was significantly higher in  $CaMKII\delta_C/RyR2^{R4496C}$  versus WT. \* $P < 0.05$  versus WT. #  $P < 0.05$  versus  $CaMKII\delta_C/RyR2^{R4496C}$ .**

## 5 Discussion

### 5.1 CaMKII $\delta_C$ associates with and phosphorylates cardiac Na<sup>+</sup> channels

The voltage-gated Na<sup>+</sup> channels composed of pore-forming  $\alpha$  and auxiliary  $\beta$  subunits are responsible for the rising phase of the action potential in cardiac muscle. Action potentials are fundamentally required to initiate myocyte shortening and therefore cardiac contractions. Cardiac function depends on the amplitude, timing and voltage dependence of Na<sup>+</sup> current through Na<sup>+</sup> channels. Altered Na<sup>+</sup> channel gating and changes in intracellular sodium homeostasis play an important role in the pathophysiology of heart failure. Tiny alterations in channel function could result in altered ion fluxes, which may have a great impact on the action potential characteristics and E-C coupling. So far, it was only known that cardiac Na<sup>+</sup> channels are regulated through phosphorylation by PKC and PKA.

The present study shows for the first time that CaMKII $\delta_C$  associates with and phosphorylates cardiac Na<sup>+</sup> channels. The localization of Na<sup>+</sup> channel  $\alpha$  subunits in isolated adult mouse and rabbit ventricular myocytes was also determined. The isoform Nav1.5 (SCN5A) of the  $\alpha$  subunit is the predominant isoform in the heart. However, the brain-type isoforms Nav1.1, Nav1.3, and Nav1.6 were shown to be expressed in ventricular myocytes having distinct subcellular localization and function (Maier et al 2002). The immunofluorescence experiments presented here using labeled Nav1.5 channels confirmed the specific localization of this subtype of sodium channels within the transverse tubular system in rabbit as well as mouse myocytes. This result is in contrast to data published by Sebastian Maier and colleagues (Maier et al 2002; Maier et al 2004) who localized the Nav1.5 only in intercalated disks but not in transverse tubules of adult isolated mouse ventricular cells. However, Nav1.5 subcellular localization in transverse tubules and intercalated discs as shown here is in agreement with a report by Mohler and colleagues (Mohler et al., 2004) who studied Nav1.5 in isolated cardiomyocytes of adult rat. In addition, other authors also confirmed that Nav1.5 is localized only in transverse tubules (Haufe et al., 2005; Dominguez et al., 2008). The use of distinct sources of antibodies and technical procedures might underlie such differences, although such controversies remain to be further dissected.

Differentially localized sodium channels may have different physiological roles. Na<sup>+</sup> channels in intercalated disks are involved primarily in initiation and propagation of the cardiac action potential from cell to cell. In contrast, Na<sup>+</sup> channels in transverse tubules

may function in coordinating and synchronizing the conduction of the action potential from the cell surface of the myocyte into the interior via the transverse tubules (Maier et al., 2002).

The immunofluorescent studies presented here using double labeling of CaMKII $\delta_C$  and Nav1.5 channels revealed that cytoplasmic isoform of CaMKII $\delta_C$  co-localized with cardiac Na<sup>+</sup> channels in both mouse and rabbit ventricular myocytes. Further co-immunoprecipitation experiments confirmed that CaMKII $\delta_C$  associates with Na<sup>+</sup> channels in both mouse and rabbit tissue.

It is known that protein kinases PKA and PKC can phosphorylate and thereby regulate cardiac Na<sup>+</sup> channels. However, PKA and PKC modulate cardiac Na<sup>+</sup> channels differently. PKA-dependent phosphorylation at Ser-526 and Ser-529 in the I-II cytoplasmic linker in response to increased intracellular levels of cAMP increases whole-cell conductance without altering channel gating. Single channel experiments revealed that the increase in whole-cell conductance resulted from an increased number of functional Na<sup>+</sup> channels, possibly by altered channel trafficking (Murphy et al., 1996; Fronwieser et al., 1997). Also, some authors found a cAMP-dependent enhancement of Na<sup>+</sup> channel steady-state inactivation (Ono et al., 1989). PKC-dependent phosphorylation at Ser 1505 in the III-IV cytoplasmic linker reduces maximal conductance and enhances steady-state inactivation (Qu et al., 1996). In the present study it is shown that exogenous CaMKII can phosphorylate Na<sup>+</sup> channels and, importantly, that endogenous CaMKII in rabbit myocytes can phosphorylate the Na<sup>+</sup> channel at an intracellular Ca<sup>2+</sup> concentration that is physiologically relevant. In addition, when CaMKII was overexpressed in these myocytes, the Na<sup>+</sup> channel was more phosphorylated even at diastolic Ca<sup>2+</sup> level (50 nM). These results suggest that CaMKII association and thereby phosphorylation of Na<sup>+</sup> channels is physiologically relevant and may also regulate the channels.

Deschênes and colleagues (Deschênes et al., 2002) were the first to investigate CaMK-dependent regulation of cardiac Na<sup>+</sup> channels expressed in human embryonic kidney (HEK 293) cells. They showed that the nonselective CaMK inhibitor KN-93 induces Na<sup>+</sup> current decay consistent with an inhibition of fast inactivation and shifted steady-state inactivation in the depolarizing direction.

Wagner and colleagues (Wagner et al., 2006) assessed the role of CaMKII $\delta_C$  on Na<sup>+</sup> channel function using 2 models: CaMKII $\delta_C$  TG mice, which develop HF, as well as acute CaMKII $\delta_C$  overexpression in rabbit myocytes. They measured steady-state inactivation and activation of Na<sup>+</sup> channels and found that CaMKII does not alter activation of the channel,

but dramatically alters its inactivation. Several types of Na<sup>+</sup> current inactivation were distinguished:

1) “fast” inactivation occurring over 2-10 ms which recovers rapidly at negative membrane potential; 2) “intermediate” inactivation occurring over hundreds of milliseconds after fast inactivation recovering more slowly; 3) “slow” inactivation occurring over tens of seconds (Bers, 2001). These different inactivation modes can all influence Na<sup>+</sup> channel steady-state inactivation, action potential duration, and Na<sup>+</sup> flux balance. Transgenic CaMKII $\delta_C$  overexpression enhances accumulation of intermediate inactivation as shown by Wagner et al. Physiologically, only a small fraction of Na<sup>+</sup> channels undergo intermediate inactivation and reduce the amount of channels available for the second excitation. Thus, CaMKII $\delta_C$  may increase the fraction of channels that can enter intermediate inactivation consistent with a reduced channel function (Wagner et al., 2006). Enhanced intermediate inactivation has been implicated in Brugada syndrome. The syndrome is associated with life-threatening ventricular tachyarrhythmias (Wang et al., 2000) and has been shown to result in strikingly similar alteration in gating as observed upon increased CaMKII $\delta_C$  activity (Wagner et al., 2006).

In contrast to intermediate inactivation, for which no structural correlate has been found yet, the cytoplasmic linker between domains III and IV and C terminus of the Na<sup>+</sup> channel  $\alpha$ -subunit has been proposed to underlie fast inactivation. CaMKII $\delta_C$  overexpression slowed fast inactivation increasing the amount of Na<sup>+</sup> influx leading to enhanced intracellular Na<sup>+</sup> concentration (Wagner et al., 2006). Mutations in the III and IV cytoplasmic linker and C terminus of the Na<sup>+</sup> channel slow the inactivation process leading to LQT3 (Bennett et al., 1995). Impaired fast Na<sup>+</sup> channel inactivation mimics the functional defects of mutant Na<sup>+</sup> channels associated with LQT3 (Wagner et al., 2006). Slowed Na<sup>+</sup> current inactivation could prolong action potential duration, leading to early afterdepolarization or LQT3-like propensity for arrhythmias as well as may elevate intracellular Na<sup>+</sup> concentration causing Ca<sup>2+</sup> overload–induced spontaneous sarcoplasmic reticulum Ca<sup>2+</sup> release and transient inward current via Na<sup>+</sup>/Ca<sup>2+</sup> exchange, which lead to delayed afterdepolarizations (Bers, 2001).

Thus, CaMKII $\delta_C$  enhances intermediate inactivation, while at the same time impairing fast inactivation and enhancing persistent Na<sup>+</sup> current (Wagner et al., 2006). Similar changes in Na<sup>+</sup> channel gating were shown for a human mutant Na<sup>+</sup> channel (Asp insertion at 1795 in the C terminus), which shows simultaneous LQT3-like and Brugada-like phenotypes (Veldkamp et al., 2000). At slow heart rates, mutant 1795*insD* Na<sup>+</sup> channel impaired fast



inactivation and increased  $\text{Na}^+$  current influx favoring action potential prolongation, which is consistent with LQT3 syndrome (Bennett et al., 1995). However, at higher heart rates, *1795insD* induces reduced  $\text{Na}^+$  channel availability and action potential shortening underlying Brugada syndrome. Therefore, it is conceivable that increased  $\text{CaMKII}\delta_C$  activity in heart failure may alter  $\text{Na}^+$  channel gating, thereby generating the substrate for arrhythmias.  $\text{CaMKII}\delta_C$  TG mice indeed showed an increased propensity for arrhythmias in vivo (Wagner et al., 2006). The QRS duration in  $\text{CaMKII}\delta_C$  TG mice was prolonged indicating slowed intraventricular conduction, which is proarrhythmic in Brugada syndrome. Repolarization was disturbed in TG mice, which favors arrhythmias in LQT3 patients. Action potential duration was prolonged which could contribute to EAD and LQT3-like arrhythmias. The resulting increased intracellular  $\text{Na}^+$  concentration could also enhance SR  $\text{Ca}^{2+}$  content via NCX, leading to spontaneous SR  $\text{Ca}^{2+}$  release and DAD. Thus, the  $\text{CaMKII}\delta_C$ -dependent  $\text{Na}^+$  channel modulation can be an acquired form of combined LQT3 and Brugada syndrome, which may contribute to arrhythmias when  $\text{CaMKII}$  activity is increased as in HF.

In the present study, acute  $\text{CaMKII}\delta_C$  overexpression in rabbit cardiomyocytes did not alter protein expression levels. This suggests that  $\text{CaMKII}\delta_C$ -dependent  $\text{Na}^+$  channel regulation may not involve primary effects on  $\text{Na}^+$  channel expression. However,  $\text{CaMKII}\delta_C$  TG mice exhibiting heart failure showed significantly more  $\text{Na}^+$  channel expression, which could be a consequence of the heart failure phenotype.

In summary, it was shown for the first time that  $\text{CaMKII}$  associates and phosphorylates  $\text{Na}^+$  channels. In the face of an increased propensity for arrhythmias in heart failure and increased  $\text{CaMKII}$  expression levels and activity, it is possible that regulation of  $\text{Na}^+$  channel function by  $\text{CaMKII}$  may contribute to these adverse effects.

## **5.2 Functional characterization of $\text{RyR2}^{\text{R4496C}+/}$ mice harboring a human CPVT mutation**

Catecholaminergic polymorphic ventricular tachycardia is a disease caused by mutations in the  $\text{RyR2}$  gene encoding the cardiac ryanodine receptor characterized by adrenergically mediated bidirectional and polymorphic VT and ventricular fibrillation (Leenhardt et al., 1995; Priori et al., 2002). Interestingly, patients with CPVT apparently have functionally normal hearts (Leenhardt et al., 1995; Laitinen et al., 2004) and the mouse model harboring

the R4496C mutation in RyR2 shows neither macroscopic alteration of the heart nor any tissue abnormalities (Cerrone et al., 2003). The clinical phenotype of CPVT patients consists of ventricular arrhythmias inducible with exercise stress testing (Leenhardt et al., 1995; Priori et al., 2002). The presence of the R4496C mutation predisposed the murine heart to the development of ventricular tachycardia and fibrillation after administration of caffeine and adrenergic agonists. It is remarkable that ventricular tachycardia in RyR2<sup>R4496C+/-</sup> mice had the typical bidirectional morphology that is considered the most distinguishing characteristic of CPVT patients. The mutation that was identified in CPVT family is located in the C terminal portion of the channel and leads to the replacement of arginine at the position 4497 with a cysteine (Cerrone et al., 2003). Because this mutation was associated with a highly malignant phenotype it has been selected by several groups for their in vitro studies. The R4496C mutation has been expressed and investigated in a heterologous system. Jiang and colleagues (Jiang et al., 2002) first studied the mouse RyR2 mutant R4496C corresponding to the R4497C human mutation by expression in HEK 293 cells and single-channel analysis showed that this mutation enhanced the basal channel activity and the propensity for spontaneous Ca<sup>2+</sup> release. Recently, this group confirmed their results and suggested that the R4496C mutation increases the channel sensitivity to activation by luminal Ca<sup>2+</sup> (Jiang et al., 2004). George and colleagues (George et al., 2003) investigated the same mutation by expression in a cardiac muscle cell line (HL-1 cardiomyocytes) and demonstrated that the R4496C mutant shows no enhancement of basal activity; however, intracellular Ca<sup>2+</sup> release was significantly augmented in cells expressing mutant RyR2 after addition of caffeine agonist or beta adrenergic stimulation. Nonetheless, all of the investigators agree that the abnormal Ca<sup>2+</sup> handling observed in R4496C RyR2 is likely to promote the development of DAD and triggered arrhythmias. Expression studies assessing mutant RyR2 function were carried out in a variety of models which may explain the controversial findings. It is likely, however, that appropriate regulation of RyR2 requires the precise interaction of a multitude of accessory proteins, which may be absent in the heterologous systems, so the analysis in native cardiac myocytes is important to clarify the mechanism by which the mutation leads to cardiac arrhythmias. In order to investigate whether RyR2<sup>R4496C+/-</sup> myocytes develop DAD in the absence of adrenergic stimulation, isolated cells from the hearts of knock-in mice were patch-clamped and action potentials recorded. The study showed that DAD and triggered activity were already present in unstimulated RyR2<sup>R4496C+/-</sup> myocytes (Liu et al., 2006).

In the present study, functional characterization of mice harboring a human RyR2 mutation (R4496C) associated with CPVT was performed using echocardiography (to assess *in vivo* cardiac function) as well as measurements of intracellular  $\text{Ca}^{2+}$  homeostasis (to evaluate global E-C coupling in isolated cardiomyocytes). The isolated RyR2<sup>R4496C<sup>+/-</sup></sup> mouse hearts showed no signs of hypertrophy and analysis of cardiomyocytes gave normal values. Echocardiographic measurements confirmed that RyR2<sup>R4496C<sup>+/-</sup></sup> knock-in mice have structurally and functionally normal hearts. Experiments to assess E-C coupling were performed in isolated single ventricular cardiac myocytes. In the heart, E-C coupling is the central mechanism by which electrical activation is translated into cardiac contraction. Cardiac contractions are directly governed by free cytosolic  $\text{Ca}^{2+}$ . Therefore, precise regulation of intracellular  $\text{Ca}^{2+}$  is critical for normal cardiac function. In detail, E-C coupling proceeds in a few steps: during depolarization small amounts of  $\text{Ca}^{2+}$  enters the cell through voltage-dependent L-type  $\text{Ca}^{2+}$  channels. This inward  $\text{Ca}^{2+}$  current activates RyR2s to release further  $\text{Ca}^{2+}$  from the SR into the cytosol. The rise in cytosolic  $\text{Ca}^{2+}$  activates the myofilaments and triggers contraction. The main mechanisms for  $\text{Ca}^{2+}$  elimination from the cytosol are pumping of  $\text{Ca}^{2+}$  back into SR by SERCA2a and the extrusion of  $\text{Ca}^{2+}$  out of myocytes by NCX (Bers, 2002). The investigation of  $\text{Ca}^{2+}$  transients and single cell shortening at several pacing rates in the present study revealed that the  $\text{Ca}^{2+}$  transient amplitude and fractional shortening in RyR2<sup>R4496C<sup>+/-</sup></sup> knock-in and WT myocytes were similar, which is consistent with the normal heart function in RyR2<sup>R4496C<sup>+/-</sup></sup> mice under physiological conditions. Moreover, at these pacing rates, the  $\text{Ca}^{2+}$  transient decay time and half-relaxation time of fractional shortening were also similar, suggesting a normal function of the SERCA2a activity. The SERCA2a and PLB protein expression levels were increased in homogenates prepared from RyR2<sup>R4496C<sup>+/-</sup></sup> mouse hearts. However, the ratio of SERCA2a/PLB was unchanged, indicating unaltered SR  $\text{Ca}^{2+}$  uptake function, that is consistent with the functional data assessed. NCX function and expression were also unaltered.

In addition to stimulating  $\text{Ca}^{2+}$  release during normal E-C coupling,  $\text{Ca}^{2+}$  release from the SR ( $\text{Ca}^{2+}$  sparks) can also occur spontaneously as a result of spontaneous opening of the RyR2 channels (Cheng et al., 1993). In cardiomyocytes isolated from RyR2<sup>R4496C<sup>+/-</sup></sup> knock-in mice, diastolic  $\text{Ca}^{2+}$  leak from the SR revealed a 2-fold increased  $\text{Ca}^{2+}$  spark frequency with high amplitudes and longer durations, suggesting increased open probability of RyR2 in mutant mice. The increased activity of the RyR2 could depend on the amount of  $\text{Ca}^{2+}$  stored in the SR, however, the SR  $\text{Ca}^{2+}$  load in RyR2<sup>R4496C<sup>+/-</sup></sup> knock-in mice was not

different from control. Thus the higher  $\text{Ca}^{2+}$  sparks occurrence in  $\text{RyR2}^{\text{R4496C}/-}$  myocytes is not due to either a higher level of  $\text{Ca}^{2+}$  stored in the SR or alteration of calsequestrin level. The increased CaSpF in mutant  $\text{RyR2}^{\text{R4496C}/-}$  mice is probably caused by “leaky” ryanodine receptor because of the mutation itself. This might also explain the apparent E-C coupling enhancement (higher fractional SR  $\text{Ca}^{2+}$  release) found in the present study. This enhanced cardiac diastolic  $\text{Ca}^{2+}$  leak may lead to the generation of DAD found by Liu and colleagues (Liu et al., 2006) resulting in arrhythmias (Pogwizd et al., 2001; Shannon et al., 2003). In detail, the directed leak of SR  $\text{Ca}^{2+}$  toward the NCX may lead to spontaneous depolarizations of the sarcolemma (Pogwizd et al., 2001). This may contribute to electrical instability, early or delayed afterdepolarizations and triggered arrhythmias (Lehnart et al., 2005; Wehrens et al., 2003). In electrically paced isolated myocytes from  $\text{RyR2}^{\text{R4496C}/-}$  mice, an increased amount of cellular arrhythmias at baseline was found in the present study, which is likely a consequence of the increased diastolic SR  $\text{Ca}^{2+}$  leak.

In conclusion, the R4496C mutation in cardiac RyR2 leads to increased fractional SR  $\text{Ca}^{2+}$  release during systole as well as enhanced diastolic  $\text{Ca}^{2+}$  leak from the SR, indicating increased RyR2 open probability and leading to a higher propensity for the development of DAD and triggered arrhythmias.

### **5.3 Overexpression of CaMKII $\delta_C$ in mouse hearts bearing the R4496C mutation leads to arrhythmias and increased mortality**

CaMKII is involved in the modulation of cellular  $\text{Ca}^{2+}$  regulation, including E-C coupling and has been implicated in the development of heart failure (Maier and Bers, 2002; Braun and Schulman, 1995). Transgenic mice that overexpress CaMKII $\delta_C$  show a reduction in twitch shortening,  $\text{Ca}^{2+}$  transient amplitude, SR  $\text{Ca}^{2+}$  content, as well as in SERCA2a and PLB expression. In contrast, the frequency of  $\text{Ca}^{2+}$  sparks was greatly enhanced. There was also enhanced NCX function and expression (Maier et al., 2003). In the present study, transgenic overexpression of cytosolic CaMKII $\delta_C$  in the  $\text{RyR2}^{\text{R4496C}/-}$  knock-in mutant mouse causes cardiac hypertrophy, contractile dysfunction and altered myocyte  $\text{Ca}^{2+}$  handling similar to previously published work in CaMKII $\delta_C$  TG mice (Maier et al., 2003). Most interestingly, in contrast to CaMKII $\delta_C$  transgenic mice with 80% survival after 10 weeks, CaMKII $\delta_C$ / $\text{RyR2}^{\text{R4496C}}$  double mutant mice died spontaneously at the age of 8-14

weeks with only 50% alive after 10 weeks. Possible reasons for these differences may be alterations in intracellular  $\text{Ca}^{2+}$  handling and/or cellular arrhythmias.

The most prominent and largely accepted disorder of E-C coupling in heart failure is decreased intracellular  $\text{Ca}^{2+}$  transients resulting from reduced SR  $\text{Ca}^{2+}$  load (Maier et al., 2003; Pieske et al., 1999) causing contractile dysfunction (Yano et al., 2005; Hasenfuss and Pieske, 2002). Reduction in SR  $\text{Ca}^{2+}$  reuptake via SERCA2a and increased SR  $\text{Ca}^{2+}$  leak through RyR2 are the main causative mechanisms for this phenomenon (Maier et al., 2003; Wehrens et al., 2004; Hasenfuss 1998; Ai et al., 2005; Marx et al., 2000). The  $\text{CaMKII}\delta_{\text{C}}/\text{RyR2}^{\text{R4496C}}$  mice in the present study not only demonstrate this HF phenotype but also show similar changes with respect to intracellular  $\text{Ca}^{2+}$  handling.

As mentioned above, reuptake via SERCA2a is the dominating mechanism for cytosolic  $\text{Ca}^{2+}$  elimination in the healthy heart. SERCA2a protein expression and/or activity were found to be reduced in the failing human heart (Meyer et al., 1995; Schwinger et al., 1999). PLB in its unphosphorylated state is an endogenous inhibitor of SERCA2a (Brittsan and Kranias, 2000). CaMKII can phosphorylate PLB at Thr-17, which increases SERCA2a activity and thus improves contractile function (Zhang et al., 2003). In the present study SERCA2a protein expression was decreased whereas PLB protein levels were unchanged in  $\text{CaMKII}\delta_{\text{C}}/\text{RyR2}^{\text{R4496C}}$  mice meaning that the ratio of SERCA2a relative to PLB is reduced. This indicates increased basal SERCA2a inhibition which may explain the prolonged relaxation kinetics. In addition, we detected similarly altered SERCA2a function with increased stimulation frequency in  $\text{CaMKII}\delta_{\text{C}}/\text{RyR2}^{\text{R4496C}}$  and  $\text{CaMKII}\delta_{\text{C}}$  as compared to WT mice. FDAR was prominent in all groups, with enhanced FDAR in double mutant and  $\text{CaMKII}\delta_{\text{C}}$  transgenic mice (similar to the previous study with  $\text{CaMKII}\delta_{\text{C}}$  TG mice). FDAR is an important intrinsic mechanism that facilitates relaxation with increasing heart rate. FDAR is also reflected in the rate of  $\text{Ca}^{2+}$  decline and is attributable to enhanced SR  $\text{Ca}^{2+}$  uptake (Maier and Bers, 2002). Thus, although FDAR might be activated by enhanced SR  $\text{Ca}^{2+}$  uptake via PLB phosphorylation by CaMKII-dependent increased phosphorylation at Thr-17 of PLB (Ai et al., 2005; Zhang et al., 2003), it may be compensated by underphosphorylation of Ser-16 (Ai et al., 2005; Kohlhaas et al., 2006) as well as the reduction in SERCA2a and the decreased in SERCA2a/PLB ratio may lead to net decreased SR  $\text{Ca}^{2+}$  uptake. NCX is the other major mechanism for cytosolic  $\text{Ca}^{2+}$  elimination and the main transporter of  $\text{Ca}^{2+}$  from the cell (Bers, 2002). The driving force of the NCX is the trans-sarcolemmal electrochemical differences of  $\text{Na}^{+}$  and  $\text{Ca}^{2+}$  and of the sarcolemmal membrane potential. In the “forward

mode”, the NCX eliminates one  $\text{Ca}^{2+}$  ion in exchange for three  $\text{Na}^+$  ions, but as mentioned above, it can also operate in a “reverse mode”, thus allowing  $\text{Ca}^{2+}$  to enter the cell. (Bers, 2001). Increased NCX expression and function are frequent findings in failing myocardium from several species including humans, but unchanged expression was also reported (Hasenfuss et al., 1999; Sipido et al., 2002). In the present study, no significant changes were found with respect to NCX protein expression in  $\text{CaMKII}\delta_{\text{C}}/\text{RyR2}^{\text{R4496C}}$  mice. However its function, measured as exponential rate time-constant of  $\text{Ca}^{2+}$  decline during caffeine-induced  $\text{Ca}^{2+}$  transients, was slightly increased in  $\text{CaMKII}\delta_{\text{C}}/\text{RyR2}^{\text{R4496C}}$  and  $\text{CaMKII}\delta_{\text{C}}$  myocytes, indicating increased  $\text{Ca}^{2+}$  extrusion from the cell through NCX.

In  $\text{CaMKII}\delta_{\text{C}}/\text{RyR2}^{\text{R4496C}}$  mouse hearts SR  $\text{Ca}^{2+}$  content was reduced to a similar extent as compared to  $\text{CaMKII}\delta_{\text{C}}$ , which may result from the decreased SR  $\text{Ca}^{2+}$  uptake or the enhanced SR  $\text{Ca}^{2+}$  leak as it was shown for other heart failure models (Hasenfuss 1998; Shannon et al., 2003). Contractile function and twitch  $\text{Ca}^{2+}$  transient amplitude at the single cell level at all frequencies were significantly decreased in  $\text{CaMKII}\delta_{\text{C}}/\text{RyR2}^{\text{R4496C}}$  and  $\text{CaMKII}\delta_{\text{C}}$  mice compared to control. This observation can be explained by a decreased amount of SERCA2a protein level and function as well as the reduction in SR  $\text{Ca}^{2+}$  content. This phenotype was also observed in studies using  $\text{CaMKII}\delta_{\text{C}}$  transgenic mice (Zhang et al., 2003; Maier et al., 2003) thus it correlates nicely to the in vivo data of the current study.

The fractional  $\text{Ca}^{2+}$  release, which provides an idea of how much  $\text{Ca}^{2+}$  is released at each twitch with respect to the total amount of  $\text{Ca}^{2+}$  stored within the SR, was significantly increased in  $\text{CaMKII}\delta_{\text{C}}/\text{RyR2}^{\text{R4496C}}$  and  $\text{CaMKII}\delta_{\text{C}}$  mice, although the lower SR  $\text{Ca}^{2+}$  content by itself would tend to greatly reduce fractional SR  $\text{Ca}^{2+}$  release. Thus, whereas SR  $\text{Ca}^{2+}$  content was reduced, the fraction of SR  $\text{Ca}^{2+}$  released during a twitch was increased, suggesting altered RyR2 open probability in  $\text{CaMKII}\delta_{\text{C}}/\text{RyR2}^{\text{R4496C}}$  double mutant and  $\text{CaMKII}\delta_{\text{C}}$  transgenic mice. This phenotype was also observed in previous studies using  $\text{CaMKII}\delta_{\text{C}}$  transgenic mice (Maier et al., 2003; Zhang et al., 2003).

In  $\text{CaMKII}\delta_{\text{C}}/\text{RyR2}^{\text{R4496C}}$  double mutant mice,  $\text{Ca}^{2+}$  sparks have increased frequency, higher amplitude and longer duration, demonstrating increased diastolic SR  $\text{Ca}^{2+}$  leak, despite reduced SR  $\text{Ca}^{2+}$  content and diastolic  $\text{Ca}^{2+}$  concentration, which actually should depress CaSpF (Cheng et al., 1993). In  $\text{CaMKII}\delta_{\text{C}}$  transgenic mice  $\text{Ca}^{2+}$  sparks have also increased frequency and duration but unchanged amplitude. One possible mechanism for this effect is an increased RyR2 opening at rest. RyR2 plays a central role in E-C coupling, it is therefore highly regulated. Recent studies have shown that CaMKII is associated with

the RyR2 (Maier et al., 2003; Currie et al., 2004; Wehrens et al., 2004), it can phosphorylate the RyR2 (Currie et al., 2004; Maier et al., 2003; Rodriguez et al., 2003; Wehrens et al., 2004; Witcher et al., 1991) and that this CaMKII-dependent RyR2 phosphorylation increases CaSpF and duration in PLB-KO mouse myocytes (without increased SR Ca<sup>2+</sup> content) (Guo et al., 2004; Guo et al., 2006). In contrast, when blocking CaMKII (using KN-93) Ca<sup>2+</sup> spark frequency decreases dramatically (Maier et al., 2003). In HF there is CaMKII-dependent enhancement of diastolic SR Ca<sup>2+</sup> leak via RyR2 and these diastolic SR Ca<sup>2+</sup> release events can contribute to the reduced SR Ca<sup>2+</sup> content (Shannon et al., 2003; Guo et al., 2006). Previous studies with CaMKII $\delta_C$  transgenic mice showed increased CaMKII association with RyR2, enhanced RyR2 phosphorylation, as well as increased fractional SR Ca<sup>2+</sup> release and resting CaSpF (despite lower SR Ca<sup>2+</sup> content and diastolic Ca<sup>2+</sup>) (Maier et al., 2003; Zhang et al., 2003). Acute CaMKII $\delta_C$  overexpression in rabbit ventricular myocytes increased fractional SR Ca<sup>2+</sup> release and CaSpF due to phosphorylation of RyR2 (Kohlhaas et al., 2006). The results indicate that CaMKII can enhance RyR2 opening, both at rest (as SR Ca<sup>2+</sup> sparks) and during E-C coupling (as fractional SR Ca<sup>2+</sup> release). The CaMKII-dependent enhancement of diastolic SR Ca<sup>2+</sup> leak may also contribute to the activation of a transient inward NCX current that cause DAD and triggered arrhythmias. Indeed, in the present study cellular arrhythmias were observed more frequently in CaMKII $\delta_C$ /RyR2<sup>R4496C</sup> mice versus CaMKII $\delta_C$  at baseline. In addition, this result was confirmed by data of Sedej and colleagues (Sedej et al., 2008) who showed significantly increased action potential durations in CaMKII $\delta_C$ /RyR2<sup>R4496C</sup> and CaMKII $\delta_C$  myocytes in contrast to WT using patch-clamp technique. Most importantly, DAD and spontaneous action potentials were clearly more often found in CaMKII $\delta_C$ /RyR2<sup>R4496C</sup> as compared to CaMKII $\delta_C$  mouse myocytes, whereas WT showed almost no arrhythmias. DAD frequency was significantly increased in CaMKII $\delta_C$ /RyR2<sup>R4496C</sup> versus CaMKII $\delta_C$  myocytes. This possibly explains high mortality in double mutant mice. We propose that CaMKII-dependent enhancement of SR Ca<sup>2+</sup> leak in CaMKII $\delta_C$ /RyR2<sup>R4496C</sup> mice may increase the propensity for DAD and arrhythmias. Here we also found that the expression level of calsequestrin was decreased in CaMKII $\delta_C$ /RyR2<sup>R4496C</sup> mice. Calsequestrin is a high-capacity, low-affinity Ca<sup>2+</sup>-binding protein that represents a major Ca<sup>2+</sup>-reservoir element within the SR lumen (Jones et al., 1998). It has been reported that expression of genes encoding calsequestrin was repressed in both diseased human and rat hearts. This reduced expression might be viewed as an adaptive response to a reduced Ca<sup>2+</sup> store within the sarcoplasmic reticulum (Zwadlo and

Borlak, 2005; Borlak and Thum, 2003; Temsah et al., 2001) but it may very well contribute to increased RyR2 sensitivity in CaMKII $\delta_C$ /RyR2<sup>R4496C</sup> mice.

In conclusion, this study demonstrated that CaMKII $\delta_C$  overexpression in mouse hearts harboring the R4496C knock-in mutation in RyR2 leads to contractile dysfunction both in vivo and in vitro associated with defects in Ca<sup>2+</sup> handling. The combination of the R4496C mutation with increased CaMKII $\delta_C$  activity provides an arrhythmogenic substrate. The strong increase in mortality in these mice may be explained by a combination of spontaneous fatal arrhythmias and impaired contractility. This is in contrast to RyR2<sup>R4496C+/-</sup> mice which show CPVT without structural heart disease only in the presence of adrenergic stimulation.



## 6 References

**Ai X., Curran J.W., Shannon T.R., Bers D.M., Pogwizd S.M.** Ca<sup>2+</sup>/calmodulin-dependent protein kinase modulates cardiac ryanodine receptor phosphorylation and sarcoplasmic reticulum Ca<sup>2+</sup> leak in heart failure. *Circ Res.* 97:1314-1322, **2005**

**Anderson M.E., Braun A.P., Schulman H., Premack B.A.** Multifunctional Ca/calmodulin-dependent protein kinase mediates Ca-induced enhancement of the L-type Ca current in rabbit ventricular myocytes. *Circ Res.* 75:854-61, **1994**

**Anderson M.E., Braun A.P., Wu Y., Lu T., Schulman H., Sung R.J.** KN-93, an inhibitor of multifunctional Ca<sup>2+</sup>/calmodulin-dependent protein kinase, decreases early afterdepolarizations in rabbit heart. *J Pharmacol Exp Ther.* 287:996-1006, **1998**

**Bassani R.A., Mattiazzi A., Bers D.M.** CaMKII is responsible for activity-dependent acceleration of relaxation in rat ventricular myocytes. *Am J Physiol.* 268:H703-12, **1995**

**Bennett P., Yazawa K., Makita N., George A.** Molecular mechanism for an inherited cardiac arrhythmia. *Nature.* 376:683-685, **1995**

**Bers D.M.** Cardiac excitation-contraction coupling. *Nature.* 415:198-205, **2002**

**Bers D.M.** Excitation-contraction coupling and cardiac contractile force. 2nd ed. Kluwer. Dordrecht, Netherlands, **2001**

**Bers D.M., Guo T.** Calcium signaling in cardiac ventricular myocytes. *Ann N Y Acad Sci.* 1047:86-98, **2005**

**Borlak J., Thum T.** Hallmarks of ion channel gene expression in end-stage heart failure. *FASEB J.* 17:1592-1606, **2003**

**Braun A.P., Schulman H.** The multifunctional calcium/calmodulin-dependent protein kinase: from form to function. *Annu Rev Physiol.* 57:417-445, **1995**

**Brittsan A.G., Kranias E.G.** Phospholamban and cardiac contractile function. *J Mol Cell Cardiol.* 32:2131-9, **2000**

**Brugada P., Brugada J.** Right bundle branch block, persistent ST segment elevation and sudden cardiac death: a distinct clinical and electrocardiographic syndrome. A multicenter report. *J Am Coll Cardiol.* 20:1391-1396, **1992**

**Catterall W.A.** From ionic currents to molecular mechanisms: the structure and function of voltage-gated sodium channels. *Neuron.* 26:13-25, **2000**

**Cerrone M., Colombi B., Santoro M., di Barletta M.R., Scelsi M., Villani L., Napolitano C., Priori S.G.** Bidirectional ventricular tachycardia and fibrillation elicited in a knock-in mouse model carrier of a mutation in the cardiac ryanodine receptor. *Circ Res.* 96:e77-e82, **2005**

**Cheng H., Lederer W.J., Cannell M.B.** Calcium sparks: elementary events underlying excitation-contraction coupling in heart muscle. *Science.* 262:740-744, **1993**

**Cheung W.Y.** Calmodulin plays a pivotal role in cellular regulation. *Science.* 207:19-27, **1980**

**Colomer J.M., Mao L., Rockman H.A., Means A.R.** Pressure overload selectively up-regulates  $Ca^{2+}$ /calmodulin-dependent protein kinase II in vivo. *Mol Endocrinol.* 17:183-92, **2003**

**Colomer J.M., Means A.R.** Chronic elevation of calmodulin in ventricles of transgenic mice increases the autonomous activity of calmodulin-dependent protein kinase II, which regulates atrial natriuretic factor gene expression. *Mol Endocrinol.* 14:1125-1136, **2000**

**Currie S., Loughrey C.M., Craig M.A., Smith G.L.** Calcium/calmodulin-dependent protein kinase II $\delta$  associates with the ryanodine receptor complex and regulates channel function in rabbit heart. *Biochem J.* 377:357-66, **2004**

**Davis B.A., Schwartz A., Samaha F.J., Kranias E.G.** Regulation of cardiac sarcoplasmic reticulum calcium transport by calcium-calmodulin-dependent phosphorylation. *J Biol Chem.* 258:13587-91, **1983**

**DeSantiago J., Maier L.S., Bers D.M.** Frequency-dependent acceleration of relaxation in the heart depends on CaMKII, but not phospholamban. *J Mol Cell Cardiol.* 34:975-84, **2002**

**Deschênes I., Neyroud N., DiSilvestre D., Marbán E., Yue D.T., Tomaselli G.F.** Isoform-specific modulation of voltage-gated Na<sup>+</sup> channels by calmodulin. *Circ Res.* 90:49e-57, **2002**

**Dominguez J.N., Rosa A., Navarro F., Franco D., Aranega A.E.** Tissue distribution and subcellular localization of the cardiac sodium channel during mouse heart development. *Cardiovascular Res.* 78:45-52, **2008**

**Dzhura I., Wu Y., Colbran R.J., Balsler J.R., Anderson M.E.** Calmodulin kinase determines calcium-dependent facilitation of L-type calcium channels. *Nat Cell Biol.* 2:173-7, **2000**

**Edman C.F., Schulman H.** Identification and characterization of  $\delta_B$ -CaM kinase and  $\delta_C$ -CaM kinase from rat heart, two new multifunctional Ca<sup>2+</sup>/calmodulin-dependent protein kinase isoforms. *Biochim Biophys Acta.* 1221:89-101, **1994**

**Fill M., Copello J.A.** Ryanodine receptor calcium release channels. *Physiol Rev.* 82:893-922, **2002**

**Fozzard H.A., Hanck D.A.** Structure and function of voltage-dependent sodium channels: comparison of brain II and cardiac isoforms. *Physiol Rev.* 76:887-926, **1996**

**Frohnwieser B., Chen L., Schreibmayer W., Kallen R.** Modulation of the human cardiac sodium channel  $\alpha$ -subunit by cAMP-dependent protein kinase and the responsible sequence domain. *J Physiol.* 498:309-318, **1997**

**George C.H., Higgs G.V., Lai F.A.** Ryanodine receptor mutations associated with stress-induced ventricular tachycardia mediate increased calcium release in stimulated cardiomyocytes. *Circ Res.* 93:531-540, **2003**

**Grueter C.E., Abiria S.A., Dzhura I., Wu Y., Ham A.J.L., Mohler P.J., Anderson M.E., Colbran R.J.** L-type  $\text{Ca}^{2+}$  channel facilitation mediated by phosphorylation of the  $\beta$  subunit by CaMKII. *Mol Cell.* 23:641-50, **2006**

**Guo T., Zhang T., Brown J.H., Bers D.M.** Effects of CaMKII on cardiac Ca release channels in myocytes. *Biophys J.* 86:241a, **2004**

**Guo T., Zhang T., Mestril R., Bers D.M.** Ca/calmodulin-dependent protein kinase II phosphorylation of ryanodine receptor does affect calcium sparks in mouse ventricular myocytes. *Circ Res.* 99:398-406, **2006**

**Hagemann D., Kuschel M., Kuramochi T., Zhu W., Cheng H., Xiao R.P.** Frequency-encoding Thr17 phospholamban phosphorylation is independent of Ser16 phosphorylation in cardiac myocytes. *J Biol Chem.* 275:22532-6, **2000**

**Hain J., Onoue H., Mayrleitner M., Fleischer S., Schindler H.** Phosphorylation modulates the function of the calcium release channel of sarcoplasmic reticulum from cardiac muscle. *J Biol Chem.* 270: 2074-81, **1995**

**Hasenfuss G., Pieske B.** Calcium cycling in congestive heart failure. *J Moll Cell Cardiol.* 34:951-969, **2002**

**Hasenfuss G., Schillinger W., Lehnart S.E., Preuss M., Pieske B., Maier L.S., Prestle J., Minami K., Just H.** Relationship between  $\text{Na}^{+}$ - $\text{Ca}^{2+}$  exchanger protein levels and diastolic function of failing human myocardium. *Circulation.* 99:641-8, **1999**

**Hasenfuss G.** Alterations of calcium-regulatory proteins in heart failure. *Cardiovasc Res.* 37:279-289, **1998**

**Haufe V., Camacho J.A., Dumaine R., Günther B., Bollensdorff C., Segond von Banchet G., Benndorf K., Zimmer T.** Expression pattern of neuronal and skeletal muscle voltage-gated Na<sup>+</sup> channels in the developing mouse heart. *J Physiol.* 564:683-696, **2005**

**Hoch B., Meyer R., Hetzer R., Krause E.G., Karczewski P.** Identification and expression of delta-isoforms of the multifunctional Ca<sup>2+</sup>/calmodulin-dependent protein kinase in failing and nonfailing human myocardium. *Circ Res.* 84:713-21, **1999**

**Hook S.S., Means A.R.** Ca<sup>2+</sup>/CaM-dependent kinases: from activation to function. *Annu Rev Pharmacol Toxicol.* 41:471-505, **2001**

**Hudmon A., Schulman H., Kim J., Maltez J.M., Tsien R.W., Pitt G.S.** CaMKII tethers to L-type Ca<sup>2+</sup> channels, establishing a local and dedicated integrator of Ca<sup>2+</sup> signals for facilitation. *J Cell Biol.* 171:537-47, **2005**

**Isom L.L.** Sodium channel beta subunits: anything but auxiliary. *Neuroscientist.* 7:42-54, **2001**

**Isom L.L., De Jongh K.S., Catterall W.A.** Auxiliary subunits of voltage-gated ion channels. *Neuron.* 12:1183-1194, **1994**

**January C.T., Riddle J.M.** Early afterdepolarizations: mechanism of induction and block. A role for L-type Ca<sup>2+</sup> current. *Circ Res.* 64:977-90, **1989**

**Jiang D., Xiao B., Yang D., Wang R., Choi P., Zhang L., Cheng H., Chen S.R.** RyR2 mutations linked to ventricular tachycardia and sudden death reduce the threshold for store-overload-induced Ca<sup>2+</sup> release (SOICR). *Proc Natl Acad Sci USA* 101:13062-13067, **2004**

**Jiang D., Xiao B., Zhang L., Chen S.R.** Enhanced basal activity of a cardiac Ca<sup>2+</sup> release channel (ryanodine receptor) mutant associated with ventricular tachycardia and sudden death. *Circ Res.* 91:218-25, **2002**

**Kirchhefer U., Schmitz W., Scholz H., Neumann J.** Activity of cAMP-dependent protein kinase and Ca<sup>2+</sup>/calmodulin-dependent protein kinase in failing and nonfailing human hearts. *Cardiovasc Res.* 42:254-61, **1999**

**Kohlhaas M., Zhang T., Seidler T., Zibrova D., Dybkova N., Steen A., Wagner S., Chen L., Brown J.H., Bers D.M., Maier L.M.** Increased sarcoplasmic reticulum calcium leak but unaltered contractility by acute CaMKII overexpression in isolated rabbit cardiac myocytes. *Circ Res.* 98:235-44, **2006**

**Lai Y., Nairn A.C., Greengard P.** Autophosphorylation reversibly regulates the Ca/calmodulin-dependent protein kinase II. *Proc Natl Acad Sci.* 83:4253-7; **1986**

**Laitinen P., Swan H., Piippo K., Viitasalo M., Toivonen L., Kontula K.** Genes, exercise and sudden death: molecular basis of familial catecholaminergic polymorphic ventricular tachycardia. *Ann Med.* 36(Suppl1):81-6, **2004**

**Lee J.C., Edelman A.M.** A protein activator of Ca<sup>2+</sup>/calmodulin-dependent protein kinase Ia. *J Biol Chem.* 269:2158-2164, **1994**

**Leenhardt A., Lucet V., Denjoy I., Grau F., Ngoc D.D., Coumel P.** Catecholaminergic polymorphic ventricular tachycardia in children. A 7-year follow-up of 21 patients. *Circulation.* 91:1512-1519, **1995**

**Lehnart S.E., Wehrens X.H., Marks A.R.** Defective ryanodine receptor interdomain interactions may contribute to intracellular Ca<sup>2+</sup> leak: a novel therapeutic target in heart failure. *Circulation.* 111:3342-3346, **2005**

**Li L., Satoh H., Ginsburg K.S., Bers D.M.** The effect of Ca-calmodulin-dependent protein kinase II on cardiac excitation-contraction coupling in ferret ventricular myocytes. *J Physiol.* 501:17-32, **1997**

**Liu N., Colombi B., Memmi M., Zissimopoulos S., Rizzi N., Negri S., Imbriani M., Napolitano C., Lai F.A., Priori S.G.** Arrhythmogenesis in catecholaminergic

polymorphic ventricular tachycardia. Insights from a RyR2 R4496C knock-in mouse model. *Circ Res.* 99:292-298, **2006**

**Lokuta A.J., Rogers T.B., Lederer W.J., Valdivia H.H.** Modulation of cardiac ryanodine receptors of swine and rabbit by a phosphorylation-dephosphorylation mechanism. *J Physiol.* 487:609-22, **1997**

**Lou L.L., Lloyd S.J., Shulman H.** Activation of the multifunctional Ca/calmodulin-dependent protein kinase by autophosphorylation: ATP modulates production of an autonomous enzyme. *Proc Natl Acad Sci.* 83:9497-501, **1986**

**Lu T., Lee H-C., Kabat J.A., Shibata E.F.** Modulation of rat cardiac sodium channel by the stimulatory G protein  $\alpha$  subunit. *J Physiol.* 518:371-384, **1999**

**Maier L.S., Bers D.M.** Calcium, calmodulin, and calcium-calmodulin kinase II: heartbeat to heartbeat and beyond. *J Mol Cell Cardiol.* 34:919-39, **2002**

**Maier L.S., Bers D.M.** Role of  $\text{Ca}^{2+}$ /calmodulin-dependent protein kinase (CaMK) in excitation-contraction coupling in the heart. *Cardiovasc Res.* 73:631-640, **2007**

**Maier L.S., Zhang T., Chen L., DeSantiago J., Brown J.H., Bers D.M.** Transgenic  $\text{CaMKII}\delta_{\text{C}}$  overexpression uniquely alters cardiac myocyte  $\text{Ca}^{2+}$  handling: reduced SR  $\text{Ca}^{2+}$  load and activated SR  $\text{Ca}^{2+}$  release. *Circ Res.* 92:904-11, **2003**

**Maier S.K.G., Westenbroek R.E., McCormic K.A., Curtis R., Scheuer T., Catterall W.A.** Distinct subcellular localization of different sodium channel  $\alpha$  and  $\beta$  subunits in single ventricular myocytes from mouse heart. *Circulation.* 109:1421-1427, **2004**

**Maier S.K.G., Westenbroek R.E., Schenkman K.A., Feigl E.O., Scheuer T., Catterall W.A.** An unexpected role for brain-type sodium channels in coupling of cell surface depolarization to contraction in the heart. *PNAS.* 99: 4073-8, **2002**

**Marx S.O., Reiken S., Hisamatsu Y., Gaburjakova M., Gaburjakova J., Yang Y.M., Rosemlit N., Marks A.R.** Phosphorylation-dependent regulation of ryanodine receptors: a novel role for leucine-isoleucine zippers. *J Cell Biol.* 154:699-708, **2001**

**Marx S.O., Reiken S., Hisamatsu Y., Jayaraman T., Burkhoff D., Rosemlit N., Marks A.R.** PKA phosphorylation dissociates FKBP12.6 from the calcium release channel (ryanodine receptor): defective regulation in failing hearts. *Cell.* 101:365-376, **2000**

**Meissner G.** Regulation of mammalian ryanodine receptors. *Front Biosci.* 7:d2072-d2080, **2002**

**Meyer M., Schillinger W., Pieske B., Holubarsch C., Heilmann C., Posival H., Kuwajima G., Mikoshiba K., Just H., Hasenfuss G.** Alterations of sarcoplasmic reticulum proteins in failing human dilated cardiomyopathy. *Circulation.* 92:778-784, **1995**

**Meyer T., Hanson P.I., Stryer L., Schulman H.** Calmodulin trapping by calcium-calmodulin-dependent protein kinase II. *Science.* 256:1199-202, **1992**

**Mohler P.J., Rivolta I., Napolitano C., LeMaillet G., Lambert S., Priori S.G., Bennett V.** Nav1.5 E1053K mutation causing Brugada syndrome blocks binding to ankyrin-G and expression of Nav1.5 on the surface of cardiomyocytes. *PNAS.* 101:17533-8, **2004**

**Motoike H.K., Liu H., Glaaser I.W., Yang A-S., Tateyama M., Kass R.S.** The Na<sup>+</sup> channel inactivation gate is a molecular complex: novel role of the COOH-terminal domain. *J Gen Physiol.* 123:155-165, **2004**

**Murphy B.J., Rogers J., Perdichizzi A.P., Colvin A.A., Catterall W.A.** cAMP-dependent phosphorylation of two sites in the  $\alpha$  subunit of the cardiac sodium channel. *J Biol Chem.* 271:28837-28843, **1996**

**Ono K., Kiyosue T., Arita M.** Isoproterenol, DBcAMP, and forskolin inhibit cardiac sodium current. *Am J Physiol Cell Physiol.* 256:C1131-C1137, **1989**



- Passier R., Zeng H., Frey N., Naya F.J., Nicol R.L., McKinsey T.A., Overbeek P.A., Richardson J.A., Grant S.R., Olson E.N.** CaM kinase signaling induces cardiac hypertrophy and activates the MEF2 transcription factor in vivo. *J Clin Invest.* 105:1395-1406, **2000**
- Pieske B., Maier L.S., Bers D.M., Hasenfuss G.** Ca<sup>2+</sup> handling and Ca<sup>2+</sup> content in isolated failing and nonfailing human myocardium. *Circ Res.* 85:38-46, **1999**
- Pogwizd S.M., Schlotthauer K., Li L., Yuan W., Bers D.M.** Arrhythmogenesis and contractile dysfunction in heart failure: roles of sodium-calcium exchange, inward rectifier potassium current, and residual beta-adrenergic responsiveness. *Circ Res.* 88:1159-1167, **2001**
- Priebe L., Beuckelmann D.J.** Simulation study of cellular electric properties in heart failure. *Circ Res.* 82:1206-1223, **1998**
- Priori S.G., Napolitano C., Memmi M., Colombi B., Drago F., Gasparini M., DeSimone L., Coltorti F., Bloise R., Keegan R., Cruz Filho F.E., Vignati G., Benatar A., DeLogu A.** Clinical and molecular characterization of patients with catecholaminergic polymorphic ventricular tachycardia. *Circulation.* 106:69-74, **2002**
- Priori S.G., Napolitano C., Tiso N., Memmi M., Vignati G., Bloise R., Sorrentino V.V., Danieli G.A.** Mutations in the cardiac ryanodine receptor gene (hRyR2) underlie catecholaminergic polymorphic ventricular tachycardia. *Circulation.* 103:196-200, **2001**
- Qu Y., Rogers J., Tanada T., Catterall W., Scheuer T.** Phosphorylation of S1505 in the cardiac Na<sup>+</sup> channel inactivation gate is required for modulation by protein kinase C. *J Gen Physiol.* 108:375-379, **1996**
- Ramirez M.T., Zhao X., Schulman H., Brown J.H.** The nuclear  $\delta_B$  isoform of Ca<sup>2+</sup>/calmodulin-dependent protein kinase II regulates atrial natriuretic factor gene expression in ventricular myocytes. *J Biol Chem.* 272:31203-31208, **1997**

**Rodriguez P., Bhogal M.S., Coyler J.** Stoichiometric phosphorylation of cardiac ryanodine receptor on serine-2809 by calmodulin-dependent kinase II and protein kinase A. *J Biol Chem.* 278:38593-600, **2003**

**Saito T., Fukuzawa T., Osaki J., Sakuragi H., Yao N., Haneda T., Fujino T., Wakamiya N., Kikuchi K., Hasebe N.** Roles of calcineurin and calcium/calmodulin-dependent protein kinase II in pressure overload-induced cardiac hypertrophy. *J Mol Cell Cardiol.* 35:1153-60, **2003**

**Schillinger W., Janssen P.M., Emami S., Henderson S.A., Ross R.S., Teucher N., Zeitz O., Philipson K.D., Prestle J., Hasenfuss G.** Impaired contractile performance of cultured rabbit ventricular myocytes after adenoviral gene transfer of Na<sup>+</sup>-Ca<sup>2+</sup> exchanger. *Circ Res.* 87:581-7, **2000**

**Schwinger R.H., Munch G., Bölek B., Karczewski P., Krause E.G., Erdmann E.** Reduced Ca<sup>2+</sup> sensitivity of SERCA2a in failing human myocardium due to reduced serin-16 phospholamban phosphorylation. *J Mol Cell Cardiol.* 31:479-491, **1999**

**Sedej S, Kockskämper J, Heinzl FR, Groborz J, Gronau P, Dybkova N, Maier LS, Colombi B, Napolitano C, Priori SG, Pieske B.** Increased vulnerability to ouabain-induced arrhythmias in myocytes from mouse hearts harboring a human CPVT mutation. 74<sup>th</sup> Annual Meeting of the German Cardiac Society:P1544, **2008** (Abstract)

**Shannon T.R., Pogwizd S.M., Bers D.M.** Elevated sarcoplasmic reticulum Ca leak in intact ventricular myocytes from rabbits in heart failure. *Circ Res.* 93:592-594, **2003**

**Simmerman H.K.B., Collins J.H., Theibert J.L., Wegener A.D., Jones L.R.** Sequence analysis of PLB: identification of phosphorylation sites and two major structural domains. *J Biol Chem.* 261:13333-41, **1986**

**Sipido K.R., Volders P.G., Vos M.A., Verdonck F.** Altered Na/Ca exchange activity in cardiac hypertrophy and heart failure: a new target for therapy? *Cardiovasc Res.* 53:782-805, **2002**

**Stühmer W., Conti F., Suzuki H., Wang X.D., Noda M., Yahagi N., Kubo H., Numa S.** Structural parts involved in activation and inactivation of the sodium channel. *Nature*. 339:597-603, **1989**

**Temsah R.M., Kawabata K., Chapman D., Dhalla N.S.** Modulation of cardiac sarcoplasmic reticulum gene expression by lack of oxygen and glucose. *FASEB J*. 15:2517-7, **2001**

**Tokumitsu H., Enslen H., Soderling T.R.** Characterization of a Ca<sup>2+</sup>/calmodulin-dependent protein kinase cascade: molecular cloning and expression of calcium/calmodulin-dependent protein kinase kinase. *J Biol Chem*. 270:19320-19324, **1995**

**Towbin H., Staehelin T., Gordon J.** Electrophoretic transfer of proteins from polyacrylamide gels to nitrocellulose sheets: procedure and some applications. *Proc Natl Acad Sci*. 76:4350-4354, **1979**

**Veldkamp M.W., Viswanathan P.C., Bezzina C., Baartscheer A., Wilde A.A.M., Balse J.R.** Two distinct congenital arrhythmias evoked by a multidysfunctional Na<sup>+</sup> channel. *Circ Res*. 86:91e-97e, **2000**

**Viswanathan P.C., Balse J.R.** Inherited sodium channelopathies: a continuum of channel dysfunction. *Trends Cardiovasc Med*. 14:28-35, **2004**

**Vogel H.J.** Calmodulin: a versatile calcium mediator protein. *Biochem Cell Biol*. 72: 357-376, **1994**

**Wagner S., Dybkova N., Rasenack E.C.L., Jacobshagen C., Fabritz L., Kirchof P., Maier S.K.G., Zhang T., Hasenfuss G., Brown J.H., Bers D.M., Maier L.S.** Ca<sup>2+</sup>/calmodulin-dependent protein kinase II regulates cardiac Na<sup>+</sup> channels. *J Clin. Invest*. 116:3127-3138, **2006**

**Wagner S., Maier L.S.** Modulation of cardiac Na<sup>+</sup> and Ca<sup>2+</sup> currents by CaM and CaMKII. *J Cardiovasc Electrophysiol*. 17:S26-S33, **2006**

**Wagner S., Seidler T., Picht E., Maier L.S., Kazanski V., Teucher N., Schillinger W., Pieske B., Isenberg G., Hasenfuss G., Kögler H.** Na<sup>+</sup>-Ca<sup>2+</sup> exchanger overexpression predisposes to reactive oxygen species-induced injury. *Cardiovasc Res.* 60:404-12, **2003**

**Wang D.W., Makita N., Kitabatake A., Balsler J.R., George A.L.** Enhanced Na<sup>+</sup> channel intermediate inactivation in Brugada syndrome. *Circ Res.* 87:E37-E43, **2000**

**Watson C.L., Gold M.R.** Lysophosphatidylcholine modulates cardiac I<sub>Na</sub> via multiple protein kinase pathways. *Circ Res.* 81:387-395, **1997**

**Wehrens X.H., Lehnart S.E., Huang F., Vest J.A., Reiken S.R., Mohler P.J., Sun J., Guatimosim S., Song L.S., Rosemblyt N., D'Armiento J.M., Napolitano C., Memmi M., Priori S.G., Lederer W.J., Marks A.R.** FKBP 12.6 deficiency and defective calcium release channel (ryanodine receptor) function linked to exercise-induced sudden cardiac death. *Cell.* 113:829-40, **2003**

**Wehrens X.H., Lehnart S.E., Reiken S.R., Marks A.R.** Ca<sup>2+</sup>/calmodulin-dependent protein kinase II phosphorylation regulates the cardiac ryanodine receptor. *Circ Res.* 94:e61-70, **2004**

**Witcher D.R., Kovacs R.J., Schulman H., Cefali D.C., Jones L.R.** Unique phosphorylation site on the cardiac ryanodine receptor regulates calcium channel activity. *J Biol Chem.* 266:11144-52, **1991**

**Witcher D.R., Kovacs R.J., Schulman H., Cefali D.C., Jones L.R.** Unique phosphorylation site on the cardiac ryanodine receptor regulates calcium channel activity. *J Biol Chem.* 266:11144-52, **1991**

**Wu Y., Colbran R.J., Anderson M.E.** Calmodulin kinase is a molecular switch for cardiac excitation-contraction coupling. *Proc Natl Acad Sci.* 98:2877-81, **2001**

**Wu Y., MacMillan L.B., McNeill R.B., Colbran R.J., Anderson M.E.** CaM kinase augments cardiac L-type  $\text{Ca}^{2+}$  current: a cellular mechanism for long Q-T arrhythmias. *Am J Physiol.* 276:H2168-H2178, **1999**

**Wu Y., Roden D.M., Anderson M.E.** Calmodulin kinase inhibition prevents development of the arrhythmogenic transient inward current. *Circ Res.* 84:906-912, **1999**

**Wu Y., Temple J., Zhang R., Dzhura I., Zhang W., Trimble R., Roden D.M., Passier R., Olson E.N., Colbran R.J., Anderson M.E.** Calmodulin kinase II and arrhythmias in mouse model of cardiac hypertrophy. *Circulation.* 106:1288-1293, **2002**

**Xiao R.P., Cheng H., Lederer W.J., Suzuki T., Lakatta E.G.** Dual regulation of Ca/calmodulin kinase II activity by membrane voltage and by calcium influx. *Proc Natl Acad Sci.* 91:9659-63, **1994**

**Yang D., Zhu W.Z., Xiao B., Brochet D.X.P., Chen S.R.W., Lakatta E.G., Xiao R.P., Heping Cheng H.**  $\text{Ca}^{2+}$ /calmodulin kinase II-dependent phosphorylation of ryanodine receptors suppresses  $\text{Ca}^{2+}$  sparks and  $\text{Ca}^{2+}$  waves in cardiac myocytes. *Circ Res.* 100:399-407, **2007**

**Yano M., Ikeda Y., Matsuzaki M.** Altered intracellular  $\text{Ca}^{2+}$  handling in heart failure. *J Clin Invest.* 115:556-564, **2005**

**Yuan W., Bers D.M.** Ca-dependent facilitation of cardiac Ca current is due to Ca-calmodulin dependent protein kinase. *Am J Physiol.* 267:H982-93, **1994**

**Zeng J., Rudy Y.** Early afterdepolarizations in cardiac myocytes: mechanism and rate dependence. *Biophys J.* 68:949-964, **1995**

**Zhang R., Khoo M.S.C., Wu Y., Yang Y., Grueter C.E., Ni G., Price E.E., Thiel W., Guatimosin S., Song L.S., Madu E.C., Shah A.N., Vishnivetskaya T.A., Atkinson J.B., Gurevich V.V., Salama G., Lederer W.J., Colbran R.J., Anderson M.E.** Calmodulin kinase II inhibition protects against structural heart disease. *Nat Med.* 11:409-17, **2005**

**Zhang T., Brown J.H.** Role of  $\text{Ca}^{2+}$ /calmodulin-dependent protein kinase II in cardiac hypertrophy and heart failure. *Cardiovasc Res.* 63:476-486, **2004**

**Zhang T., Johnson E.N., Gu Y., Morissette M.R., Sah V.P., Gigena M.S., Belke D.D., Dillmann W.H., Rogers T. B., Schulman H., Ross J. Jr., Brown J.H.** The cardiac-specific nuclear  $\delta_B$  isoform of Ca/calmodulin-dependent protein kinase II induces hypertrophy and dilated cardiomyopathy associated with increased protein phosphatase 2A activity. *J Biol Chem.* 277:1261-1267, **2002**

**Zhang T., Maier L.S., Dalton N.D., Miyamoto S., Ross J.J., Bers D.M., Brown J.H.** The  $\delta_C$  isoform of CaMKII is activated in cardiac hypertrophy and induces dilated cardiomyopathy and heart failure. *Circ Res.* 92:912-9, **2003**

**Zhu W.S., Wang S.Q., Charik K., Yang D., Zhang T., Brown J.H, Devic E., Kobilka B.K., Cheng H., Xiao R.P.** Linkage of beta 1-adrenergic stimulation to apoptotic heart cell death through protein kinase A-independent activation of  $\text{Ca}^{2+}$ /calmodulin kinase II. *J Clin Invest.* 111:617-25, **2003**

**Zwadlo C., Borlak J.** Disease-associated changes in the expression of ion channels, ion receptors, ion exchangers and  $\text{Ca}^{2+}$ -handling proteins in heart hypertrophy. *Toxicol Appl Pharmacol.* 207:244-256, **2005**

## Acknowledgements

I would like to thank Professor Lars Maier for giving me the opportunity to work on this project, for his generous help and constant support.

I am very grateful to Professor Rüdiger Hardeland for reviewing my PhD thesis and to Professor Detlef Doenecke for being my coreviewer.

I want to give my special thanks to Dr. Darya Zibrova and Astrid Steen from whom I learned the best laboratory practice, for their help in my work.

I am thankful to Dr. Stefan Wagner and Dr. Stefan Neef for their help and cooperation, for teaching me confocal and epifluorescence microscopy. I appreciate their helpful advice and the time they spent discussing our results.

I thank Dr. Michael Kohlhaas and Dr. Can Sag for their cooperation, practical advice and the answers to all my questions.

I want to give my special thanks to Timo Schulte and Thomas Sowa for their help in organizing my work and for their constant support.

My warm thanks to all my colleagues, with whom I worked side by side over the last few years in the department, for the creation of a scientific working atmosphere.

I am thankful to Gudrun Müller for the huge yields of isolated rabbit cardiomyocytes.

My very special thanks I give to my husband, Sasha, for his wholehearted and active support, patience and understanding.

Finally, I want to give a very special thanks to my mother for her moral support that was so necessary for me during this whole period.

## Appendix

### Curriculum Vitae

#### Personal data

Name	Nataliya Dybkova
Date of birth	7.12.1972
Place of birth	Kiev, Ukraine
Citizenship	Ukraine
Marital status	Married

#### Education

1979-1992	School education, Kiev, Ukraine
1993-1998	University study Biological faculty of Kiev National Taras Shevchenko University, Kiev, Ukraine
1997	Degree: Bachelor of Science in biology, teacher of biology Bachelor scientific project "The effect of nerobol anabolic on Na <sup>+</sup> /K <sup>+</sup> -ATPase activity of microsomes of skeletal, unstriped and heart muscles"
1998	Degree: Specialist of Science in biochemistry, teacher of biology Specialist scientific project "Investigation of the effect of acetylsalicylic acid on the state of membranes of endoplasmatical reticulum of the rat liver under conditions of their intoxication by tetrachlormethane"
2003-2005	Research assistant in Department of Cardiology and Pneumology of Georg-August University Clinic (Göttingen)
March 2005-May 2008	Experimental work for the present dissertation in Department of Cardiology and Pneumology of Georg-August University Clinic (Göttingen)

#### Publications

1. Maier LS, Wahl-Schott C, Horn W, Weichert S, Pagel C, Wagner S, **Dybkova N**, Müller OJ, Näbauer M, Franz WM, Pieske B. Increased SR Ca<sup>2+</sup> cycling contributes to improved contractile performance in SERCA2a-overexpressing transgenic rats. *Cardiovasc Res.* 67:636-646.2005.
2. Kohlhaas M, Zhang T, Seidler T, Zibrova D, **Dybkova N**, Steen A, Wagner S, Chen L, Heller Brown J, Bers DM, Maier LS. Increased sarcoplasmic reticulum calcium leak but



- unaltered contractility by acute CaMKII overexpression in isolated rabbit cardiac myocytes. *Circ Res.* 98:235-244.2006.
3. Wagner S, **Dybkova N**, Rasenack ECL, Jacobshagen C, Fabritz L, Kirchhof P, Maier SKG, Zhang T, Hasenfuss G, Heller Brown J, Bers DM, Maier LS. Ca/calmodulin-dependent protein kinase II regulates cardiac Na channels. *J Clin Invest.* 116:3127-3138.2006.
  4. Yurukova S, Kilić A, Leineweber K, **Dybkova N**, Maier LS, Brodde O-E, Kuhn M. Ca<sup>2+</sup>/Calmodulin kinase II - mediated increased cardiac relaxation responses to  $\beta$ -adrenergic receptor stimulation in ANP receptor deficient mice. *Cardiovasc Res.* 73:678-688.2007.
  5. Sag CM, **Dybkova N**, Neef S, Maier LS. Effects on recovery during acidosis in cardiac myocytes overexpressing CaMKII. *J Mol Cell Cardiol.* 43:696-709.2007.
  6. Zhang T, Kohlhaas M, Backs J, Phillips W, Mishra S, **Dybkova N**, Chang S, Bers DM, Maier LS, Olson EN, Heller Brown J. Cytoplasmic and nuclear isoforms of CaMKII differentially affect calcium handling but similarly regulate HDAC/MEF2 transcriptional response. *J Biol Chem.* 282:35078-35087.2007.
  7. Wagner S, Hacker E, **Dybkova N**, Fabritz L, Kirchhof P, Bers DM, Maier LS. Ca/calmodulin kinase II differentially modulates transient outward potassium current in heart failure. *Circulation.* (in Revision).
  8. **Dybkova N**, Sedej S., Napolitano C., Neef S., Rokita A.G., Hünlich M., Kockskämper J., Priori S.G., Pieske B., Maier L.S. Overexpression of CaMKII $\delta_C$  in RyR2<sup>R4496C</sup> knock-in mice leads to spontaneous sudden cardiac death and altered intracellular Ca<sup>2+</sup> handling. *Circulation.* (submitted)

## Abstracts

1. Kohlhaas M, Seidler T, Zhang T, Zibrova D, **Dybkova N**, Heller Brown J, Bers DM, Maier LS. Intracellular calcium handling in isolated rabbit cardiac myocytes overexpressing cytoplasmic vs. nuclear CaMKII $\delta$  isoform. *Europ Heart J.* 25 (Suppl):178-179.2004.

2. **Dybkova N**, Wagner S, Bers DM, Maier LS. First evidence of the association of CaMKII $\delta$ c with the cardiac Na channel. *Z Kardiol.* 95 (Suppl 1):V262.2006.
3. Kohlhaas M, **Dybkova N**, Bers DM, Maier LS. CaMKII-Inhibition vermindert das diastolische SR Ca Leck. *Z Kardiol.* 95 (Suppl 1):P963.2006.
4. Wagner S, Hacker E, **Dybkova N**, Fabritz L, Kirchhof P, Bers DM, Maier LS. Ca/Calmodulin Kinase II differentially modulates transient outward potassium current in heart failure. *Circulation.* 114 (Suppl II):60.2006.
5. Knöll R, Pfeiffer C, Maier LS, **Dybkova N**, Chen J, Hasenfuss G, Chien KR. A new MLP interacting protein (MiP1) is an important mediator in human cardiomyopathy. *Z Kardiol.* 96 (Suppl 1):V1776.2007.
6. Rokita AG, Unsöld B, Teucher N, Schmidt K, Sowa T, Hünlich M, **Dybkova N**, Neef S, Wagner S, Maier LS. Differential regulation of Ca/calmodulin-dependent protein kinase II (CaMKII) in cardiac hypertrophy in the mouse: pressure overload versus volume overload. *Circulation.* 116 (Suppl II):154-155.2007.
7. **Dybkova N**, Napolitano C, Rokita AG, Neef S, Hünlich M, Kockskämper J, Priori SG, Pieske B, Maier LS for the CONTICA study group. Overexpression of CaMKII $\delta$ c in RyR2R4496C knock-in mice leads to spontaneous sudden cardiac death and altered intracellular Ca handling. 74. Jahrestagung der DGK:V49.2008.
8. Sedej S, Kockskämper J, Heinzl FR, Groborz J, Gronau P, **Dybkova N**, Maier LS, Colombi B, Napolitano C, Priori SG, Pieske B. Increased vulnerability to ouabain-induced arrhythmias in myocytes from mouse hearts harboring a human CPVT mutation. 74<sup>th</sup> Annual Meeting of the German Cardiac Society:P1544.2008.